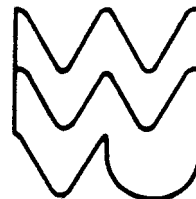


West  
Virginia  
University



CROSS-STRIKE STRUCTURAL DISCONTINUITIES: TEAR FAULTS AND  
TRANSFER ZONES IN THE CENTRAL APPALACHIANS OF WEST VIRGINIA

by Thomas H. Wilson  
Research Associate  
Devonian Shale Program

UGR FILE # 498

U. S. Department of Energy  
Contract number **DE-AC21-76ET12138**  
formerly **DE-AC21-76MC05194**

December 1980

Department of Geology & Geography  
College of Arts & Sciences  
Morgantown, West Virginia 26506

UGR File #498  
W.Va, Univ. Dept. of Geology & Geography  
December 1980

CROSS-STRIKE STRUCTURAL DISCONTINUITIES -  
TEAR FAULTS AND TRANSFER ZONES IN  
THE CENTRAL APPALACHIANS OF WEST VIRGINIA

by

Thomas H. Wilson  
Research Associate  
Devonian Shale Program

U. S. Department of Energy Contract no. DE-AC21-76ET12138  
formerly DE-AC21-76MC05194

West Virginia University  
Department of Geology and Geography  
Morgantown, West Virginia 26506

December 1980

TABLE OF CONTEXTS

	Page
Table of Contents. . . . .	i
List of Figures, Tables and Plates . . . . .	v
Acknowledgements . . . . .	xi
Abstract . . . . .	.xiii
I. INTRODUCTION . . . . .	1
A. Purpose . . . . .	1
B. Terminology . . . . .	3
C. Previous Work . . . . .	4
<u>1. The Parsons CSD</u> . . . . .	4
<u>2. The Petersburg CSD.</u> . . . . .	5
<u>3. Systematic Jointing Within</u> <u>Discontinuities</u> . . . . .	7
II. STRUCTURAL ANALYSIS OF THE MIDDLE MOUNTAIN SYN- CLINE AND ELSHORN MOUNTAIN ANTICLINE . . . . .	9
A. Geologic Mapping in the Middle Mountain Syncline and Elkhorn Mountain Anticline . . . . .	9
<u>1. Introduction.</u> . . . . .	9
<u>2. Stratigraphy.</u> . . . . .	12
<u>3. Structural Setting.</u> . . . . .	13
<u>4. Surface and Subsurface Structure n</u> <u>the Map Area</u> . . . . .	14
<u>5. The Petersturg CSD.</u> . . . . .	22
<u>6. The Valley and Ridge Extension of</u> <u>the Parsons CSD</u> . . . . .	23
B. Systematic Jointing in the Middle Mountain Syncline . . . . .	25

Table of Contents continued...

	<u>Page</u>
1. <u>Introduction</u> . . . . .	25
2. <u>Characteristics of Systematic Jointing in the Middle Mountain Syncline</u> . . . . .	29
a. <u>Discussion</u> . . . . .	.
b. <u>Joint development relative to folds and faults</u> . . . . .	36
c. <u>Joint intensity and spacing relative to folds and faults</u> . . . . .	38
C. <u>Conclusions</u> . . . . .	42
III. <u>SUBSURFACE STRUCTURAL INTERPRETATIONS</u> . . . . .	43
A. <u>Introduction</u> . . . . .	44
B. <u>Regional Cross Sections</u> . . . . .	44
1. <u>Construction</u> . . . . .	44
a. <u>Surface structure and stratigraphic thicknesses</u> . . . . .	44
b. <u>Structural lithic units</u> . . . . .	45
c. <u>Stiff structural lithic units</u> . . . . .	49
d. <u>Soft structural lithic units</u> . . . . .	52
e. <u>Descriptions of the sections</u> . . . . .	53
2. <u>Valley and Ridge Structures</u> . . . . .	53
3. <u>The Bergton-Crab Run and Adams Run Anticlines</u> . . . . .	63
4. <u>Structures Between the Little North Mountain Fault and the Blue Ridge Fault</u> . . . . .	64
5. <u>Plateau Structure</u> . . . . .	65
C. <u>Structural Interpretation</u> . . . . .	65
1. <u>Structure in the Cambrian-Ordovician Stiff Structural Lithic Unit</u> . . . . .	65



Table of contents continued...

	<u>Page</u>
2. <u>Structure in the Silurian-Devonian Stiff Structural Lithic Unit.</u> . .	73
D. Structural Model for the Parsons and Petersburg Cross-Strike Structural Discontinuities . . . . .	78
E. Balancing Structural Cross Sections . .	82
F. Balancing Cross Sections and Pressure Solution. . . . .	87
IV. CENTRAL APPALACHIAN GRAVITY MODELS. . . . .	94
A. Introduction. . . . .	94
B. Causes of Disagreement. . . , .	95
C. Regional Gravity Profiles . . . . .	98
D. Valley and Ridge Models . . . . .	139
1. <u>Perry's (1971) Section DD'.</u> . . . .	109
2. <u>The Middle Mountain Syncline.</u> . . . .	112
3. <u>Sites' (1978) Section CC' . . . . .</u>	116
4. <u>Jacobeen's and Kanes' (1974) Section.</u>	116
E. Conclusion. . . . .	122
V. SUGGESTIONS TO FUTURE WORKERS. . . . .	126
VI. CONCLUSIONS . . . , . . . . .	132
REFERENCES CITED . . . . .	136
APPENDIX I - Rotated and Unrotated Joints. . . . .	147
A. Joint Strike and Dip in Rotated and Unrotated Bedding . . . . .	148
B. Equal Area Projections of Rotated and Unrotated Joints. . . . .	169

Table.of contents continued...

	<u>Page</u>
APPENDIX II - Joint Spacings and Intensities . . . . .	188
A. Introduction. . . . .	189
B. Joint Spacing and Pseudovalue . . . . .	191
C. Intensity, Mean Pseudovalue, and Confidence Limits on the Mean. . . . .	224
D. Average Group Intensities and p-Values. . . . .	225
APPENDIX III - Stratigraphy. . . . .	225
A. Thicknesses of Stratigraphic Units. . . . .	229
B. Deep Well Locations . . . . .	241
C. Fence Diagrams. . . . .	243
APPENDIX IV - List of Pertinent Gravity Data for the Middle Mountain Gravity Profile. . . . .	246
V I T A . . . . .	248
Approval of Examining Committee. . . . .	249

# LIST OF FIGURES, TABLES , AND PLATES

<u>FIGURE</u>	<u>Page</u>
1 - Location Map of the Parsons and Petersburg CSD's	6
2 - Location map of the Middle Mountain Syncline and Elkhorn Mountain Anticline Field Area	11
3 - Geologic Map of the Middle Mountain Syncline and Elkhorn Yountain Anticline	1.5
4 - Cross Section CC' Across the Middle Mountain Syncline and Elkhorn Mountain Anticline	17
5 - Cross Section BB' Across the Middle Mountain Syncline and Elkhorn Yountain Anticline	18
6 - Cross Section AA' Across the Middle Mountain Syncline and Elkhorn Mountain Anticline	21
7 - Rose Diagrams of Systematic Joint Trends in the Middle Yountain Syncline (see the legend on the caption page of Figure 3)	30
8 - Strike of the Maximum Frequency Joint Set Plotted at the Sample Site	31
9 - Mean Joint Intensity and 95% Confidence Limits on the Mean	32
10 - Station Locations and Subdivisions of the Systematic Joint Study	37
11 - Locations of the Structural Cross Sections	54
12 - Structural Interpretation I of the Valley and Ridge Structures North of the Petersburg and Parsons CSD's (after Jacobeen and Kanes, 1974)	55
13 - Structural Interpretations II of Valley and Ridge Structures North of the Petersburg and Parsons CSD's	56
14 - Sites' Structural Cross Section CC' Across the Northeast Portion of the Valley and Ridge Province	60
15 - Surface and Subsurface faults in the Cambrian-Ordovician Carbonates	66

List of figures, tables and plates continued...

<u>FIGURE</u>	<u>Page</u>
16 - Terrain-corrected Bouguer Gravity Map Taken from Plate I of Kulander and Dean (1978)	72
17 - Schematic Diagram of a Transfer Zone Developed Above a Sole Fault (from Dahlstrom, 1969)	74
18 - Schematic Representation of Inferred Subsurface Cambrian-Ordovician Structure	75
19 - Transfer Zone Model Proposed for the Parsons Cross-Strike Structural Discontinuity	80
20 - Illustrated Methods of Thrust Propagation (from Marshak and Geiser, 1930)	88
21 - Shortening of a Multilayer	90
22 - Folds of the Central Appalachian High Plateau and the Locations of Gwinn's Lineaments (after Gwinn, 1964)	93
23 - Modelled Gravity Profiles are Located on the Contours of Residual Bouguer Gravity (from Kulander and Dean, 1978)	99
24 - Calculated and Residual Bouguer Gravity Along Structural Interpretation SS' South of the Parsons CSD are Plotted and Compared	100
25 - Calculated and Residual Bouguer Gravity Along the Structural interpretation NN' North of the Parsons CSD are Compared	101
26 - Structural Sections NN' and SS' are Located along With the Petersburg and Parsons CSD's on Contours of Terrain-corrected Bouguer Gravity taken from Kulander and Dean, 1973	102
27 - Calculated and Terrain-corrected Bouguer Gravity are Plotted and Compared for Structural Interpretation SS' South of the Parsons CSD	103
28 - Calculated and Terrain-corrected Bouguer Gravity are Plotted and Compared for Structural Interpretation NN' North of the Parsons CSD	104

List of figures, tables and plates continued..

<u>FIGURE</u>	<u>Page</u>
29 - Calculated and Residual Bouguer Gravity are Plotted and Compared for Perry's (1971) Section DD'	110
30 - Calculated and Observed Gravity, are "lotted and Compared for a Subsurface Structural Interpretation Across the Middle Mountain Syncline and Elkhorn Mountain Anticline	114
31 - Calculated and Residual Bouguer Gravity are Plotted and Compared for Sites' (1978) Section CC'	117
32 - Structural Interpretation I of Valley and Ridge Structures North of the Petersburg and Parsons CSD's (after Jacobeen and Kanes, 1974)	120
33 - Structural Interpretation II of Valley and Ridge Structures North of the Parsons and Petersburg CSD's	121
34 - Calculated Gravity for Structural Interpretation I of Valley and Ridge Structures North of the Petersburg and Parsons CSD's	125
35 - Calculated Gravity for Structural Interpretation II of Valley and Ridge Structures North of the Parsons and Petersburg CSD's	126
36 - Location Map of Appalachian CSD's Taken from Wheeler, 1980	130
37 - Equal Area Projections of Poles to Rotated and Unrotated Systematic Joints from Group 1	171
38 - Equal Area Projection of Poles to Rotated and Unrotated Systematic Joints from Group 2	173
39 - Equal Area Projection of Poles to Rotated and Unrotated Systematic Joints from Group 3	175
40 - Equal Area Projections of Poles to Rotated and Unrotated Systematic Joints from Group 4	177
41 - Equal Area Projections of Poles to Rotated and Unrotated Systematic Joints from Group 5	179
42 - Equal Area Projections of Poles to Rotated and Unrotated Systematic Joints from Group 6	181

List of figures, tables and plates continued...

<u>FIGURE</u>	<u>Page</u>
43 - Equal Area Projection of Poles to Rotated and Unrotated Systematic Joints from Group 7	183
44 - Equal Area Projection of Poles to Rotated and Unrotated Systematic Joints from Group 8	185
45 - Equal Area Projection of poles to Rotated and Unrotated Systematic Joints from Group 9	187
46 - Dee-i, Wells Projected Gnto Structural Sections SS' and NN' are Located T-Jells have been projected along the local structural trend. Well locations and depths to the to? of the Ordovician and deeper units are taken from Cardwell (1976). <sup>242</sup>	
47 - Fence Diagram of Thicknesses of Mississippian to Lower Devonian Units Constructed from Measured Sections and Well Logs (see text for references).	244
<b>48</b> - Fence Diagram of Cambrian to Middle Devonian Structural Lithic Units Constructed from Well Locations and Thickness taken from Cardwell (i977)	245
<u>TABLES</u>	
1 - Structural Lithic Units	47
2 - Shortening Measurements from the Structural Interpretation North of the Parsons Structural Discontinuity	s3
3 - Shortening Measurements from the Structural Interpretation South of the Parsons Structural Discontinuity	84
4 - Average Densities Assigned to Stratigraphic Intervals for Sections NN' and SS' (averages calculated using densities taken from Kulander and Dean, 1978)	106
5 - Average Densities Assigned to Stratigraphic Intervals for Perry's (1971) Section DD', Sites' (1978) Section CC! (averages were calculated using densities taken from Kulander and Dean, 1978)	111

## List of figures, tables and plates continued...

<u>TABLES</u>	<u>Page</u>
6 - Average Densities Assigned to Stratigraphic Intervals in the Middle Mountain Syncline (average calculated using densities taken from Kulander and Dean, 1378)	115
7 - Average Densities Assigned to Stratigraphic Intervals for the Jacobeen and Kanes (1974) Section Line (averages calculated using densities taken from Kulander and Dean, 1978)	118
8 - Trend and Plunge of Cluster Poles, the Standard Deviation of Poles in Each Cluster and the Number of Poles in Each Cluster for the Rotated and Unrotated Systematic Joints of Group 1	170
9 - Trend and Plunge of Cluster Poles, the Standard Deviation of Poles in Each Cluster and the Number of Poles in each Cluster for the Rotated and Unrotated Systematic Joints of Group 2	172
10 - Trend and Plunge of Cluster Poles, the Standard Deviation of Poles in Each Cluster and the Number of Poles in Each Cluster are Listed for the Systematic Joints of Group 3	174
11 - Trend and Plunge of Cluster Poles, the Standard Deviation of Poles in Each Cluster and the Number n of Poles in Each Cluster are Listed for the Systematic Joints of Group 4	176
12 - Trend and Plunge of Cluster Poles, the Standard Deviation of Poles in Each Cluster and the Number n of Poles in Each Cluster are Listed For the Systematic Joints of Group 5	178
13 - Trend and Plunge of Cluster Poles, the Standard Deviation of Poles in Each Cluster and the Number n of Poles in Each Cluster are Listed for the Systematic Joints of Group 6	180
14 - Trend and Plunge of Cluster Poles, the Standard Deviation of Poles in Each Cluster and the Number n of Poles in Each Cluster are Listed for the Systematic Joints of Group 7	182

List of figure-,, tables and plates continued...

<u>TABLES</u>	<u>Page</u>
15 - Trend and Plunge of Cluster Poles, the Standard Deviation of Poles in Each Cluster and the Number n of Poles in Each Cluster are Listed for the Systematic Joints of Group 8	184
16 - Trend and Plunge of Cluster Poles, the Standard Deviation of Poles in Each Cluster and the Number n of Poles in Each Cluster are Listed for the Systematic Joints of Group 9	186

<u>PLATES</u>	
1 - Structural interpretations NN' and SC' north and south of the Parsons CSD. The sections extend from the Blue Ridge across Virginia and West Virginia to the Ohio State line and depict sub-surface structures in the Valley and Ridge, High Plateau and much of the remaining Plateau further to the west. . . . . in back pocket	
2 - Section JJ' is an interpretation of Valley and Ridge structures in Mineral and Hampshire Counties of West Virginia. The section indicates a complete duplication of the Cambrian-Ordovician sequence on interpretation suggested by Jacobeen and Kanes (1975).	248
3 - Section LL' is a longitudinal section along Valley and Ridge structures. The section extends from the southern border of Pendleton County, West Virginia through Grant and most of Mineral Counties of West Virginia.	249
4 - Gravity stations occupied in the Middle Mountain-Elkhorn Mountain study area are located at the scale of the 7-1/2' quadrangles.	250



### ACKNOWLEDGEMENTS

The majority of this work was supported under a Department of Energy, Eastern Gas Shales Contract (number DE-Ac21-76Mc05194, formerly EY-76-C-05-5195) with Dr. Robert C. Shumaker of West Virginia University. Initial stages of the project were funded by the donors of the Petroleum Research Fund of the American Chemical Society through Dr. Russell L. Wheeler, by the West Virginia Geological and Economic Survey, and Sigma Xi.

For those ideas in this report that may survive harsh scrutiny and criticism, I must share credit with Dr. R. Wheeler and Dr. R. Shumaker. Dr. Wheeler stimulated an initial interest in Appalachian structural problems and shared a wealth of information in the detailed structural characteristics of CSD's here in the Appalachians and elsewhere. Dr. Shumaker has been working on many of the structural problems present in the subsurface Cambrian-Ordovician carbonate sequence since the mid-sixties and pointed out the need for transition from the complete duplication of the Cambrian-Ordovician sequence north of the Petersburg CSD to the imbricate stacking of that sequence to the south of the CSD.

Appreciation is extended to the following gentlemen for critically reviewing this manuscript and for discussion and suggestions during the research: Professor Milton Heald, Professor Richard Williams and Professor William Dunne, all of the department of Geology at West Virginia University, and Dr. Douglas Patchen of the West Virginia Geological and Economic Survey.

Special thanks go to the following individuals for discussion on specialized areas of the research: Dick Beardsley, Columbia Gas Transmission Corporation; Bill Bagnall and Rick Drabish, also of Columbia Gas Transmission Corporation; Dudley Cardwell, West Virginia Geological and Economic Survey; Phil Berger, University of Cincinnati, Ohio; Roy Sites, Sterling Drilling Company, Charleston, West Virginia; Byron Kulander, Wright State, Ohio; Stuart Dean, University of Toledo, Ohio; John Dennison, University of North Carolina; Bili Perry, Jr., U. S. Geological Survey, Denver Colorado; Eberhard Werner, West Virginia University; Jan Dixon, ARCO Oil and Gas, Denver! Colorado; Brian Long, West Virginia Office of Surface Mining; Jim Ruotsalo, West Virginia University.

Special thanks also go to the following individuals for field assistance, and/or discussions, which may or may not have been related to this project: Phil Berger, Jim Ruotsola, Bob Westfall, Al Brown, Roy Sites, Brian Long, Jan Dixon, Gavrielle Glich, Scott McColloch and John LaCaze. Many thanks also to John Wright for drafting many of the illustrations in this manuscript.

### ABSTRACT

The structural characteristics of two cross-strike structural discontinuities (CSD's) in the central **sedimentary** Appalachians of West Virginia and Virginia were examined using limited field studies, structural cross sections, and gravity modelling. Detailed mapping and joint intensity studies were confined to the *Valley* and Ridge Middle Mountain syncline and adjacent Elkhorn Mountain anticline in Pendleton County, West Virginia where these structures are intersected by an extension of the Parsons CSD. A gravity profile across these structures was also surveyed and modelled. Two structural cross sections were constructed across the sedimentary Appalachians to compare structural features north and south along the length of the Parsons CSD. Additional cross sections' north of both the Parsons and Petersburg CSD's were constructed to provide additional details on subsurface Valley and Ridge structure in West Virginia. Comparisons of the theoretical gravity with already existing observed gravity data were made along these and other previously published structural sections through the area.

Detailed mapping along the Middle Mountain syncline and Elkhorn Mountain anticline indicates that structural shortening within the Parsons CSD is taken up by small and

more numerous faults than outside the CSD. Splay faults cutting the Silurian-Devonian structural lithic unit transfer slip into the Middle Devonian shales thickening that sequence particularly in the more intensely faulted CSD. Relative increases in joint intensity are associated with faulted and more intensely folded rocks so that joint intensity within the CSD is generally greater than outside the CSD. Reports from other areas along the Parsons and Petersburg CSD's are consistent with this interpretation. A gravity profile across the area indicates that the Cambrian-Ordovician structural lithic unit is folded and faulted beneath the Elkhorn Mountain syncline and that splay faults have cut through that sequence transferring slip into the overlying Martinsburg Formation.

A subsurface structural model of the Cambrian-Ordovician structural lithic unit is inferred from structural cross sections. The Parsons and Petersburg CSD's are expressed at the surface primarily in Silurian and younger formations. However, the expressions of the CSD's are not confined to these formations. Along the Parsons CSD the Cambrian-Ordovician unit is tear faulted between the noses of the Elkins Valley and Deer Park anticlines of the Plateau province and across the plunging noses of the Bergton-Crab Run and Adams Run anticlines in the Valley and Ridge Province. The Valley and Ridge segment of the Petersburg CSD coincides with a transfer zone and inferred zone of

..

tear faults in the underlying Cambrian-Ordovician structural lithic unit.

The structural details mapped along the Middle Mountain-Elkhorn Mountain fold pair and mentioned above can also be explained if the Parsons CSD in the exposed Silurian-Devonian structural lithic unit is a fault transfer zone. Areas mapped previously by other workers along segments of the Parsons CSD in the Plateau and also along the Petersburg CSD in the Valley and Ridge and Plateau provinces are consistent with the fault transfer Interpretation of structures in the exposed Silurian-Devonian and higher level structural lithic units along these CSD's. Thus, the structural characteristics of the Parsons and Petersburg CSD's at all structural levels can be explained as cross strike alignments of transfer zones, tear faults, or both,

## INTRODUCTION

### A. Purpose

Structural discontinuities have been of interest to geologists for many years (see Chapter III). The academic and economic importance of an increased understanding of structural discontinuities is recognized by Wheeler, et al. (1974, p. 197):

First, the lineaments appear to be among the largest cross strike structures of the central sedimentary Appalachians. Thus, whether or not Gwinn's interpretation of them as tear faults is correct, they are a fundamental *part* of the structural geometry of that region. Second, an understanding of the lineaments is necessary to interpreting the structural evolution of the central Appalachians. Third, correct interpretation of the rock movements that produced the lineaments can illuminate tectonic processes occurring in the marginal, hydrocarbon-prospective zones of orogens generally. Fourth, lineaments' economic importance arises from the possibility that such structures may create fracture porosity, interrupt reservoirs, create structural traps, influence migration of fluids along strike, and affect the validity of structural extrapolations along strike. Finally, because understanding of the lineaments will increase our knowledge of orogens generally, such understanding will contribute to the increasingly important effort to find these smaller, deeper, more subtly hidden reserves of hydrocarbons that still remain in deformed sedimentary rocks.

The current study is designed, in part, to characterize the structural effects of the Pax-sons CSD on exposed Devonian shales of the Middle Mountain syncline of the Valley

and Ridge province in eastern West Virginia (see Chapter II). Much of the current research of the Department of Energy's Eastern Gas Shales Project is directed toward predicting the locations of fractured reservoirs in the gas-producing Devonian Shales. The Middle Devonian shales exposed in the Valley and Ridge province are mechanically similar to the gas-productive Upper Devonian Brown shale to the west, beneath the Allegheny Plateau. Field studies of the Middle Mountain area will be discussed in detail in Chapter II.

In addition to the field studies , pre-existing regional structural data on the central sedimentary Appalachian will be integrated and presented as structural cross sections. The construction of these cross sections and their interpretation are discussed in Chapter III. A three dimensional structural model will be proposed for the region of the Central Appalachians that includes the Parsons and Petersburg CSD's. .

In Chapter IV , theoretical gravity will be calculated for the structural cross sections and will be compared to gravity data collected and compiled by Kulander and Dean (1978). New data collected in the Middle Mountain area is also modelled.

Suggestions to future workers will be made in Chapter V.

The major conclusions of the work presented here will be outlined in Chapter VI.

## B. Terminology

The descriptive term cross-strike structural discontinuity (or CSD) is introduced by Wheeler, et al. (1978), and defined by Wheeler (1980, in press) as

...structural. . .alignments, at high angles to regional strikes, that are recognizable because they disrupt strike-parallel structural, geophysical, geomorphic, sedimentologic or other patterns.

Two zones of cross-strike structural discontinuity in northeast West Virginia were named the "Parsons lineament" and the "Petersburg discontinuity" (Wheeler, et al., 1974). Wheeler (1980) discusses cross-strike structural discontinuities (CSD's) and commonly refers to the Parsons and Petersburg cross-strike structural discontinuities as either structural, lineaments or as just lineaments. Thus, it seems permissible to choose a shortened form of descriptive term once it has been established that one is referring to a cross-strike structural discontinuity when using that shortened form. Because this report discusses a cross-strike alignment of discontinuities of various structural features within the Paleozoic sedimentary cover in the Valley and Ridge and Plateau provinces of West Virginia and Virginia, the use of the term cross-strike structural discontinuity is preferred. Use of the shortened form, lineament is not



preferred, since the term lineament often carries with it the connotation of LANDSAT, U2, or short air-photo lineament. Although LANDSAT and U2 lineaments are associated with the Parsons and Petersburg CSD's (Trumbo, 1976; Wheeler, et al, 1976), no one such lineament or group of lineaments coincides with the known or inferred extent of these CSD's. Further, LANDSAT, U2, and short airphoto lineaments are not the concern of this study. Hence, to avoid the possibility of any confusion with these types of lineaments, the shortened form --structural discontinuity, or just discontinuity-- is often used here. Where the Petersburg and Parsons CSD's are referred to specifically, the abbreviation CSD is always used.

### C. Previous Work

#### 1. The Parsons Structural Discontinuity

Alignments of structural discontinuity presently associated with part of the Parsons CSD (Figure 1) were previously recognized by Gwinn(1964). Detailed mapping along the Parsons CSD by Henderson (1973), Wheeler and others (1974), Mullenex (1975), and Trumbo (1976), indicate that minor and intermediate-scale folds are more abundant northeast of and within the Parsons CSD in the Plateau province of eastern Tucker County, West Virginia. A zone of disruption in dip contours is used to define

the width of the discontinuity (Wheeler, et al. (1976a).

The Parsons CSD has also been recognized on LANDSAT Imagery as two parallel northwest-trending LANDSAT lineaments (Wheeler, et al 1976a). Trumbo (1976) and Wheeler, et al (1976a) also report that the zone between these two LANDSAT photolineaments contains photolineaments observed on U2 color infrared images which have significantly different trends than those to the northeast or southwest.

An alignment of fold terminations can be observed in Rockingham County, Virginia (Rader and Perry, 1976a, 1976b). The Parsons CSD has been extended along a more southeasterly trend than Gwinn's lineament through Pendleton County, West Virginia (Figure 1) , to include this alignment of fold terminations (Wheeler, 1978). The expression of the discontinuity in Pendleton County is comparatively subtle in terms of regional structure. However, Wilson (1979) has shown that intermediate-scale folds and reverse faults are more abundant within the discontinuity and die out to the northeast, where the proposed extension of the discontinuity crosses an outcrop belt of the Middle Devonian shales.

## 2. The Petersburg Structural Discontinuity

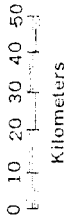
The Petersburg CSD appears to intersect the Parsons CSD in the eastern Plateau province, in a rugged area mapped

# GEOLOGIC MAP OF WEST VIRGINIA

## WEST VIRGINIA GEOLOGICAL AND ECONOMIC SURVEY

1969

**PETERSBURG**  
**| CSD**



only by Reger (1921) (Figure 1). The Parsons and Petersburg CSD's are similar in many respects, and their origins and developments may be intimately related. Sites (1978, p. 26) says the following about the Petersburg CSD:

The Petersburg lineament is not a simple transverse fault. Instead, three factors are observed that coincide with the location of the lineament: (1) plunge of anticline into synclines; (2) the existence of several small, lineament parallel cross faults mostly with a left lateral, strike slip motion; and (3) increased longitudinal faulting and folding with the non-cross fault controlled water gap.

As with the Parsons CSD, the width of the Petersburg CSD is defined by disruptions in dip contours (Sites and Wheeler, 1976; McColloch, 1977; Sites, 1978). Sites (1978) also notes considerable geomorphic expression of the Petersburg CSD, disruption in fold patterns, an increase in longitudinal jointing in fold noses, changes in stratigraphic thickness across the discontinuity, and expression as a LANDSAT lineament. Wheeler, et al. (1979) have presented a tabulation of the phenomena which characterize these discontinuities and others found in the central and southern Appalachians, the Andes, and the Irish Caledonides.

### 3. Systematic Jointing Within Discontinuities

Recent techniques developed by Vialon, and others (1976) and modified by Wheeler (1979) have been used successfully to show that the Parsons and Petersburg CSD's

are more intensely jointed (Dixon, 1979; Wheeler and Dixon, 1980). The most closely spaced joint set within these discontinuities is the set whose strike parallels the trend of the discontinuity (Dixon, 1979). Joint intensity studies have been very productive thus far. Many of the characteristics of jointing can be associated with detachment tectonics. However, the presence of increased joint intensity within the Petersburg CSD where it crosses the Allegheny structural front (Dixon, 1979) may involve deeper-level tear faults, and/or transfer zones (see Chapter III).

## II. STRUCTURAL ANALYSIS OF TX MIDDLE MOUNTAIN SYNCLINE AND ELKHORN MOUNTAIN ANTICLINE

### A. Geologic Mapping in the Middle Mountain Syncline and Elkhorn Mountain Anticline

#### 1. Introduction

Part of the Middle Mountain syncline of the Valley and Ridge province in West Virginia (see Figure 2) was chosen as a site for extensive field studies because it exposes the Middle Devonian shales\* and plunges across the Parsons and Petersburg CSD's. The organically-rich Middle Devonian shales exposed in the Middle Mountain syncline are the mechanical equivalent of the Devonian Brown shales in the western subsurface of the Appalachian Plateau province to the west. A significant amount of gas is produced from the Devonian Brown shales, and considerable effort has been directed through the Department of Energy's Eastern Gas Shales Project to exploration for new reserves of gas in these shales (Patchen, 1977). The effects on exposed Middle Devonian shales of deformation in the underlying and more competent Silurian and Lower Devonian formations may be very similar to the effect on buried

\*Middle Devonian shales as used in this text will include the Harrell Formation which is the lowermost formation of the Upper Devonian sequence.

productive shales that overlay structures in the Middle Devonian Onondaga Limestone to the west under the Plateau. Deformation of these more competent limestones and sandstones in the low Plateau anticlines is much more intense than that at higher structural levels (Gwinn, 1964).

Field studies were focused in the vicinity of the proposed intersection (Wheeler, 1978, 1980) of the Parsons CSD with the Middle Mountain syncline (see Figure 2). A southwest-to-northeast plunge in Devonian Oriskany structure across the proposed extension of the discontinuity can be observed on the West Virginia state geologic map (Cardwell, et al., 1968). This plunge in structural level was examined through detailed surface mapping of exposed stratigraphic formations and studies of systematic joint intensities throughout exposed Middle and Upper Devonian formations. In addition, this work continues previous structural studies of this area undertaken by the author (Wilson, 1979a, 1979b).

This chapter will attempt to answer the following questions: Do interruptions in structure along the length of the Middle Devonian syncline and adjacent Elkhorn Mountain anticline represent part of the inferred regional cross-strike structural discontinuity? What similarities and dissimilarities exist between structural features observed in these Valley and Ridge structures and those

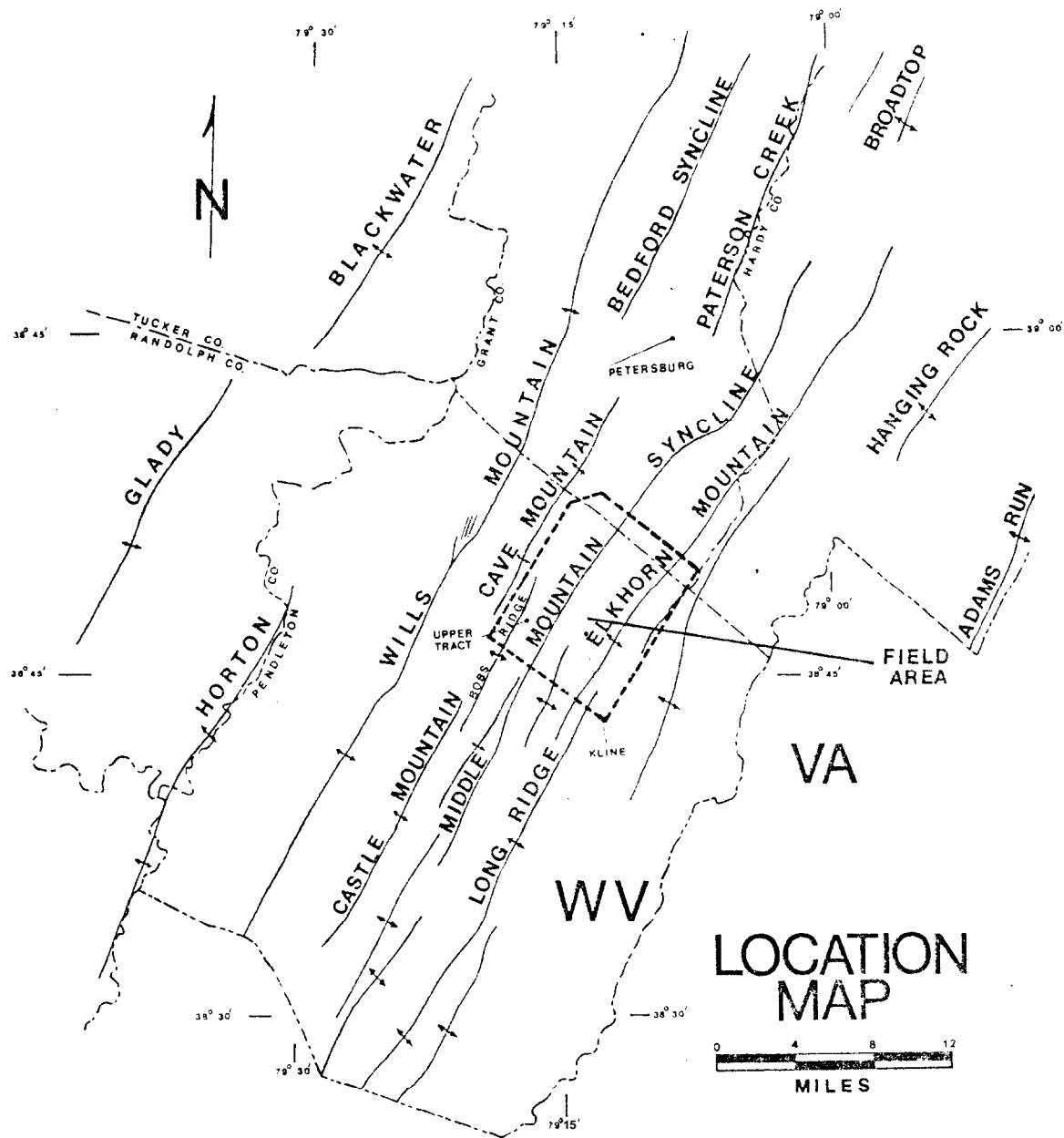


Figure 2 Location map of the Middle Mountain Syncline and Elkhorn Mountain Anticline Field Area



reported for the areas across the Parsons CSD of the Plateau (Henderson, 1973; Wheeler, et al, 1974, 1976; Mullenex, 1976; Trumbo, 1976; Dixon, 1979)? Also, how are the structural features within the Fiddle Mountain area similar or dissimilar to those reported for the Petersburg CSD (Wilson, 1976; Wheeler, et al, 1974; McColloch, 1977; LaCaze, 1975; Sites, 1978; Dixon, 1980)?

## 2. Stratigraphy

Silurian and Devonian units are exposed within areas of the Middle Mountain syncline and Elkhorn Mountain anticlines mapped by the author (see Figure 3). Field identification was made on the basis of numerous published descriptions of the Silurian and Devonian formations exposed within this study area and in surrounding areas. Detailed mapping and descriptions of: the stratigraphy along the Wills Mountain anticline adjacent to the west of this area are presented by Perry (1971). Sites (1971) presents descriptions of Silurian and Lower Devonian formations exposed in the Cave Mountain anticline northwest of the study area. Sites (1978) describes Silurian, and Lower and Middle Devonian formations exposed in the Petersburg region north of this study area. Descriptions of the Lower and Middle Devonian section along the Patterson Creel; anticline in Pendleton and Hardy Counties, West Virginia, presented in

McColloch (1976) were also useful. Additional information on Middle and Upper Devonian units is presented in Dennison (1961, 1963), Dennison and Hasson (1974), Hasson (1972), and Hasson and Dennison (1974). Perhaps the most complete description of the rock units exposed in the study area is found in the Pendleton County Report (Tilton, Prouty, and Price, 1927).

### 3. Structural Setting

The Middle Mountain syncline lies in the Valley and Ridge province of the Appalachians of West Virginia (see Figure 2). Adjacent to the Middle Mountain syncline along its northwest flank is the Cave Mountain anticline, an allochthonous block, thrust along high-angle listric surfaces arising from a thrust in the Ordovician Reedsville Formation (Sites and Wheeler, 1977). The Cave Mountain anticline lies on the southeast limb of the Wills Mountain anticline, which rises from a decollement in the Cambrian Waynesboro Formation (Perry, 1971, 1975; Jacobeen and Kanes, 1974, 1975; Sites, 1978) and represents the northwesternmost large structure of the Valley and Ridge province. The Elkhorn Mountain anticline is sheared by several low-angle reverse faults in a manner less intense than, but similar to, that of the Cave Mountain anticline, and represents a detachment rising out of the Ordovician Reedsville Formation along with possible detachments in the Silurian Wills

Creek and/or Ordovician Juniata Formations.






As mentioned above (section A.1 of this chapter), a northeastward drop in Devonian Oriskany Sandstone structure can be observed across the extension of the Parsons CSD. The Wills Mountain anticline also plunges across the Parsons CSD (see geologic maps of Cardwell, et al, 1968; Tilton, et al, 1927; Perry, 1975). Bobs Ridge anticline, Cave Mountain anticline, and other anticlines between the Wills Mountain anticline and Middle Mountain syncline terminate within or near the extension of the Parsons discontinuity (Figure 2). Similarly, to the southeast of the Middle Mountain syncline, the Long Ridge anticline overlaps with the Elkhorn Mountain anticline in the Parsons CSD. The former plunges out, but the latter continues to the northeast beyond the discontinuity. Other structural features discontinuous across the extension of the Parsons CSD will be discussed in Chapter III.

#### 4. Surface and Subsurface Structure in the Map Area

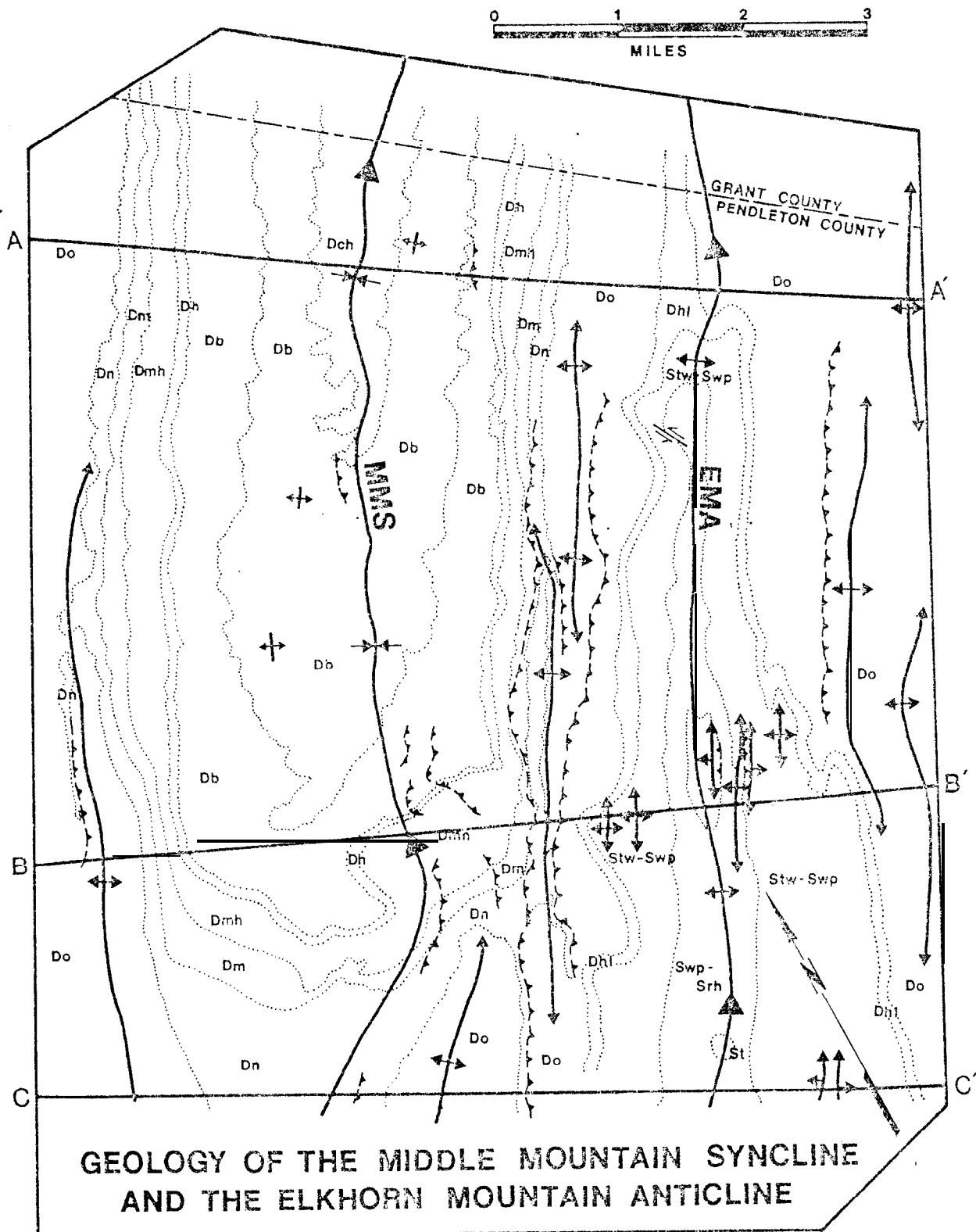
The portions of the Middle Mountain syncline and Elkhorn Mountain anticline, mapped in this study, are shown on Figure 3. Contours of bedding dip over the syncline along with a strike-line map of this structure presented in Wilson (1979a) were used to locate the axial trace of the Middle Mountain syncline. The westward bend in the

Figure 3: Geologic map of the Middle Mountain Syncline and the Elkhorn Mountain Anticline

LEGEND:

...	Stratigraphic contact
	Axial fold trace
	Anticline
	Syncline
	Reverse fault
	Strike slip fault

Dch	Chemung Group
Db	Brallier Formation
Dh	Harrell Shale
Dmh	Mahantango Formation
Dm	Marcellus Formation
Dn	Needmore Shale
Do	Oriskany Sandstone
Dhl	Helderberg Group
Stw- Swp	Tonoloway Formation to the Williamsport Formation
Swp-Srh	Williamsport Formation through the Rose Hill Formation



axial trace of the **syncline across** the **plunge** out of the Middle Devonian formations is produced by an anticline on the syncline's southeast limb that dies out northeastward beneath the Middle Devonian formations (Figure 3). The presence and extent of this anticline are illustrated in cross sections CC' & BB' (see Figures 4 and 5) (see Figure 3 for locations of the sections). Disruption of bedding dip and large standard deviations of bedding dip extend approximately two miles northeast of this anticline (Wilson, 1979a, 1979b). R. Wheeler (oral communication, 1978) has suggested that the disrupted shales may be related to a northeastward continuation of this anticline in the subsurface. Cross sections BB' (Figure 5) shows the presence of folded Lower Devonian and Silurian formations on the syncline's southeast limb. Detailed mapping of surface structures in this area also reveals that extensive folding and faulting have thickened the Devonian Needmore, Marcellus, and Mahantango Formations by two to three times their normal thicknesses (see Figure 5). The faults in the shales are related to thrust faults that cut across more brittle Lower Devonian and Silurian formations, probably representing splay thrusts that rise from a decollement in the Ordovician Martinsburg Formation to a decollement or decollements in the Middle Devonian shales (see Figures 4 and 5). Bagnall, Beardsley, and Drabish (1979)

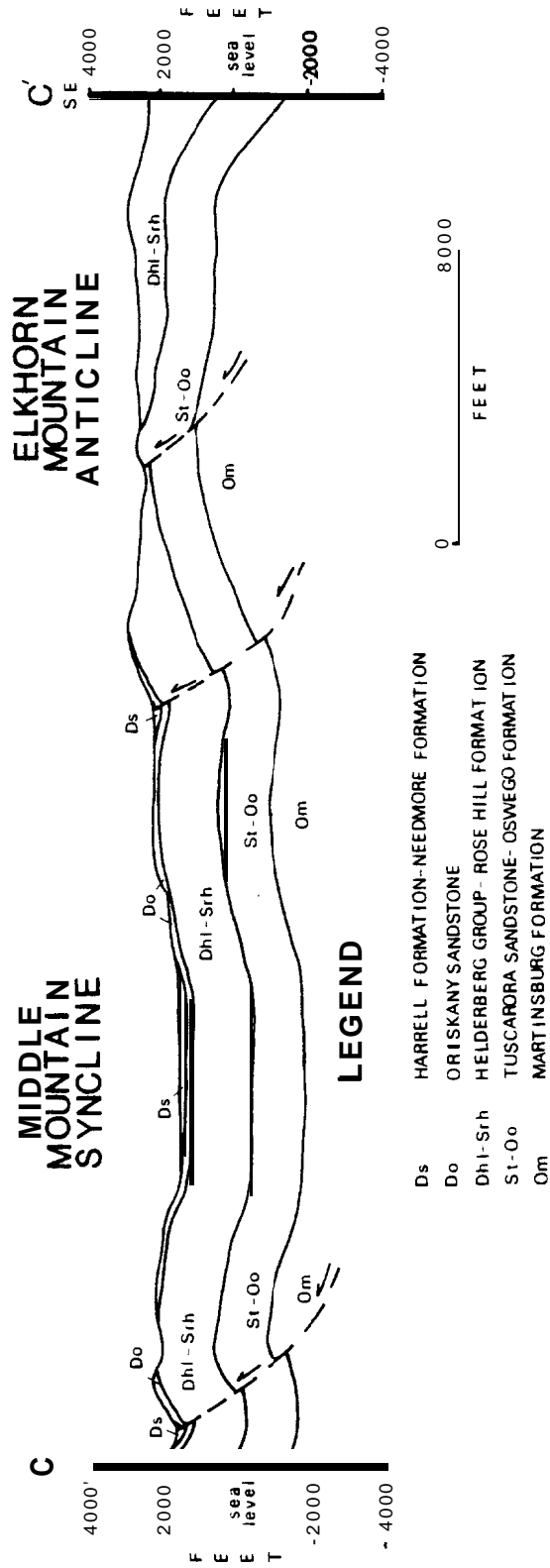


Figure 4 Cross Section CC' Across the Middle Mountain Syncline and Elkhorn Mountain Anticline

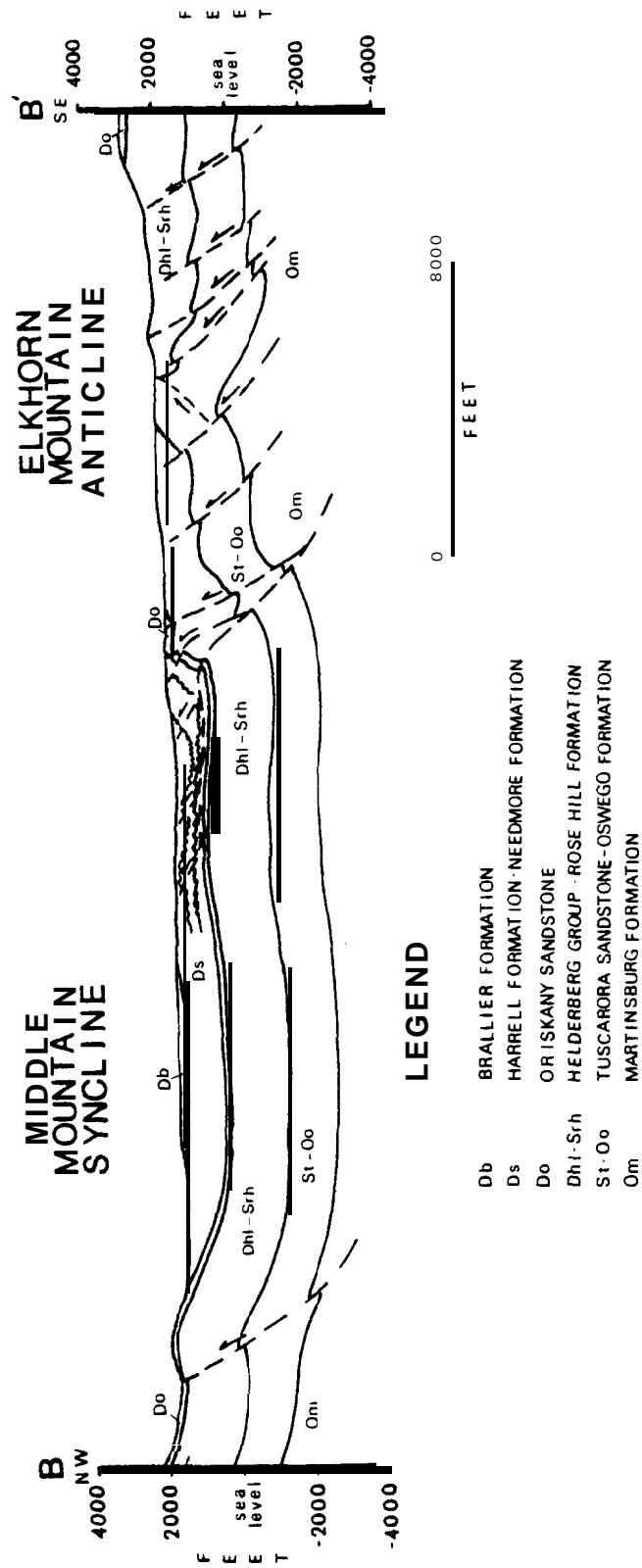


Figure 5 Cross Section BE' Across the Middle Mountain Syncline and Elkhorn Mountain Anticline



present seismic evidence for the presence of detachment within the Ordovician Juniata Formation and the Silurian Wills Creek Formation on the northwest limb of the Wills **Mountain** anticline near Reyser, West Virginia. It is possible, then, that some of the faulting on the northwest limb of the **Elkhorn** Mountain anticline is partly due to detachment in these formations.

Displacements along faults mapped in the **Middle** Devonian shales are questionable. Presence of a fault was based on several types of evidence. Roughly linear zones often separated rocks of different formations, bedding to one side being steeply dipping to overturned but becoming flat-lying or nearly so across such a zone. The Purcell Limestone within the **Marcellus** Formation (normally 16 feet thick) has been thickened in places along such zones to over 70 feet by folding and faulting. Similar increased thickness of the Purcell limestone has been inferred from cuttings from water wells drilled along such zones (Dove, oral communication 1979). In more competent units, offsets of as much as 100 feet were observed. Often, however, faulting was inferred on the basis of alignments of dip reversals along with the presence of slickensided zones over considerable distances. Thus, the faults represented on the geologic map (Figure 3) are distinct structural elements within exposed formations mapped in the area.

Although the amount of displacement along any one fault is not precisely known, the presence of considerable structural deformation aligned with local structural trends is clear.

The presence of increased numbers of faults coincides with a 2,800-foot northward drop in the level of the Lower Devonian Oriskany Sandstone between cross sections CC' to the south (Figures 3 and 4) and PA' to the north (Figures 3 and 6. The geometry of the Elkhorn-Middle Mountain structural complex undergoes considerable change across this area. In the central part of the map area (Figure 3 and Figure 5), the Elkhorn Mountain anticline is very much like an anticlinorium containing several smaller-order (Nickelson, 1964) 2,000-foot wavelength folds. In the south, the Elkhorn Mountain anticline is faulted (Figure 4) and some short-wavelength folds are present, but to a lesser extent than in the central part of the map area. In the northern part of the map area, the anticline is apparently unfaulted, and short-wavelength folds are less numerous (Figure 6). The Middle Mountain syncline within this faulted zone is nearly flat-bottomed, (Figures 4 and 5) with one 200- to 400-foot amplitude fold present in the Lower Devonian and Silurian formations. North of this zone (Figure 6), in the syncline beds plunge to deeper structural levels and the fold becomes more cylindrical in

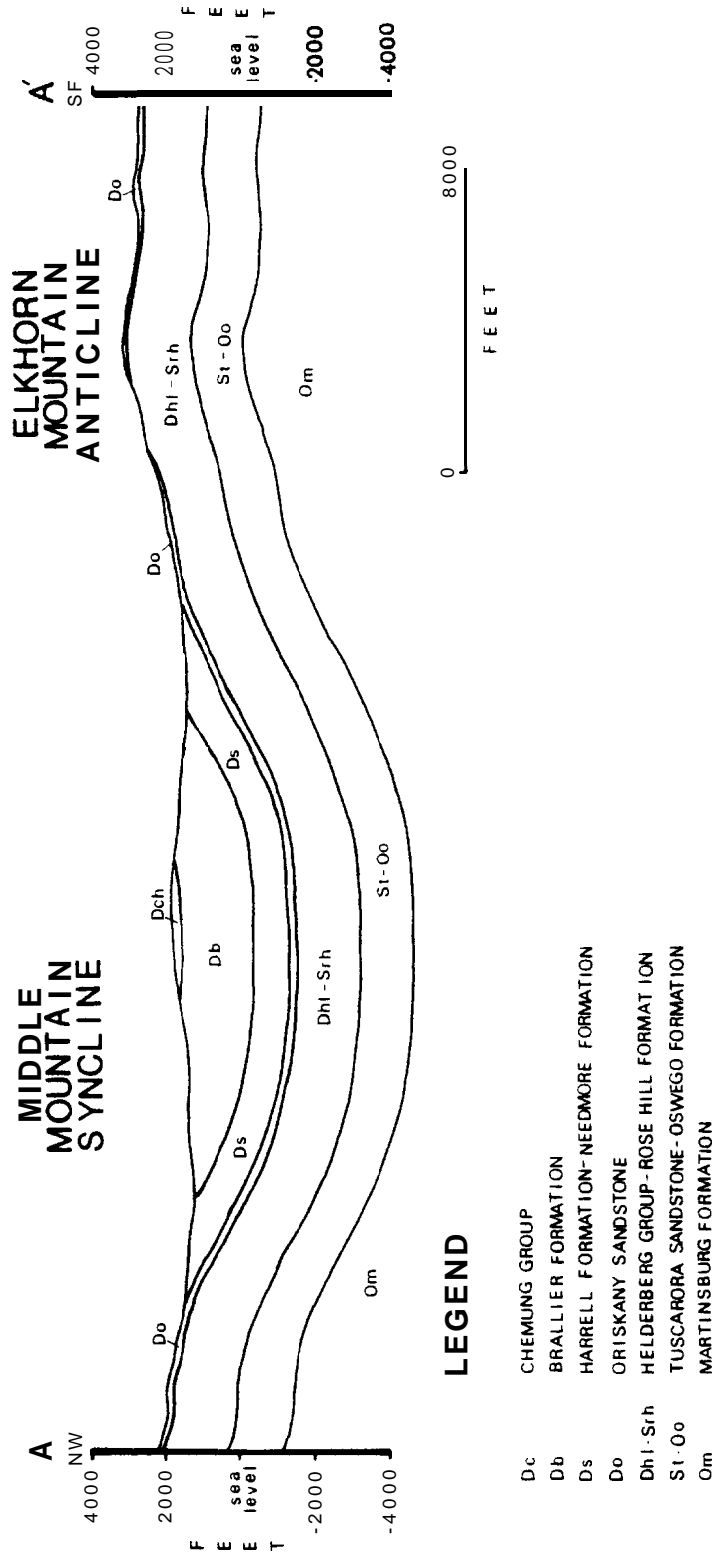


Figure 6 Cross Section A-A' Across the Middle Mountain Syncline and Elkhorn Mountain Anticline

cross section. The amplitude of the **Elkhorn Mountain anticline** at the base of the Ordovician Oswego Formation is 4,400 feet in section AA' north of the faulted zone. To the south in sections BB' and CC', the amplitudes are 2,800 and 3,000 feet, respectively. Shortening of section AA' along the base of the Ordovician Oswego Formation and the Silurian Tuscarora Sandstone is approximately 4 percent, or 1,500 feet. Shortening of sections BB' and CC' is approximately 5 percent, or 2,000 feet. Relationships between shortening in these sections is discussed further in section A.6 of this chapter.

#### 5. The Petersburg CSD

Partial mapping of the region between section AA' and the Petersburg area to the north (Figure 2) found no significant faulting or disruption of exposed Devonian formations. Some faulting may be present in Silurian and Devonian rocks across the **Elkhorn Mountain anticline** (see section NY', Plate 1). Cross section AA' and section NN' just 7 miles north of it are almost identical in profile. Sites' (1978) section CC' indicates that the Devonian and Silurian formations again rise toward the surface under the Middle Mountain **syncline** in the vicinity of the Petersburg CSD. Across and north of the Petersburg CSD, Silurian and Devonian formations maintain their structural level, with a gradual drop in structural level occurring

farther to the north beneath the Clearville **syncline** (see the longitudinal section LL' on Plate 3). The geologic map along the Petersburg discontinuity presented in Sites (1978, Plage 3) indicates that thrust faults in Devonian and Silurian formations become more numerous within the Petersburg CSD than north or south of the discontinuity.

#### 6. The Valley and Ridge Extension of the Parsons CSD

The proposed extension of the Parsons CSD coincides with a zone in the Middle Mountain **syncline** and Elkhorn Mountain **anticline** across which Devonian and Silurian formations plunge northeastward 2,800 feet in structural level. Thrust faults are more numerous within this zone. Some of these thrusts were observed to transfer displacement into the Middle Devonian shales of the **syncline**, thickening those shales by two to three times their normal thickness. These interruptions in longitudinal structure are almost identical to those across the Petersburg CSD to the north and the Parsons CSD northwest in the Plateau. Hence, the alignment of interruptions in structure in the Middle Mountain **syncline** and Elkhorn Mountain anticline with interruptions along other Valley and Ridge structures along an extension of the Parsons CSD of the Plateau implies a continuation of that discontinuity into the Valley and Ridge province.

South of section CC' of this study (Figures 3 and 4), structural features are inferred entirely from Tilton, Prouty, and Price (1927) and Cardwell, et al (1968) and are illustrated in cross sections LL' and SS (Plates 1 and 3). The Devonian and Silurian formations maintain their structural level to the south (longitudinal section LL'). These formations are folded into one-mile-wavelength folds for which some detachment-related faulting can be inferred (see section SS', Plate 1).

Although the amplitude of the Elkhorn-Middle Mountain fold pair is less in sections BB' and CC' (Figures 5 and 4), the total shortening across the structure is approximately the same to within a percent and possibly greater than the shortening across section AA' (Figure 6) to the north (section A.4 of this chapter). Thus, structural shortening of Devonian and Silurian rocks in sections BB' and CC', within and south of the Parsons CSD, is accomplished not only by the 2,800- to 3,000-foot amplitude Elkhorn-Middle Mountain fold pair but also from numerous faults and smaller folds within the structure.

The structural discontinuity, then, represents a zone across which there is a transition in the types and geometries of structures producing structural shortening. A structural model explaining the surface and inferred subsurface structural features of both the Parsons and the

Petersburg CSD's will be proposed in Chapter IV.

B. Systematic Jointing  
in the Middle Mountain Syncline

1. Introduction

Holland and Wheeler (1977) presented results from a study of systematic jointing across the Parsons CSD in the Appalachian Plateau which indicate that rocks within the discontinuity are more intensely jointed than rocks outside the discontinuity. Several interval-scale variables along with joint orientation, were measured to quantify the size of a joint and the relationships between joints. **LaCaze** (1978) reported smaller spacings for systematic joints in the Petersburg CSD than outside the discontinuity along the Allegheny structural front. A method for estimating fracture intensity developed by **Vialon** and others (1976) was modified by **Wheeler** (1979) for use as an estimate of systematic joint intensity. Analysis of **LaCaze's** (1978) data by **Wheeler** and **Dixon** (1980) indicates that joint intensity increases within the Petersburg CSD. Subsequent and more extensive observations of systematic jointing along the Parsons CSD in the Plateau and across the Petersburg CSD where it crosses the structural front confirm that these discontinuities contain more intensely jointed rock (**Dixon**, 1979).

Devonian shale gas production is, to a large extent, controlled by fracture permeability (Hunter and Young, 1953; Shumaker, 1976, 1978; Larese and Heald, 1977; **Schaeffer**, 1979). Shumaker (1978, p. 361) points out that:

We need to understand the type, orientation, and origin of the fractures responsible for gas production from the shale. If we do not document these characteristics we will surely find it difficult to predict their extent and locations, and, therefore, the extent and locations of production.

Shumaker (1978) uses the term "porous fracture **facies**" to describe the limited stratigraphic extent of **production-related** fracture permeability. Shumaker (1978, p. 362) suggests:

... that at least part and possibly all of the fractures responsible for shale gas production in eastern Kentucky and southwestern West Virginia were caused by minor tectonic transport and/or differential shortening within and above an ancient high-pressure detachment zone in the basal Devonian shales of the "undeformed" Appalachian foreland.

A thrust fault is more likely to flatten out as it propagates into a weak layer, although higher-angle faulting is possible (Rodgers and Rizer, **1979a**, 1979b). As the fault propagates into the weak layer, secondary structures and fractures will remain in the region initially near the fault tip after the fault tip has propagated out of that region (Rodgers and Rizer, **1979a**, 1979b; D. Rodgers, oral communication, 1979). Relic



secondary faults observed in the Upper Devonian Lower Huron Shale member of the Ohio Shale Formation were used to identify the interval of detachment in the Pine Mountain thrust sheet (Wilson, et al, 1978). An increased intensity of jointing was also observed in the interval of detachment (Wilson, et al, 1978). Secondary faulting will also deform the area in advance of the leading edge of a thrust fault (Anderson, 1951; Hafner, 1951; Chinnery, 1966; Rodgers and Rizer, 1979). Northwest-trending slickenlines observed in the Brown shales of the Nicholas Combs No. 7239 core (Kulander, Dean, and Barton, 1977) and slickenlines observed in the Martin County core were explained in this way (Wilson, et al, 1978) and were suggested to represent the porous fracture facies discussed by Shumaker (1978). Deformation domains defined by Wilson (1979) illustrate the stratigraphic confines of detachment-related deformation in the Middle Mountain syncline. Specifically, the Devonian Needmore Shale and Marcellus, and Mahantango Formations are intensely disrupted by numerous folds and faults that are secondary to splay thrusts that cut brittle Devonian and Silurian formations and transfer slip from the Ordovician Martinsburg Formation into the Middle Devonian shales (section A of this chapter). A sharp decrease in amount of such nearly penetrative deformation occurs across the Devonian Harrell Shale into the lower part of

the Brallier Formation, indicating that deformation is largely confined to the ductile and less competent Middle Devonian shales.

As noted earlier, subsurface structure beneath low Plateau folds is considerably more complex than that at the surface (Cwinn, 1964). Deformation of the shales exposed in the Middle Mountain **syncline** will be comparable in degree to deformation of the shales above faulted and folded Devonian Onondaga Limestone and beneath the much less intensely deformed Carboniferous rocks exposed in the Plateau. Thus, the deformed Middle Devonian shales in the Middle Mountain **syncline** represent an exposed **analogue** of a possible subsurface fractured gas reservoir.

The remaining sections of this chapter document the characteristics of systematic jointing observed in the shales of the syncline. Perhaps observations of joint orientation, joint intensity, and the relationships of joint orientation and intensity (surface area of joints per unit volume of rock) to the various structural elements in the **syncline** will lead us to a better understanding of their origin, and thus allow us to predict the extent and location of fracture-controlled production, as Shumaker (1978) suggests.

A brief discussion of rotated joints using equal area projections is presented in **Appendix IA** along with

a complete listing of joint strikes and dips in rotated and unrotated beds. Joint **spacing** and the calculation of joint intensity and other quantities used in the documentation of joint intensity are discussed in Appendix IIA. Complete lists of measured spacings and calculated intensities are provided in Appendixes IIB and IIC.

## 2. Characteristics of Systematic Jointing in the Middle Mountain Syncline

a. Discussion. As discussed in section A of this chapter, the Parsons CSD across the Elkhorn-Middle Mountain fold pair is related to specific structures observed in the field or inferred from mapping. Because of the relationships of rock failure to applied and internal stresses and to lithology, the joint orientation, spacing, and intensity data collected in the Middle Mountain **syncline** are displayed at each station location on the geologic map of that structure (Figures 7, 8, and 9). The equal area projections of rotated and unrotated joints were too cumbersome to represent on the **geologic** map, and so are presented as a series of figures in Appendix IB.

Joint strikes plotted in the roses (Figure 7) are the unrotated orientations measured directly from the folded and faulted rocks exposed in the map area. The interpretation of this type of data is considered to be a complex problem in itself. The question of timing of

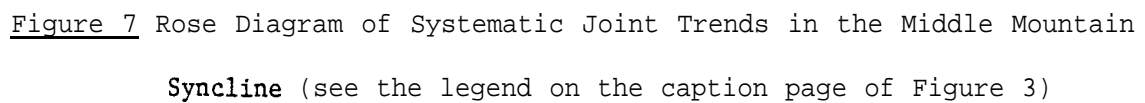


Figure 8

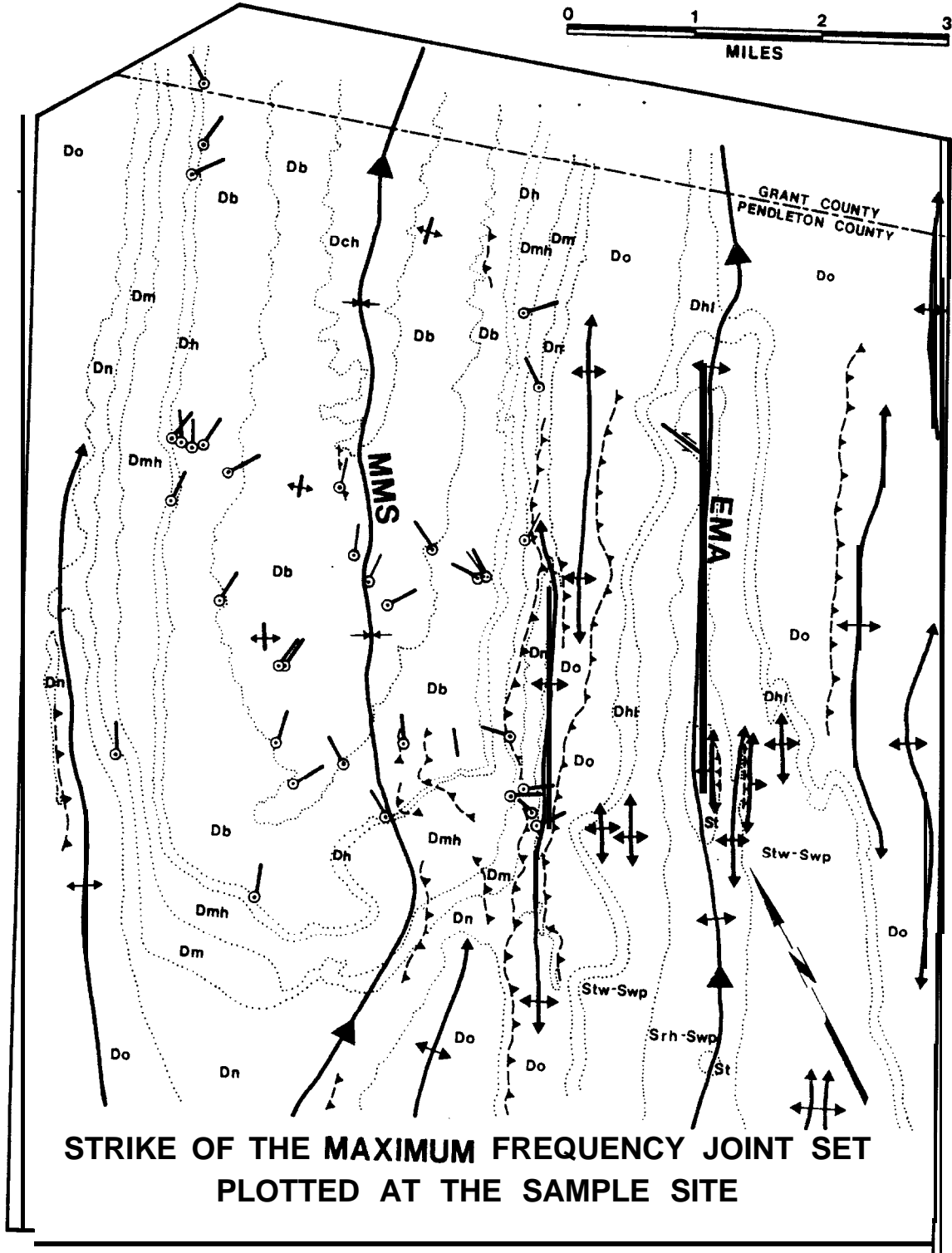
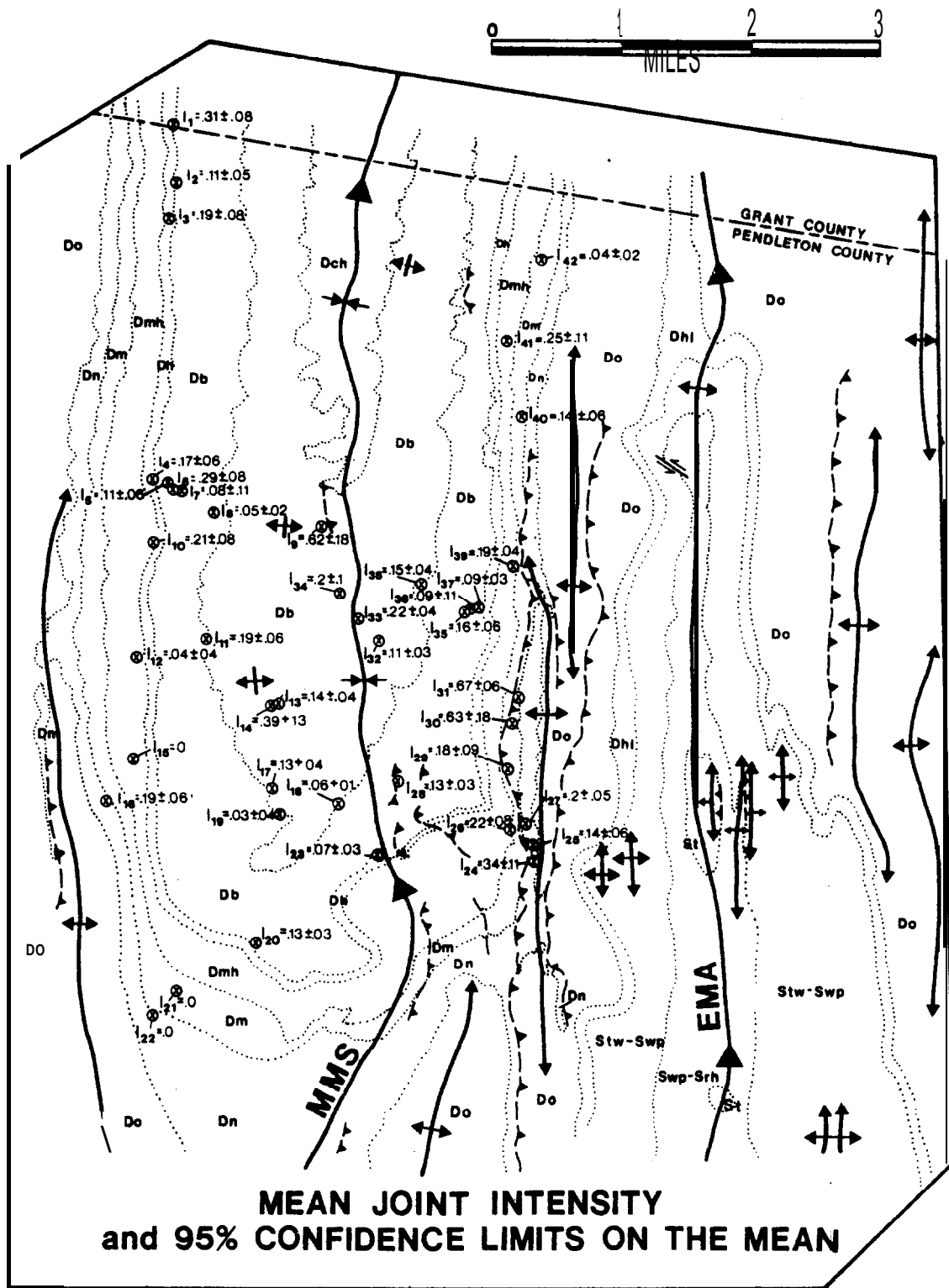


Figure 9



fracture development needs to be considered before rose plots of joint strike can be interpreted in a meaningful way. If, for instance, the development of systematic joints in a specified volume of rock occurred early in an elastic prefolding phase of brittle deformation, subsequent folding and faulting of that rock volume will probably scatter the observed strikes into an obscure pattern. Variations in the rate of sea floor spreading inferred from paleomagnetic data (Girdler, 1979) suggest that similar variations in strain rate can be expected to occur at convergent plate boundaries. Thus, a volume of rock deformed during orogenesis may experience brittle deformation at intervals throughout a particular deformational event. Indeed, the stress field at any particular instant, in a buckling layer, is quite complex (Dietrich, 1969). In effect, the patterns observed in rose plots of joint strike (Figure 7), or equal area projections of poles to joint surfaces (Appendix IB) can be and probably are complicated by several factors, particularly in structurally complex areas.

B. Kulander (oral communication, 1978) and Ii. Wheeler (oral communication, 1979) have suggested that fracture development can be dated by comparing the scatter in clusters formed on equal area projections of poles to

systematic joints in deformed beds to the scatter in clusters of poles formed by those same joints rotated back to their pre-deformational horizontal orientation. If there is greater scatter in joint orientations in the horizontal or rotated bedding, then the joints are assumed to be late or post-folding. If the converse is true, then joint formation is assumed to have occurred prior to folding in the flat-lying beds. This, however, restricts our timing to either before or early in the first episode of deformation, or late or following the last episode of deformation, and does not allow us to discriminate jointing that has developed at some intermediate stage, or between sets of systematic joints which may have developed at different times.

Timing the formation of systematic joints using this method is further restricted by the necessity of combining joint orientations from two or more exposures. An increase or decrease in the scatter among poles in normal or deformed bedding arises because the bedding at different exposures will undergo different amounts of rotation. Bedding orientation at a single exposure is commonly uniform throughout the exposure, so that angular relationships between poles to joints or any other planar or linear fabric elements are preserved. The question arises, then, of how to group the exposures for comparison.



Jointing along the hinge of a fold may precede or follow the development of joints on the limbs of the fold or those along a nearby fault. Thus, groupings for this study were chosen on the basis of common relationship to the-major structural elements in the map area and to lithology (see footnotes to Tables 8 through 16, Appendix IB, and Figure 10).

The question of timing in the formation of systematic joints is important in the assessment of whether an area will have a productive fractured gas reservoir or not. If jointing in an area occurred early in a deformational event, gas may have migrated rapidly to neighboring structural or stratigraphic traps or have been lost from the section entirely. If, however, jointing occurs late and is confined in extent, the conditions may be favorable for both reservoir formation and reservoir sealing.

In the preceding discussion, we have been concerned with the relative timing of joint formation to the development of folds and faults. It should be noted that relative ages or the sequence of formation of systematic joint sets in any given exposure can be established through observation of cross-cutting and abutting and other relationships (see Kulaner, Dean, and Barton, 1977; and Kulander, Barton and Dean, 1979). The cross-cutting and abutting relationships between joint sets have not been considered in this

study.

b. Joint development relative to folds and faults.

Systematic joints examined in the study area have been divided into nine groups on the basis of their structural location within the Middle Mountain syncline. The stations comprising each group and their relation to local structure are defined in Appendix IB, with Tables 8 through 16 (see also Figure 10).

Several problems are encountered in the evaluation of relative amounts of scatter among rotated and unrotated poles to joint surfaces plotted on equal area nets. As discussed in the previous section, angular relationships between joint surfaces measured in uniformly dipping bedding are preserved with respect to rotation of the bedding. However, in group 1, whose joints come from the same exposure, poles forming the unrotated cluster pole at N12E/02SW have a standard deviation more than four times as great as for those poles from the same cluster (N51E/07SW) in rotated beds. This indicates that considerable error can be introduced from hand-plotting and hand-rotating processes alone. In the future, useful statistical analysis of these data will require the use of computer-assisted methods to determine pole orientation, the angular relationships between poles and the positions of rotated poles.

The locations of cluster centers from all groups



were estimated by eye in both rotated and unrotated projections. The standard deviations of angles between individual poles and their cluster center was calculated for clusters identified in the rotated and **unrotated equal** area projections for each group. The center of a cluster or cluster pole, the standard deviation of the poles within a cluster about the cluster pole, and the number of poles in a cluster, are tabulated in Appendix IB, Tables 8 through 16. Inspection of the standard deviations (scatter) of poles about cluster centers indicates that few, if any, statistical differences are likely to exist between standard deviations of poles in rotated and unrotated clusters.

Hence the question of timing in the formation of systematic joints relative to the development of folds and faults remains unanswered by this method.

c. Joint intensity and spacing relative to folds and faults. Joint intensity is the amount of joint surface area per unit volume of rock in an exposure (Wheeler and Dixon, 1980). The calculation of joint intensity using pseudovalues (R. Wheeler, oral communications, 1979 and 1980) is explained in Appendix IIA. The study area was divided into nine structural and lithologic divisions (Figure 10). The average intensities for the stations within each of these nine divisions are tabulated in Appendix IID.

Examination of Appendix IID indicates that **statis-**

tically significant differences ( $p \leq .05$ ) occur only between the average intensity of systematic jointing for group 6 and groups 1-2, 3, 5, and 7. Group 6 is comprised of these stations within the intensely folded and faulted Middle Devonian shales exposed on the southeast limb of the Middle Mountain **syncline** (Figure 10). In each case, the intensity of group 6 is greater. Differences did not exist between group 6 and groups 4, 8, and 9. Group 4 is comprised of a single station (station 9, see Figure 10). A low-angle thrust fault with 80 to 100 feet to displacement cuts through this exposure in the Devonian Brallier Formation along the axis of the Middle Mountain **syncline**. Group 8 includes those stations on the northwest limb of the Middle Mountain **syncline** and north of the intensely deformed area (group 6) on the **syncline's** southeast limb. Group 9 includes those stations on the southeast limb of the **syncline** north of the deformed area covered by group 6. Although no faulting was observed in the areas covered by groups 8 and 9, high standard deviations of bedding dip (Wilson, 1979) indicate that bedding in these areas is disrupted. Rock flexures unobserved at outcrop scale produce this disruption in bedding dip.

These differences suggest what is perhaps the obvious -- more folded and more faulted rocks are more intensely jointed than less-folded and less-faulted rocks.

As indicated earlier (section A of this chapter), the zone of structural discontinuity across the Middle Mountain **syncline** contains more intensely folded and faulted rocks. Thus, the structural discontinuity will contain larger volumes of more intensely jointed rock.

On Plate III, the strike of the maximum frequency (minimum spacing) set from each exposure has been indicated. Inspection of the map indicates that transverse (northwest-striking) joints are generally more closely spaced in faulted rock. There is considerable variety in the orientations of maximum frequency sets elsewhere in the study area however, the longitudinal (northwest-striking) set is most common and the transverse set least common.

The orientations of maximum frequency joint sets suggest that minimum effective stress during jointing was parallel to strike in the reverse faulted and folded Middle Devonian shales on the southeast limb of the Middle Mountain syncline, particularly within the Parsons CSD, producing localized transverse joints. Throughout the rest of the area, minimum effective stress was at high angles to strike, producing pervasive longitudinal joints. Dixon (1980) also notes that the most intense sets are in and parallel to a structural discontinuity.

Berger and Johnson (1980) show that fold asymmetry can be produced by buckling, splay faulting, or drag along

a ramp where movement **along** the ramp either does not occur. **or**, if it does, it follows the development of the fold. This seems reasonable, because if the shear strength of a rock layer is exceeded early during folding, continued shortening is likely to occur by translation along the plane of weakness represented by the fault, rather than by folding. Their solution is for a viscous isotropic **semi**-infinite halfspace. Deformation of a sequence of brittle layers between ductile detachment intervals is likely to be more complex (see Chapter III, section B, on structural lithic units). However, it seems likely that when movement along a ramp through a brittle sequence of layers is transferred to slip within an overlying ductile detachment interval, folding of the hanging wall rocks will terminate. It is suggested, then, that intense jointing, specifically the closely spaced transverse joint sets related to faults in Middle Devonian shales, developed after folding. Jointing of the surrounding unfaulted Middle Devonian shales and the overlying Brallier Formation is less intense than in the faulted shales and may provide a seal to the **fault**-related fracture porosity. However, along strike, faulted northwest limbs of anticlines will permit migration of fluids to structurally higher positions within the faulted shale.

### C. Conclusions

The extension of the Parsons cross-strike structural discontinuity into Valley and Ridge structures (Wheeler, 1978) is thought to be valid. The zone of structural discontinuity present across the Middle Mountain **syncline** and **Elkhorn** Mountain anticline is expressed in the following ways. The structural level of the Lower Devonian Oriskany Sandstone drops 2,800 feet to the northeast across the discontinuity. Structural shortening south of the discontinuity is achieved by more abundant, higher-order (smaller) structures than those to the north of the discontinuity. Structural shortening within the discontinuity is taken up by more abundant, higher-order structures than those formed either north or south of the discontinuity. Rocks within the discontinuity are more intensely faulted, and folds are more numerous and have smaller wavelengths and amplitudes than folds north or south of the discontinuity. In addition, joint intensity studies show that the Parsons CSD in the Middle Mountain **syncline** is a zone of greater joint intensity because it is also a zone of more intensely deformed rocks. Fault-related jointing appears to have developed late in the folding process.



### III. SUBSURFACE STRUCTURAL INTERPRETATIONS

#### A. Introduction

Several theories and observations have been made concerning the origins of structural discontinuities. Transverse steps and transcurrent faults between decollement horizons were first postulated as a source for higher-level fold terminations by Wilson and Sterns (1958) for the Cumberland Plateau, later by Rodgers (1963). Cwinn (1964), and Harris (1970) for the central and southern Appalachians, and by Dahlstrom (1970) for the Canadian Rockies. The localization of discontinuities has, in some cases, been related to recurrent movement along basement-controlled faults (Price and Kluwer, 1974; Price and Lis, 1975; Lis and Price, 1976; Benvenuto and Price, 1970; Drahovzal, 1974; Home, 1975, 1971a, 1975b, 1976a, 1976b; Price, 1975; R. Wheeler, 1978, and oral communications, 1978, 1980; W. Perry, oral communication, 1980). Sedimentary facies and thickness changes have similarly been suggested to have a genetic relationship to discontinuity formation by Trumbo (1976) and Sites (1978). R. Wheeler (oral communication, 1980) has observed a statistically significant relationship between pinchouts in several Middle Devonian members and location within a discontinuity. Variations in the timing of plate collision and the northeastward deepening

of the basin may also be related to development of discontinuities in the central Appalachians (B. Kulander, oral communication, 1978); R. Shumaker, oral communication, 1979). Hence, what we know of structural discontinuities thus far suggests that a variety of factors are likely to be important in the development of any one structural discontinuity.

It is the intent of this chapter to describe surface and subsurface structural characteristics in the central Appalachians of West Virginia and to suggest an explanation for the origins of the Parsons and Petersburg CSD's.

## B. Regional Cross Sections

### 1. Construction

#### a. Surface structure and stratigraphic thicknesses.

Surface structure and stratigraphic thickness estimates are taken almost entirely from the mapped surface structure and measured sections presented in the West Virginia and Virginia County Reports. Unit contacts and surface relief were taken directly from the maps presented with these reports. Average thicknesses were calculated (when possible) from the reported measured sections at the surface along with subsurface information from oil and gas wells that often penetrated the Devonian Catskill Formation. A complete tabulation of average stratigraphic thickness is presented for counties through which the section lines pass in Appendix IIIA. Depths to the top of the Big Lime

(Greenbrier Limestone) in Tyler, Wetzel, and Marshall counties, West Virginia, are taken from Cardwell (1978). Dudley Cardwell has compiled information from available well data on depths to the top of the Onondaga (Cardwell, 1974) and depths to the top of the Ordovician and Precambrian (Cardwell, 1977) for the state of West Virginia. Wells projected onto sections NN' and SS' are located in Appendix IIIB, Figure 45. Additional information on the thicknesses of Silurian through Cambrian formations is presented by Chen (1977). Perry (1964) reports on thicknesses of Ordovician and Cambrian formations penetrated by Consolidated Gas Company's No. 1 Ray-Sponaugle well. Thicknesses from these sources, but largely from Cardwell (1977), are presented as a fence diagram for Cambrian to Middle Devonian structural lithic units in Appendix IIIC (Figure 48). A fence diagram for thicknesses of Middle Devonian through Mississippian formations is also presented in Appendix IIIC (Figure 47).

b. Structural lithic- units. The cross sectional representation of a structural lithic unit (a sequence of rock units having similar mechanical properties [Currie, Patnode, and Trump, 1962]) must be consistent with observed or inferred features of similarly deformed sequences of rock units. Structural lithic units used in these cross sections are defined according to their potential to form

major decollement intervals.

Any relatively more viscous or soft unit appears to have the potential to serve as a decollement horizon. Decollements have been observed in the following units: Pennsylvanian coal seams (Staub, 1979); the Devonian Bral-lier Formation (Wilson, unpublished results) the Devonian Brown shales (Wilson, et al, 1978; Evans, 1979); the Silurian Salina Group (Woodward, 1959; Gwinn, 1964); and the Ordovician Martinsburg and Cambrian Waynesboro For-mations (Gwinn, 1964; Perry, 1971, 1975, 1978; Sites, 1978; Bagnall, Beardsley, and Drabish, 1979; Jacobeen and Kanes, 1974, 1975). Intervening intervals, those relatively more competent, or stiff, sequences of rock units within which the formation of decollement surfaces is of minor importance, form a second group of structural lithic units. The structural lithic divisions of the Paleozoic sedimen-tary cover used for the cross sections presented here are listed in Table 1.

# STRUCTURAL LITHIC UNITS

Age	Name*	Mechanical Behavior
Pennsylvanian	Monongahela Group Conemaugh Group Allegheny Formation	
Mississippian	<b>Mauch</b> Chunk Group Greenbrier Group Pocono Group	stiff
Devonian	Hampshire Formation Chemung Group Brallier Formation	
	Harrell Shale Manhantango Formation Marcellus Formation <b>Needmore</b> Shale	soft
	Oriskany Sandstone Helderberg Group Tonoloway Formation Wills Creek Formation** Williamsport Formation McKenzie Formation Clinton Group Tuscarora Sandstone	stiff
Ordovician	Juniata Formation Oswego Formation	
	Martinsburg Formation	soft
	Trenton Group Black River Group St. Paul Group Beekmantown Group	stiff
Cambrian	Conococheague Formation Elbrook Formation	
	Lower Cambrian and Basement Rocks	stiff

TABLE 1

\*Group and formation names are taken from  
Cardwell, et al (1968)

\*\*The Wills Creek formation is the equivalent of the Salina of the Plateau. Detachment within the Salina is extensive throughout the Plateau (Gwinn, 1964; Woodward, 1959). The Wills Creek is considered a ductile structural lithic unit in the Plateau portions of the regional cross sections. Bagnall, Beardsley, and Drabish (1979) report the occurrence of detachment within the Wills Creek Formation on the northwest limb of the Wills Mountain anticline near Reyer, West Virginia.

†Bagnall, Beardsley, and Drabish (1979) also report detachment occurring in the Juniata shales.

c. Stiff structural lithic units. Sequences of formations comprising a stiff structural lithic unit are assumed to have a constant thickness in cross section normal to the boundaries of the sequence. Ideally, constant normal thickness can be maintained during folding if the fold develops by layer-parallel **flexural** slip (Donath and Parker, 1964) between individual layers within the sequence. Chapple and **Spang** (1974) noted the importance of layer-parallel slip to the development of folds in the Greenport Center **syncline** in southeastern New York. This type of fold may be concentric or parallel in cross section and may become chevron-like at depth (**Ramberg**, 1963). Johnson and Page (1976) and Johnson (1977) observed this characteristic in the folds of the **Huasna syncline** in the Coast Ranges near San Luis Obispo, California.

Johnson and Page (1976) and Johnson (1977) note that although visible evidence of **interbed** slip is conspicuously absent between most of the strata, folding developed primarily by layer-parallel slip between structural layers much larger than individual lithologic layers in the sequence. The theoretical model of Chapple and **Spang** (1974) predicts accommodation of folding by layer-parallel slip at widely spaced intervals.

The concentric to chevron-form folding is also commonly observed in the Juras and Canadian Rockies, par-

ticularly in rocks deformed above detachment intervals (Spencer, 1969).

Shear within less competent layers of the sequence may produce some thinning in the limbs and thickening of hinges in the folded sequence. Also, pressure solution, particularly in the Cambrian-Ordovician sequence of dolomites and limestones, is likely to produce thinning of fold limbs and, hence, apparent thickening of fold hinges during fold development. Hence, the above assumption provides us with only an approximation to the actual form of a folded stiff structural lithic unit. Small faulting, wedging and jointing will produce further divergence of reality from the model.

The assumption of layer-parallel slip as the dominant process in the development of folds in sequences of stiff units leads to another constraint on the cross sectional representation of deformation in a stiff sequence. The Panther Creek and Turner Valley sections of Dahlstrom (1969 and 1970) indicate that displacement along ramping reverse faults decreases up the ramp and that shortening: higher up the ramp is accomplished by increasing amounts of folding. Dahlstrom (1969, p. 747) points out the following:

The Turner Valley cross section is based on good well, seismic, and surface geological control. It shows remarkable change from more than 2 miles (3.2 km) of fault displacement at depth to virtually none at the



surface and the accommodations of this change by folding.

As mentioned in Chapter 11 (p.40 ) Berger and Johnson (1980) indicate that drag along a ramp is not necessary to fold formation and that, in fact, the fold above a ramp develops prior to the formation of the ramp. The process of fold development by layer-parallel slip implies that within a stiff structural lithic unit, layer-parallel slip increases from bottom to top through a sequence of structural layers in the unit producing increasing amounts of shortening by folding toward the top of the unit. Dahlstrom (1969, p. 747) indicates:

2. **Interbed** slippage is a necessary part of the thrust faulting process just as it is in concentric folding;
3. **Interbed** slippage can contribute to the change of displacement along a fault and, in extreme instances, could become a species of imbrication.

The cross-sectional representation of stiff units will be consistent with the above observations and theoretical behavior if we impose the constraint that the length of the cut on the hanging wall of the ramp be less than the length of the cut along the footwall. in addition to the requirement that total shortening along the top and bottom of the stiff unit be equal. This requires that layers at the bottom of a stiff structural-lithic unit be less folded and have greater displacement along the ramp than layers higher in the unit.

The constraint that the cross-sectional lengths along the top and bottom of a given stiff structural-lithic unit be equal, refers to total length across the basin (or as much of it as possible) and not to individual thrust slices. The reason for this constraint is to insure that unit volume after deformation equals that before deformation.

d. Soft structural lithic units. Deformation of soft structural lithic units is characterized by a more viscous behavior in the cross sections presented in Plate V. Field examination of the Middle Devonian shales (a soft structural lithic unit) reveals that the unit is not deformed by continuous flow but by considerable folding, faulting, jointing, and, to some extent, by solution cleavage (see Chapter II). Much of this folding, faulting, and jointing was associated with thrust faults ramping through the underlying Silurian and Devonian formations into the Middle Devonian shales. Similar behavior is inferred from gravity data for the Ordovician Martinsburg Formation in the faulted and folded subsurface of the Valley and Ridge province (Chapter IV). The thickening of soft units in areas where slip has been transferred from one detachment horizon to another is also supported by Bagnall, Reardsley and Drabish (1979). In addition, the more viscous behavior of a soft structural lithic unit is represented in cross

section by thickening the unit in the hinges of folds and thinning the unit on the limbs of folds.

e. Descriptions of the sections. The regional structural cross sections constructed for this study are displayed on Plates 1, 2 and 3. The individual sections are located in Figure 11. They consist of two cross sections north (NW') and south (SS') of the Parsons CSD (Plate 1) and extend from the Blue Ridge Front across the Valley and Ridge, and Plateau provinces to the West Virginia-Ohio border. Jacobeen's and Kanes' (1974) section has been redrawn and included as section JJ' to the north of the Parsons and Petersburg CSD's (Plate 2). The longitudinal section LL' extending along strike through Pendleton County, West Virginia into Mineral County, West Virginia across all three cross sections has also been included as Plate 3.

## 2. Valley and Ridge Structures.

There has been considerable dispute over the interpretation of Valley and Ridge structure presented by Jacobeen and Kanes (1974). Two possible interpretations of subsurface structure along their section line are presented below in Figures 12 and 13. Their interpretation (presented as JJ' Plate 2, and Figure 12) is considered valid for several reasons. First, their interpretation is based on seismic reflection data (see Jacobeen and

# LOCATIONS OF STRUCTURAL CROSS SECTIONS

## GEOLOGIC MAP OF WEST VIRGINIA WEST VIRGINIA GEOLOGICAL AND ECONOMIC SURVEY

Robert B. Erwin, State Geologist

1969

UGR File #498  
W.Va.Univ. Dept. of Geology & Geography  
December 1980

54

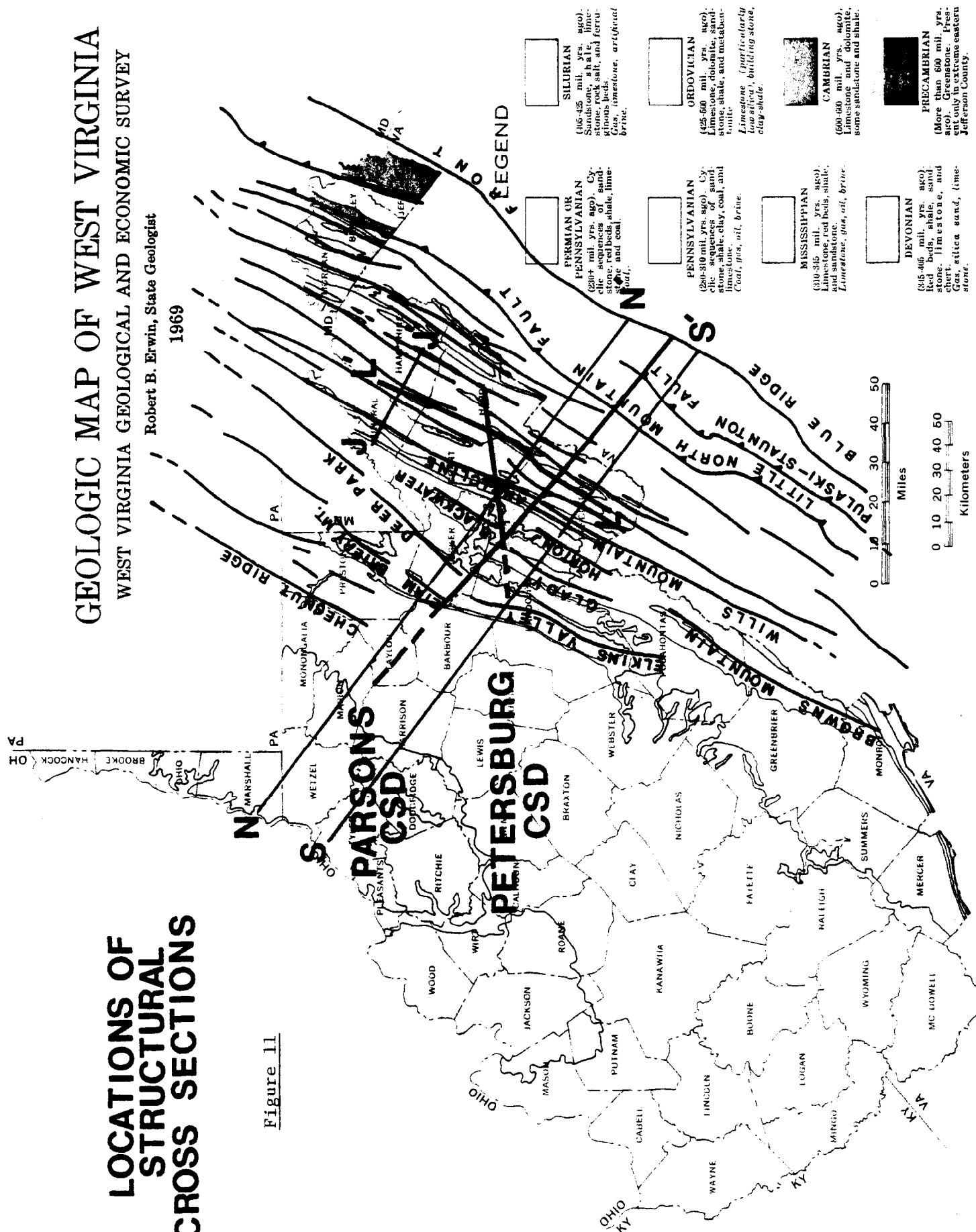


Figure 11

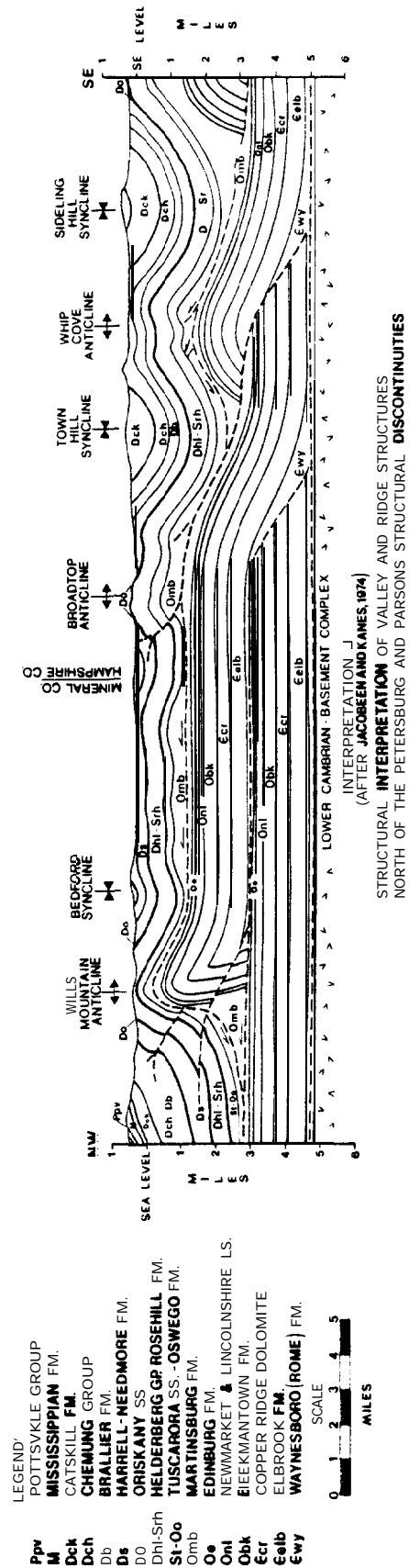


Figure 12

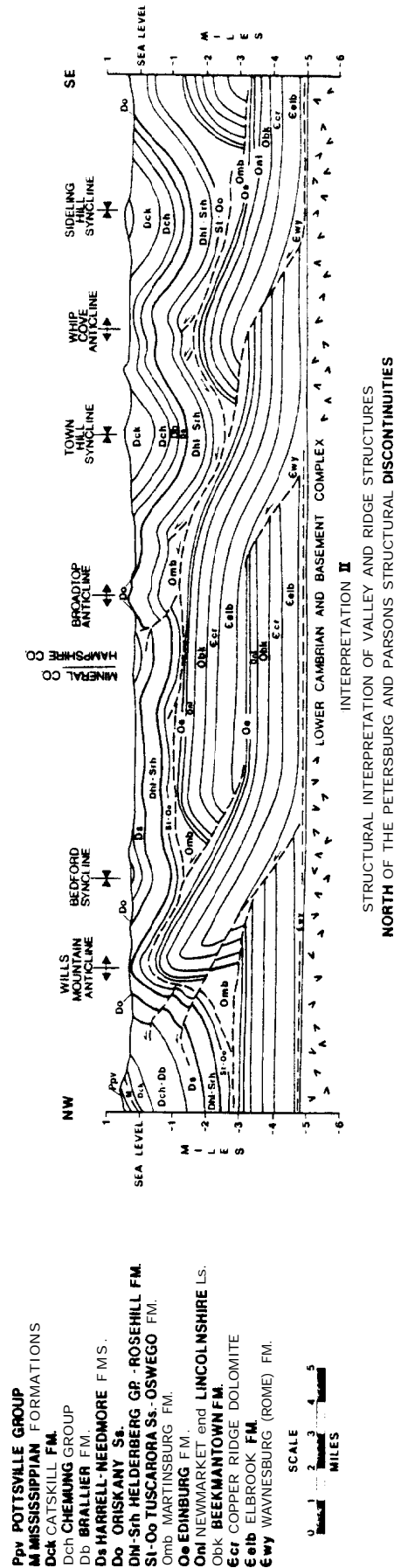


Figure 13

Kanes, 1974 and 1975) covering a large percentage of the area represented in cross section. Second, additional unpublished seismic data between the Roadtop and Wills Mountain anticlines favors their interpretation. Third, terrain-corrected Bouguer gravity from a survey along their section line run by R. Perkey (1980. oral communication) also supports their interpretation. Gravity models of both interpretations are presented in Chapter IV along with the implications of R. Perkey's (1980 oral communication) observations.

Interpretations of Valley and Ridge structure south of JJ' including the Elkhorn and Long Ridge anticlines and structures northwest to the structural front along the northwest limb of the Wills Mountain anticline are contained in sections NN' and SS' of Plate 1. The interpretations are similar to those presented by Perry (1971. 1978) and Jacobeen and Kanes (1975), both of which are supported by seismic data along or near the section line. Although there is general agreement that subsurface Cambrian and Ordovician structure across the area is represented by a series of imbrications of that brittle sequence there are some differences worth mentioning. In Perry (1971 and 1978) the length of the cut on the hanging wall is equal to the length of the cut on the footwall of major ramps through the Cambrian-Ordovician sequence. This implies

either that layer-parallel slip did not play a role in fault development and folding --contrary to observations of Chapple and Spang (1974), Johnson and Page (1976) and Johnson (1977)-- or if there was a layer-parallel slip, it occurred uniformly throughout the sequence --contrary to the observations of Dahlstrom (1969 and 1970) (see section c, chapter III). Also, in Perry's (1971 and 1978) cross sections through the area there is little or no thickening of the Ordovician Martinsburg (or Reedsville) Formation in front of splay thrusts through the Cambrian-Ordovician sequence and along which there is from one to three miles of displacement. This behavior for a relatively ductile unit disagrees with field observations presented in Chapter II, behavior inferred from a published seismic interpretation (Bagnall, Beardsley, and Drabish, 1979) and behavior inferred from a terrain-corrected Bouguer gravity profile surveyed across the Middle Mountain syncline (see Chapter IV). The cross sections of Jacobeen and Kanes (1975) represent only the gross outline of subsurface Cambrian-Ordovician structure, but generally agree with equivalent segments of sections NN' and SS'. Perry's sections disagree further with sections NN' and SS' and Jacobeen's and Kanes' sections through the area in that Perry has an additional fault slice between the Elkhorn or Long Ridge anticline and the Castle Mountain or Cave Mountain anticline. In Jacobeen's and Kanes'



sections and sections MN' and SS'(Plate 1) the Cambrian-Ordovician carbonates are faulted beneath the Wills Mountain anticline and the Elkhom or Long Ridge anticline with no indication of a fourth fault beneath the Middle Mountain syncline. Sites' (1978) section CC' agrees in many respects with Perry's sections. Sites' cross section is based in part on unpublished seismic sections (Sites, 1978, p. 123). Some of the features in his sections may only be apparent and related to thickening of the low velocity Martinsburg Formation. For example, in Sites' section CC' (see Figure 14) the Martinsburg Formation (1,700 feet thick) reaches a thickness of roughly 7,030 feet in the core of the Elkhom Mountain anticline. In addition, there is a **syncline** in the Cambrian-Ordovician **sequence** beneath a surface anticline in Silurian and Devonian formations. The Martinsburg shale beneath the Cave Mountain anticline is thickened to approximately 5,000 feet and the Cambrian-Ordovician sequence beneath is folded into a syncline. Considerable faulting mapped at the surface in Silurian and Devonian formations (Sites, 1971, 1975, and 1978) is related to detachment in the underlying Martinsburg Formation so that thickening of the Martinsburg is expected. If the added travel time through the thickened shale is not corrected for, the shale will appear anomalously thick and reflections from the top of the Cambrian-Ordovician

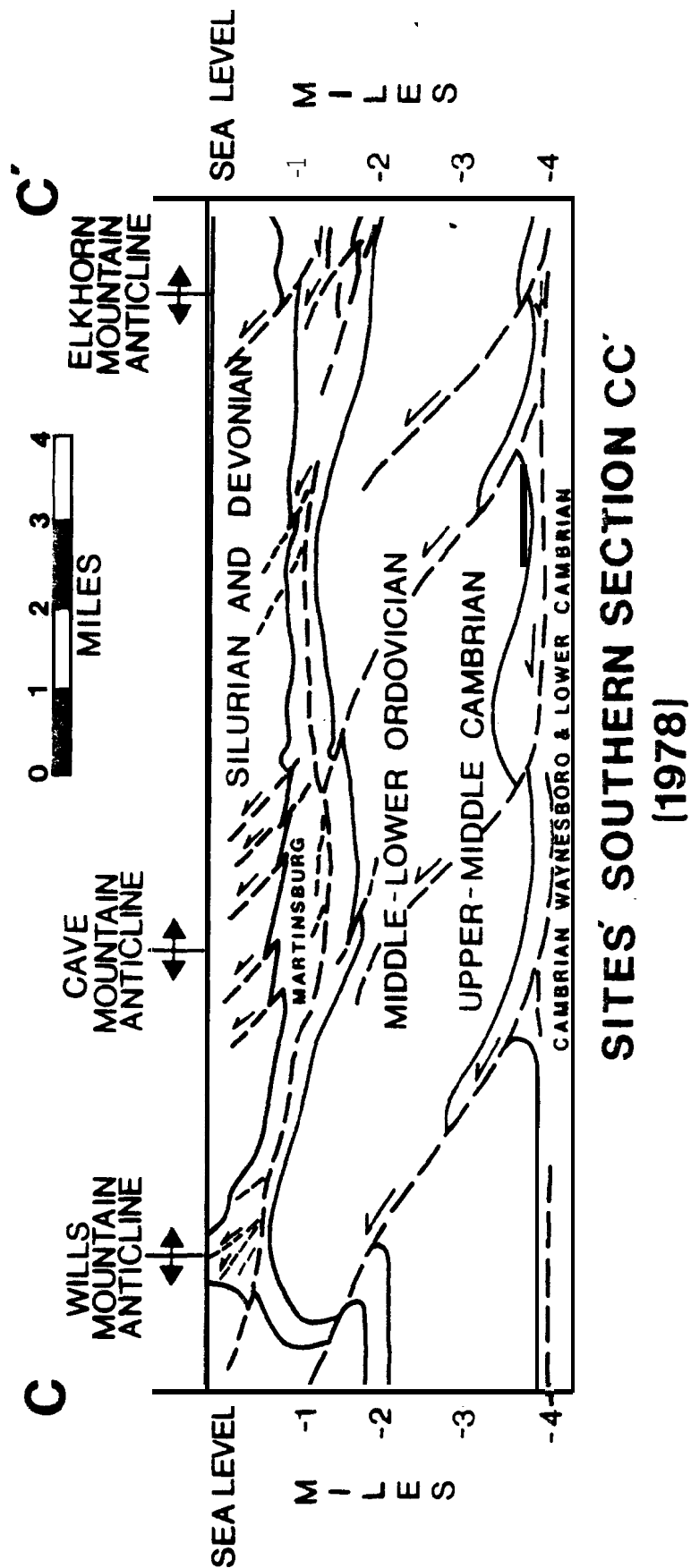


Figure 14 Sites' Structural Cross Section CC' across the Northeast Portion of the Valley and Ridge Province

dolomites and limestones will be delayed in time producing apparent synclines in that sequence. This problem is particularly evident beneath the Cave Mountain anticline where a **syncline** is portrayed in the hanging wall of the faulted Cambrian-Ordovician sequence.

Information presented in Perry (1963, 1971, 1978), Jacobeen and Kanes (1974 and 1975), Sites (1978) and Bagnall, Beardsley and Drabish (1979) are consistent in their interpretation that the Wills Mountain anticline is either wholly, or in part, due to thrusting of the Cambrian-Ordovician sequence over a ramp beneath the Broadtop anticline (Figure 12). Bagnall, Beardsley and Drabish (1979) present seismic evidence showing that the lower sheet of Cambrian-Ordovician rocks is cut and displaced slightly along ramps between the Cambrian Waynesboro Formation and the Ordovician Martinsburg Formation.

The longitudinal section LL' extends along the axis of the Middle Mountain **syncline** across the Parsons and Petersburg structural discontinuities and further to the northeast along the axis of the Clearville syncline. Basement depths calculated from seismic profiles at Cosner gap and further north at Keyser along the line of Jacobeen and Kanes were reported by R. Beardsley (1980, oral communication). The basement is represented by a straight line drawn through those depths. A double thickness of the

Cambrian-Ordovician sequence can be included across the line of **Jacobeen** and **Kanes** south beneath the Clearville **syncline** to the northern edge of the Petersburg CSD. South across the Petersburg CSD and Parsons CSD, it is not possible to include a double thickness of the Cambrian-Ordovician sequence because basement depths reported for this area (W. Beardsley, 1980 oral communication), are too shallow. Similar subsurface structural interpretations have been proposed for longitudinal sections along the Canadian Rockies (Bally, Gordy, and Stewart, 1966).

One point not discussed earlier in this section should be mentioned here. The representation of subsurface structure becomes increasingly difficult and more speculative with increasing depth. The development of disharmony in folding, particularly between the Silurian-Lower Devonian sequence and the Cambrian-Ordovician sequence, certainly may be possible, complicating an interpretation of subsurface structure based on surface structures. As an aid to inferring deep detached structure, information on characteristic wavelengths and amplitudes of folds in the Cambrian-Ordovician sequence or Silurian-Lower Devonian sequence is available from surface mapping, well data, and geophysical data. Relatively small 1/2 to 2 mile wavelength folds mapped on the Elkhorn Mountain anticline (see Chapter II) or mapped within the Cave

Mountain complex (Sites, 1971 and 1975) have been related to detachment above the Martinsburg Formation. The wavelength of the Wills Mountain anticline at the Cambrian-Ordovician level on the other hand, is from 4 to 6 miles in wavelength. In section NN' for instance, across the Elkhorn Mountain anticline there is also a rather broad 4 to 5 mile wavelength structure with roughly a 1-mile amplitude. This fold has an amplitude and wavelength implying Cambrian-Ordovician involvement. This sort of reasoning alone would not be considered a strong evidence or irrefutable proof of folding and ramping of the subsurface Cambrian-Ordovician sequence; however, since seismic evidence presented in Perry (1971 and 1978) and Jacobeen and Kanes (1975) supports this line of reasoning for the subsurface of the Wills Mountain anticline, the Cave Mountain anticline and the Elkhorn Mountain Long-Ridge anticline, similar implications regarding subsurface structure should not be overlooked in areas where subsurface information is not available.

### 3. The Bergton-Crab Run and Adams Run Anticlines.

Between the Elkhorn Mountain-Long Ridge anticline and the Little North Mountain Fault lie the Bergton-Crab Run and Adams Run anticlines (see section NN' of Plate 1). South across the Parsons CSD these two anticlines plunge

out. No geophysical or well data was found for this area. However, along section NN' the amplitudes and wavelengths of the surface folds are suggestive of Cambrian-Ordovician involvement in these anticlines which is represented in section NN'. In section SS' (Plate 1) the entire section-- Lower Cambrian through Devonian-- is shown as almost undeformed, although long wavelength, low amplitude anticlines may be present.

#### 4. Structures Between the Little North Mountain Fault and the Blue Ridge Front.

Displacement of the Cambrian-Ordovician sequence along the Little North Mountain fault increases to the south across the Parsons CSD. Also, the Staunton-Pulaski fault is not present in section NN', but has considerable displacement in section SS' (see Plate 1). In NN', ramping within a second underlying sheet of Cambrian-Ordovician dolomites and limestones is related to the **Mayland anticline**, which plunges only slightly to the south from NV' to SS' across the discontinuity. Two **synclines** in the Massanutten synclinorium formed in the Silurian Massanutten Sandstone plunge out southwest across the Parsons discontinuity leaving only the 5-mile wavelength synclinorium developed in the Cambrian-Ordovician sequences.

The crystalline rocks of the Blue Ridge have been

represented as detached above a decollement in the Cambrian Rome Formation as suggested by the recent COCORP seismic interpretation (Cook and others, 1979; Harris and Bayer, 1979).

#### 5. Plateau Structure.

Subsurface structures in the Plateau have been discussed in detail by Gwinn (1964). Plateau structures presented in cross sections NN' and SS' are generalizations of descriptions presented by Gwinn (1964). Some additional structure has been added to the Lower Devonian formations detached above the Silurian Salina Formation in the Plateau **synclines**. The Blackwater anticline plunges out southwest across the Parsons structural discontinuity into (or beneath) the Job syncline. Similarly, the Glady anticline plunges out northeast across the discontinuity beneath the Georges Creek syncline. As inferred for the Middle Mountain syncline, these anticlines can be expected to continue for some distance beneath the syncline. Thus, small doubly faulted anticlines in the Devonian Oriskany sandstone, characteristic of detachment in the Salina, have been **included** beneath the synclines.

### C. Structural Interpretation

#### 1. Structure in the Cambrian-Ordovician Stiff Structural Lithic Unit.





Major anticlines of the Valley and Ridge and High Plateau provinces are located on the geologic map of West Virginia (Figure 11). The cross sections discussed in the previous section (section B.e) indicate that several of the Plateau and Valley and Ridge anticlines are related to detachment above a decollement in the Cambrian Rome Formation. Gwinn (1964) presents cross sections based on well and seismic reflection data that show faulted Cambrian-Ordovician beneath the **Elkins** Valley anticline and Browns Mountain anticline. In the core of the Deer Park anticline, Gwinn (1964) indicates that the Juniata is thickened to approximately 4,000 feet along with considerable faulting of the Oriskany Sandstone and thickening of the Silurian formations. However, some faulting of Cambrian-Ordovician formations cannot be ruled out because of the long wavelength of the anticline, and by analogy with the **Elkins** Valley anticline, so that minor displacement along the Rome has been suggested (see section NN'). **Cardwell** and others (1968) have indicated faulting of the Cambrian-Ordovician formations beneath the Briery Mountain anticline, and Gwinn (1964) notes that some faults may be present in the Cambrian-Ordovician sequence beneath the northern segment of the Deer Park anticline. The extent of Rome detachment northwest into the Plateau inferred from the above observations and reports is represented in Figure 15. The northwest extent of Rome detachment can be

seen to vary abruptly along strike as, for example, between the northeastern plunge out of the Browns Mountain **anti**-cline and the southwestern plunge out of the **Elkins** Valley anticline. Similarly, there is an abrupt decrease in the northwest extent of Rome detachment by 4 to 5 miles between the northeastern plunge out of the **Elkins** Valley anticline and the southwestern plunge out of the Deer Park anticline. Wheeler and others (1976) indicate that in the plunging nose of the Deer Park anticline intermediate scale folds have more northeasterly trends than those further north-east within the Deer Park complex. This can be explained by a slight right-lateral tear between the noses of the two anticlines. Tearing between the two structures could easily have occurred if slip along the Rome beneath the **Elkins** Valley anticline continued over a longer period of time, or at a greater rate than slip beneath the Deer Park **anti**-cline. Dahlstrom (1969, p. 751) notes that:

In adjacent cross sections the amount of "shortening" at a specific horizon between comparable reference lines must be nearly the same unless there is a tear fault between them.

If a segment along section SS' is taken across the **Elkins** Valley anticline (Plate 1) and a comparable segment is taken along section NN' extending about 4 or 5 miles northwest from the northwest limb of the Deer Park anticline, shortening to the south at the Cambrian-Ordovician level

is approximately 1 mile, while to the north it is inferred to be zero. A similar discontinuity in shortening occurs between the **Elkins** Valley and Browns Mountain anticlines.

For these reasons, tear faults including zones of distributed faulting and rotation have been indicated between offset thrust faults or ramps through the Cambrian-Ordovician sequence (Figure 15).

The line of reasoning favoring Jacobeen's and Kanes' (1974) section (JJ', Plate 2) and the equivalent segments along strike to the southwest in sections NN' and SS' (Plate 1) was presented in the preceding section. Between the northwest limb of the Wills Fountain anticline and the southeast limb of the **Broadtop** anticline along section JJ'-- a horizontal distance of 20.5 miles-- there is a 32-mile length of the Cambrian-Ordovician sequence. Across equivalent 20.5 mile segments of NN' and SS' to the south (see Plate 1), there are 24 and 25 mile lengths respectively of the Cambrian-Ordovician sequence.

As suggested above, Dahlstrom (1969) indicates that rather significant differences in shortening between adjacent cross sections could imply or be accounted for by the presence of a tear fault between the two sections. Dahlstrom (1969, p. 751 and 752) offers another possible mechanism to account for substantial differences in shortening between adjacent cross sections:

The Lewis Thrust for instance (Dahlstrom et al, 1962), has a minimum of 23 miles (37 km) of thrust displacement at the United States border and 135 airline miles 217.2 km) to the north, the fault displacement is zero. Over the same distance the overall shortening in the mountain belt as a whole may have diminished but certainly not by 23 miles (37 km)...**there** must be some compensatory mechanism at work whereby displacement is "transferred" from one structure to another...

The compensatory mechanism for thrusts is a kind of lap joint wherein the fault whose displacement is diminishing is replaced by an echelon fault whose displacement is increasing. Clearly such a "transfer zone" could not exist unless all of the faults involved in the transfer zone are rooted in a common sole fault.

Total shortening of the Cambrian-Ordovician sequence across the basin is 6 miles greater in section NN' than in section SS'. Most of this shortening difference is related to the presence of the Bergton-Crab Run and Adams Run anticlines in section NN' (Plate 1). Since these two structures plunge out southward rather abruptly, a left-lateral tear fault or zone of wrenching is hypothesized to be present across the plunging noses of these structures. A distinct left lateral shift in surface fold traces across the inferred tear fault supports this hypothesis (see geologic map of Rockingham County, Virginia, Brent, 1960). Total shortening of the Cambrian-Ordovician sequence across the basin along JJ' is not known, but the additional 8 miles of shortening across JJ' requires

that one or more tear faults or transfer zones be present between NN' and JJ'. The longitudinal section LL' is drawn to suggest that this transfer or tear must occur across the Petersburg structural discontinuity. Terrain-corrected Bouguer gravity over the area taken from Kulander and Dean (1978) is shown in Figure 16. Gravity values increase from 6 to 11 milligals northeastward within a 12-mile long interval across the Petersburg CSD in Grant County. A comparable increase in the terrain-corrected Bouguer gravity occurs across the Wills Mountain anticline. Calculated gravity for structural cross sections presented in Chapter IV indicates that such an increase in gravity will be produced by a duplication of the Cambrian-Ordovician sequence. Thus, the gravity high across the Petersburg area (Figure 16) supports the inferred presence of the duplicated Cambrian-Ordovician sequence into the Petersburg area as illustrated in Figure 18. All available subsurface information points to the presence of a duplicated Cambrian-Ordovician sequence north of the Petersburg area, yet surface fold traces in the Silurian and Devonian sequence do not show left lateral shifts in trend (see Cardwell and others, 1968) and although left-lateral strike-slip faults are present in the plunge out of the Bedford syncline southwestward into the Petersburg CSD, displacements along them are significant (Sites, 1978). On the basis of the gravity

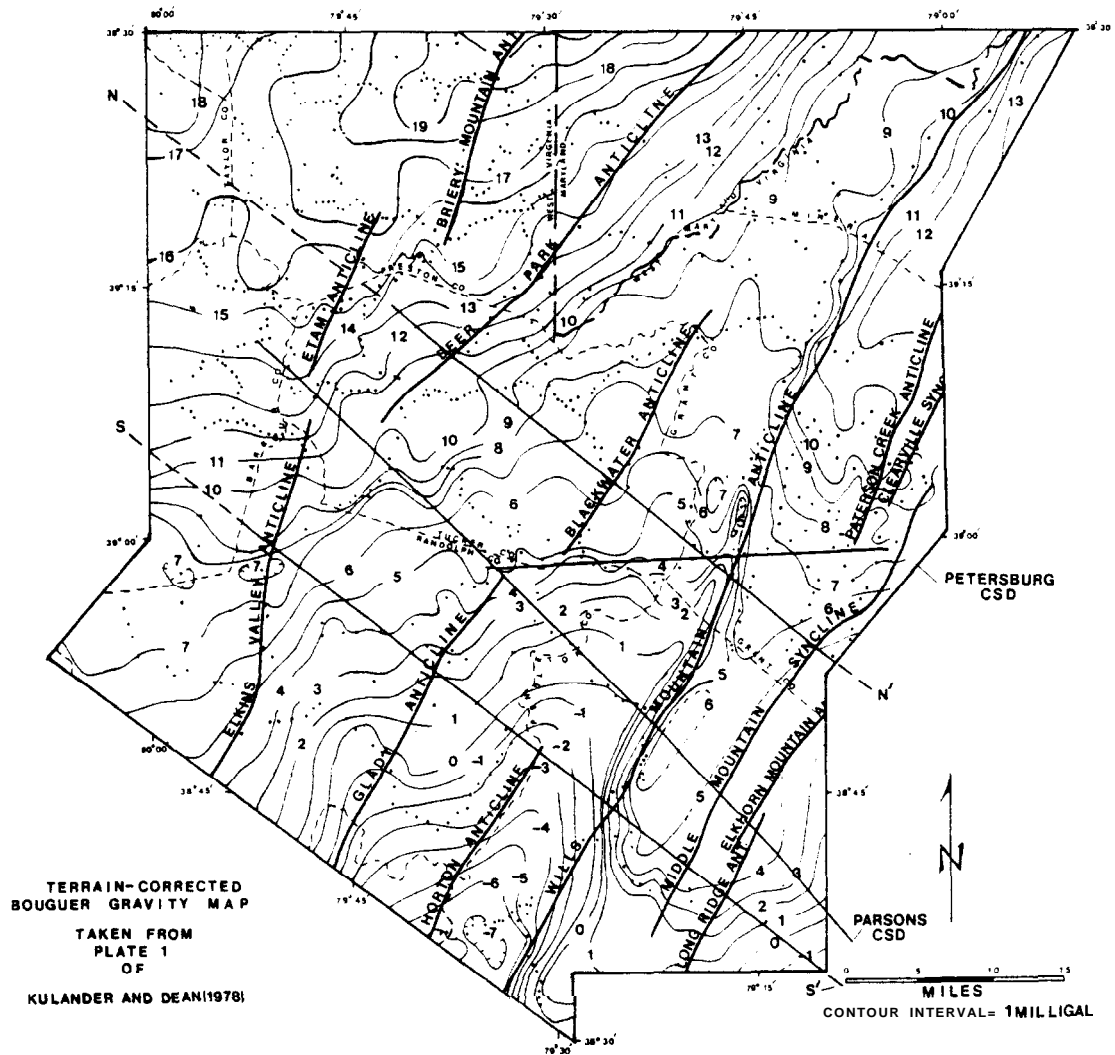
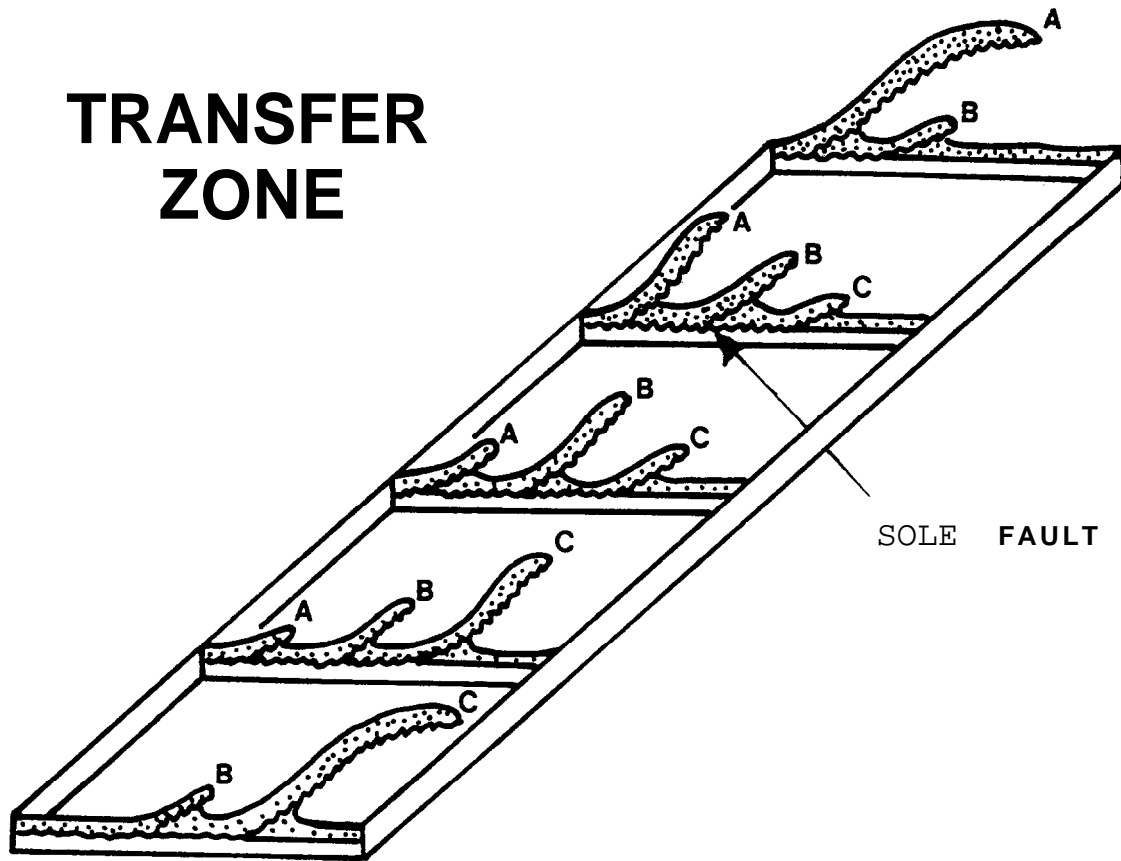


Figure 16

data and the structural cross sections, some mechanism accommodating the transition in shortening across the Petersburg area must be present. Since surface structural features do not support the presence of tear fault or tear fault zone through the shallow and exposed sequence, a more gradual transfer zone accompanied by wrenching and tearing is proposed. Figure 17, taken from Dahlstrom (1969) illustrates the three dimensional nature of the transfer zone with its roots in a sole thrust. Figure 18 illustrates the three dimensional model for the transfer zone through the Petersburg area along with the other subsurface structures proposed above for the Cambrian-Ordovician sequence.

## 2. Structure in the Silurian-Devonian Stiff Structural Lithic Unit.

In Chapter II, section A, the surface and subsurface structure of the Middle Mountain syncline was discussed. Several features were noted regarding the structure of this area. It is felt that three of these features are of fundamental importance to the structural interpretation of the Parsons and Petersburg CSD's. First, to the southwest and within the Parsons CSD, the amplitude of the Elkhorn-Mountain Middle Mountain fold pair is 3,000 and 2,800 feet respectively. Northeast of the structural dis-



**FROM DAHLSTROM(1969)**

Figure 17 Schematic Diagram of a Transfer Zone Developed Above a Sole Fault



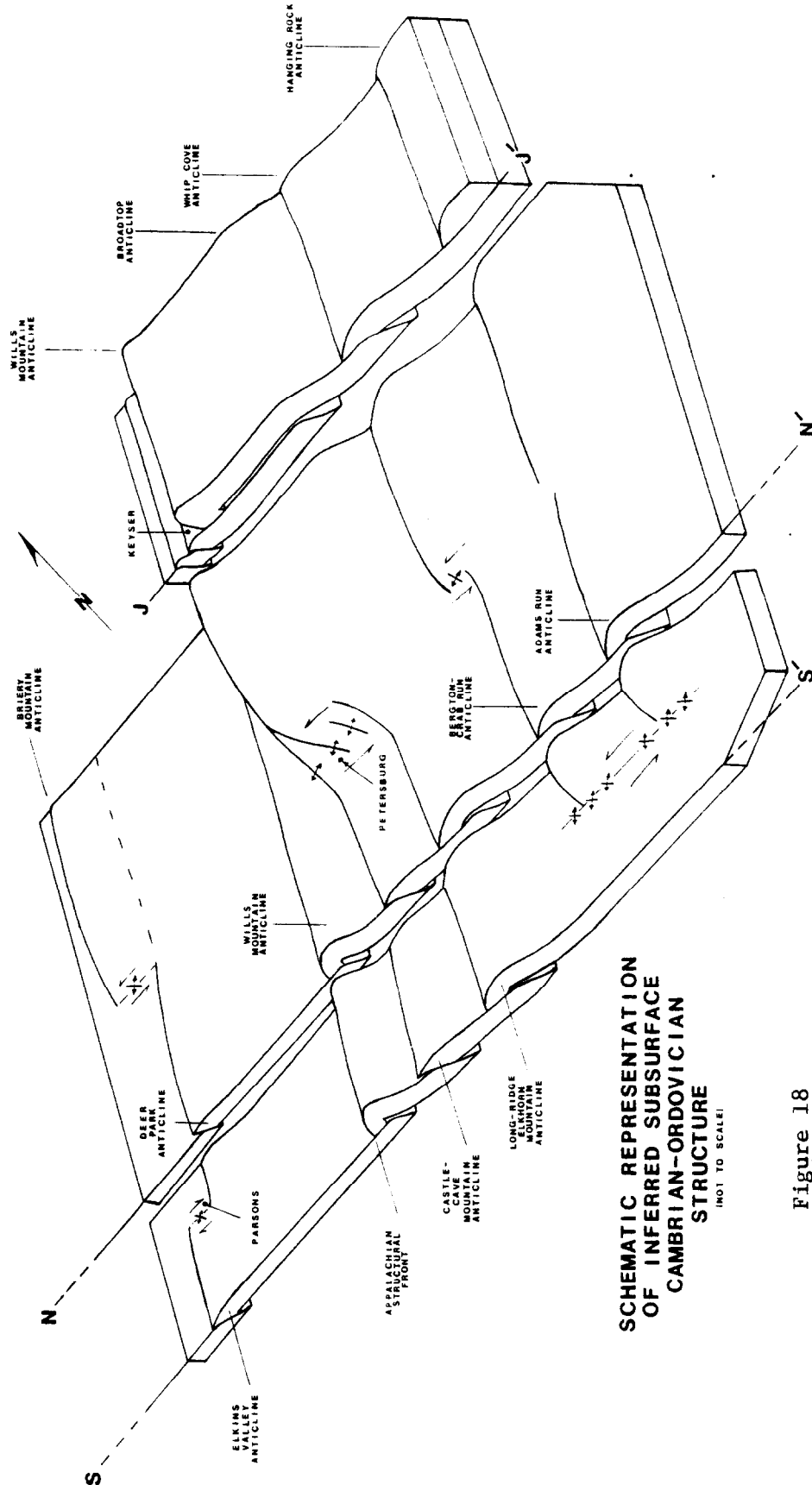


Figure 18

continuity structural relief is significantly greater at 4,400 feet. Second, total shortening southwest and within the discontinuity across the Elkhorn-Middle Mountain structure is approximately 2,000 feet or 500 feet (33%) greater than the shortening outside the discontinuity to the northeast. Third, northeast along the axis of the Middle Mountain **syncline** the Devonian Oriskany Sandstone drops 2,800 feet in structural level across the discontinuity.

In section NN' of Plate 1, it is apparent that structural relief across the **Elkhorn** Mountain anticline and Middle Mountain **syncline** is related primarily to the relief across subsurface Cambrian-Ordovician structure. Similarly, but to a lesser extent, surface structural relief across the **Elkhorn** Mountain-Middle Mountain fold pair south of the discontinuity, is related to the Cambrian-Ordovician structure (see SS' of Plate 1). The increased shortening within and south of the Parsons CSD is related to detachment in either, or all three, of the Nartinsburg, Juniata, and Wills Creek Formations--all of which are known detachment horizons producing structure in Lower Devonian formations (Gwinn, 1964; Bagnall, Beardsley, and Drabish, 1979). If the shortening of Cambrian-Ordovician structures could be subtracted from the overlying structures, Silurian and Devonian rocks northeast of the discontinuity would be roughly flat lying while faults and folds in these rocks

within and south of the discontinuity would produce an anticline in Silurian-Devonian formations plunging northeast across the discontinuity a total of 2,800 feet.

Although shortening southwest and within the discontinuity across the **Elkhorn Mountain-Middle Mountain** fold pair is only 500 feet greater than shortening to the northeast across this structure, Dahlstrom's (1969) requirement for tear faults or transfer zones is recalled. Mapping of surface structures in the area (Chapter II, section A) revealed no cross faults or tear faults. A considerable number of thrust faults with large displacements have been mapped by Sites (1971, 1978, and 1980 oral communication) in the Cave Mountain area northeast of the Parsons CSD and adjacent northwest of the Middle Mountain syncline. Again, no tear faults have been mapped across this structure as it plunges out to the southwest across the Parsons CSD (Sites, 1971). Nor is there any significant amount of cross faulting or tear faulting to the northeast along the Cave Mountain anticline where this structure plunges across the Petersburg CSD (Sites, 1971 and 1978). However, detailed mapping along both the Parsons and Petersburg CSD's has consistently revealed that the zone of structural discontinuity contains more numerous intermediate scale folds, but there are also more numerous thrust faults. It is suggested that these two cross-strike structural discon-

tinuities can be viewed as a cross-strike alignment of fault transfer zones.

D. Structural Model for the Parsons and  
Petersburg Cross-Strike Structural Discontinuities

The increasing deformation observed in the Devonian Oriskany Sandstone southwest across the Parsons CSD and along the **Elkhorn** Mountain-Middle Mountain fold pair is the result of detachment in the Martinsburg Formation ramping into Juniata, Wills Creek and Middle Devonian shale detachment intervals southwest of the discontinuity, while movement northeast of the discontinuity continued along the Marginsburg thrust. Shortening on either side of the discontinuity was equalized to the northwest, where movement along the Martinsburg sole thrust ramped upward into Juniata, Wills Creek and Middle Devonian formations producing equivalent shortening of the Silurian-Devonian sequence across the Cave Mountain anticline northeast of the Parsons CSD. Equivalent shortening occurs in the discontinuity through greater numbers of faults. A generalized model illustrating the geometry of the inferred transfer zone is presented in Figure 19. The model is further simplified by considering only two detachment intervals--the Martinsburg and Middle Devonian soft structural lithic units. The model can be modified appropriately to coincide with structures along the Petersburg CSD to the north, or

the Plateau segment of the Parsons CSD. Note, however, that the Parsons and Petersburg CSD's are marked by transfer zones not only in the Silurian-Lower Devonian sequence, but within the Cambrian-Ordovician sequence as well. In addition, the numerous intermediate scale 200-1,000 foot amplitude folds in the Chemung Group along the plunging nose of the Deer Park anticline of the Plateau are probably related to shortening above shallow detachments in either the Middle Devonian shales or in shale intervals of the Devonian Brallier Formation. Hence, the available evidence indicates that fault transfer occurring across structural discontinuities involves all detachment intervals from the Cambrian Waynesboro (Rome) Formation through the Middle Devonian formations and possibly higher level detachment intervals, although deep and shallow structural levels may transfer slip independently of each other. Along some segments of the discontinuity transfer may be limited to only a few brittle units. Between the southeast limbs of the Wills Mountain and Elkhorn Mountain anticlines along the Parsons CSD, the lack of transfer within the Cambrian-Ordovician sequence accounts for the less pronounced surface expression of the discontinuity. Instead of the Middle Mountain syncline and Elkhorn Mountain anticline plunging out completely across the discontinuity, those structures primarily related to structure in the

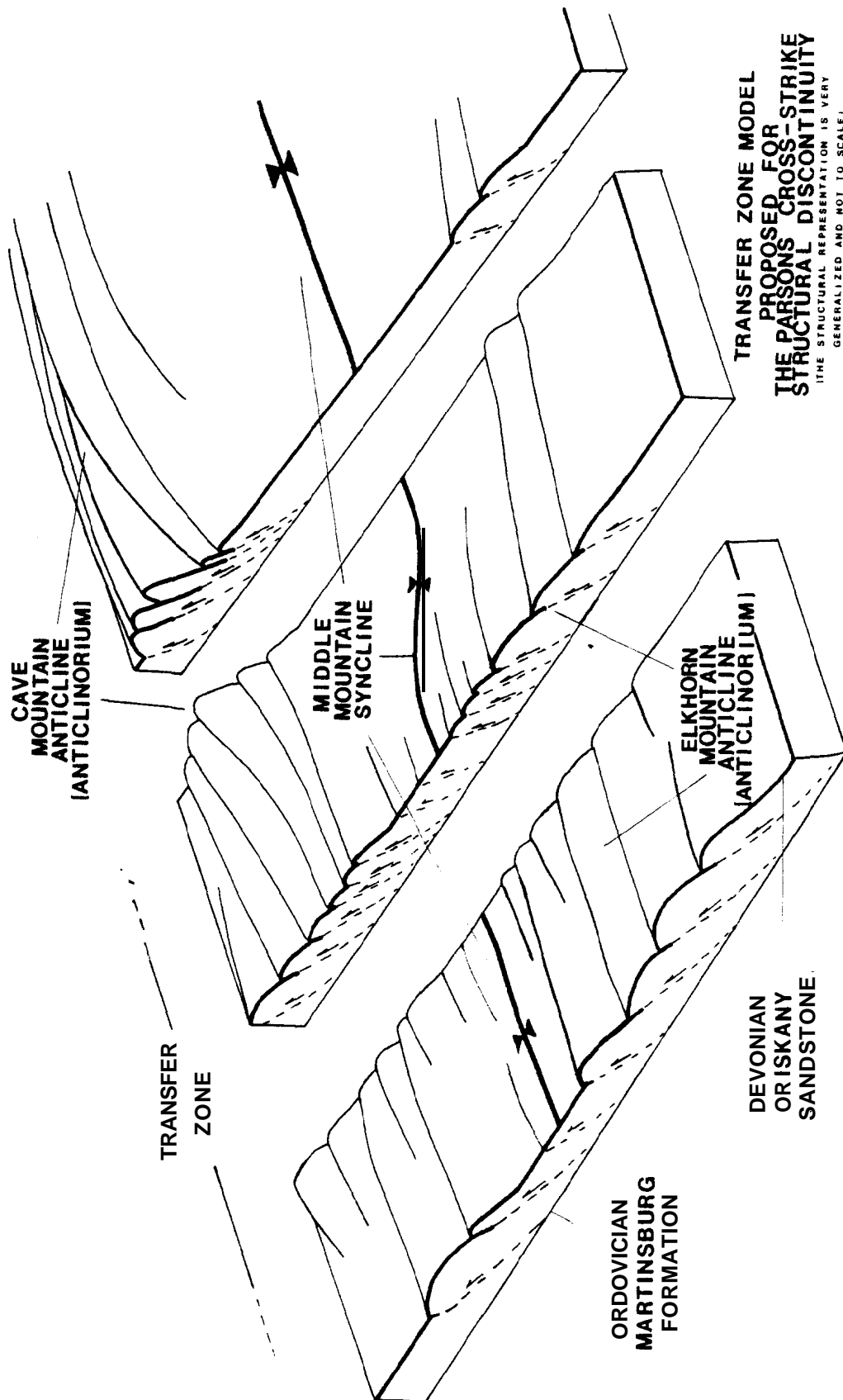


Figure 19

Cambrian-Ordovician sequence, only show a change in amplitude and a drop in structural level across the discontinuity. Similar thickening of the Ordovician Martinsburg Formation and folding of the overlying Silurian-Lower Devonian sequence is encountered northeast along the axis of the Massanutten synclinorium across the Parsons CSD. Northwest along the discontinuity in the Plateau, the Horton, Blackwater and Glady anticlines plunge out completely across the discontinuity. The Cambrian-Ordovician sequence is flat lying beneath these structures. Movement along a Martinsburg sole thrust is transferred to higher level detachment intervals forming the Horton anticline southwest of the Parsons CSD while northeast of the discontinuity, contained displacement along the Martinsburg is transferred to higher level detachment intervals further northwest **beneath** the Blackwater anticline and so on back and forth forming next the Glady anticline, the Deer Park and **Elkins** Valley anticlines. The northeast swing of fold axes along the Deer Park indicates that the tear or fault zone in the underlying Cambrian-Ordovician sequence is younger than detachment in the Martinsburg. This sequence of detachment developing progressively deeper is accepted for the central Appalachians in general (Perry, 1978; Sites, 1978) although there are local exceptions (Sites, 1978).

The Petersburg CSD similarly represents a zone

across which shortening above a Martinsburg sole thrust is transferred via numerous faults and small folds to fewer faults with larger displacements and fewer folds with larger amplitudes on either side of the zone. Sites' (1978) Figure 10 (p. 3) is an excellent representation of structural shortening northeast and southwest of the discontinuity, however, very little shortening is illustrated in the discontinuity and the increased intensity of faulting and folding in the discontinuity are not shown. In addition, a broad transfer zone, 10 to 15 miles in width, (see section LL') occurs in the Cambrian-Ordovician sequence across the Petersburg CSD.

#### E. Balancing Structural Cross Sections

Tables 2 and 3 list shortening measurements across the Valley and Ridge segment, the Plateau segment, and the total width of the sedimentary basin for sections NN' and SS'. Theoretically, total shortening across the basin should be constant, or nearly so, for each unit in the sequence. Similarly, shortening across adjacent sections must be nearly the same unless separated by a tear fault. However, along section NN', the Martinsburg shale is shortened 30.3 miles, almost twice as much as that for the Cambrian-Ordovician sequence (16.2 miles) and more than seven times that of the Oswego Sandstone (4.1 miles) (see Table 2). Similar disagreements are present in section SS'



SHORTENING MEASUREMENTS  
FROM THE STRUCTURAL INTERPRETATION  
NORTH OF THE PARSONS STRUCTURAL DISCONTINUITY

	<u>Cambrian and Ordovician Dolomites and Limestones</u>	<u>Ordovician Martinsburg Formation</u>	<u>Ordovician Oswego Sandstone</u>
VALLEY AND RIDGE*			
H (miles)	33.1	33.1	33.1
L (miles)	48.7	53.4	36.1
D (miles)	15.6	20.3	3.0
%S	32	38	8.3
EASTER.!? PLATEAU**			
†H (miles)	33	33	33
L (miles)	33.5	43	34.1
D (miles)	0.5	10	1.1
%S	1.5	23.3	3.2
TOTAL			
H (miles)	66.1	66.1	66.1
L (miles)	82.2	96.4	70.2
D (miles)	16.2	30.3	4.1
%S	19.7	31.4	5.8

TABLE 2

\*Valley and Ridge refers to structure between the Little North Mountain Fault and the northwest limb of the Wills Mountain anticline.

\*\*Eastern Plateau refers to structures between the northwest limb of the Wills Mountain anticline and the northwest limb of the Etam anticline

†H is the horizontal distance along the section line.

L is the total length of the unit contained in the interval H along the section line. For the soft Martinsburg Fm L is the total area of the formation divided by its thickness

$$D = L - H$$

$$S = (D/L) \times 100$$

SHORTENING MEASUREMENTS  
FROM THE STRUCTURAL INTERPRETATION  
SOUTH OF THE PARSONS STRUCTURAL DISCONTINUITY

	<u>Cambrian and Ordovician Dolomites and Limestones</u>	<u>Ordovician Martinsburg Formation</u>	<u>Ordovician Oswego Sandstone</u>
VALLEY AND RIDGE*			
H (miles)	31	31	31
L (miles)	40	42.2	36
D (miles)	9	11.2	5
%s	22.5	26.5	13.9
EASTERN PLATEAU**			
†H (miles)	32	32	32
L (miles)	33	39.2	33.5
D (miles)	1	7.2	1.5
%S	3	18.4	4.5
TOTAL			
H (miles)	63	63	63
L (miles)	73	81.4	69.5
D (miles)	10	18.4	6.5
%S	13.7	22.6	9.4

TABLE 3:

\*Valley and Ridge refers to structures between the Little North Mountain Fault and the northwest limb of the Wills Mountain anticline.

\*\*Eastern Plateau refers to structures between the northwest limb of the Wills Mountain anticline and the northwest limb of the Elkins Valley anticline.

†H is the horizontal distance along the section line.

L is the total length of the unit contained in the interval H along the section line. For the soft Martinsburg Fm, L is the total area of the formation divided by its thickness.

$$D = L - H$$

$$S = (D/L) \times 100$$

(Table 3). In addition, there is disagreement in the amounts of shortening along the same units in adjacent cross sections (see Tables 2. and 3).

There are several possible explanations for this disagreement. Regional sections constructed at a scale of 1 inch to the mile, cannot detail intermediate scale surface structure. Detailed mapping of surface structures consistently shows considerably greater amounts of shortening than documented in previous regional studies (Sites, 1978 and 1980 oral communication; see also Henderson, 1973, Mullenex, 1974, and Trumbo, 1976). In addition, it is difficult to estimate structural shortening related to thickened units from 1 or possibly 2 wells into the core of a structure. Thus, the anomalously low shortening reported for the Ordovician Oswego Sandstone and thus for the overlying Juniata Formation, and Silurian and Devonian formations is certainly much greater. The excessive shortening reported for the Ordovician Martinsburg Formation may be attributed to too little thinning of limbs, too much thickening of hinges, and far too much thickening in front of Cambrian-Ordovician faults. However, it may be that the shortening in the Martinsburg is not excessive, but actually a close approximation of the total shortening. The outline of the Cambrian-Ordovician sequence is inferred from some seismic data, and some gravity data, but generally

is inferred from relief in surface structure. Reports on the thickness of this sequence vary from approximately 6,500 feet (Zurgani, 1975) to 9,500 feet (see Sites' 1978, section CC'). Measured sections through exposed portions of the sequence (Brent, 1960) in Rockingham County, Virginia, indicate a total thickness of 8,500 feet. Perry (1964) similarly indicates an 8,500-foot thickness from the Ray-Sponaule well in Pendleton County, West Virginia. Each of these reports comes from structurally complex areas so that the 8,500-foot thickness may be greater than the undeformed thickness of that sequence. However, the 8,500-foot thickness for the Cambrian-Ordovician sequence used in the sections of Jacobeen and Kanes (1974 and 1975) and Perry (1971 and 1978) has been used for the Valley and Ridge portions of sections NN' and SS' (Plate 1). The shortening of the sequence measured from the general outline of Cambrian-Ordovician structure is certainly an underestimate. Because all unit thicknesses used in the construction of these cross sections were acquired by averaging measured sections which may have been structurally thickened to varying degrees, the unit thicknesses will contain an average or representative amount of excess thickness related to structural shortening. The uncertainties in these shortening estimates indicate that the calculated values of shortening from NN' and SS' are of little meaning. Future detailed

mapping along the total length of any available cross sections across the basin could provide a better estimate of total shortening across the basin. However, the large amount of work required to find that number, in itself, would not be worthwhile. An accurate estimate of total shortening in the Silurian-Devonian sequence of the Plateau could be acquired simply by an accurate assessment of that sequence's undeformed thickness.

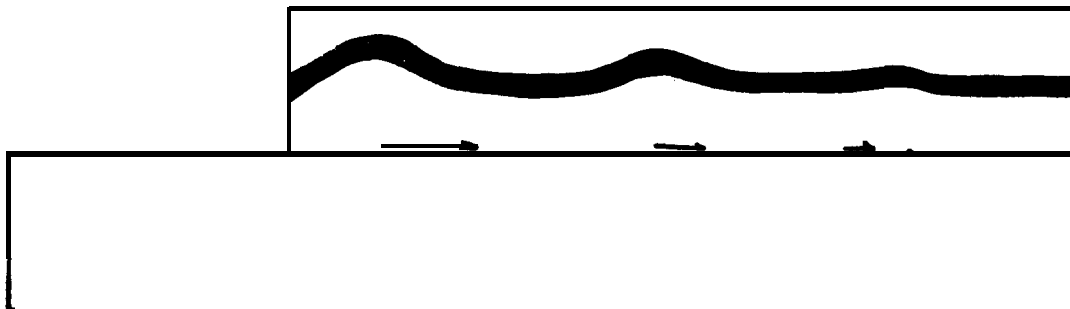
In spite of the balancing flaws, the generalized portrayal of regional structures has been very useful in finding solutions to basic problems in central Appalachian structure and their construction is recommended for future regional structural studies. Specifically, they have been useful in developing a three-dimensional model of regional subsurface structure.

#### F. Balancing Cross Sections and Pressure Solution

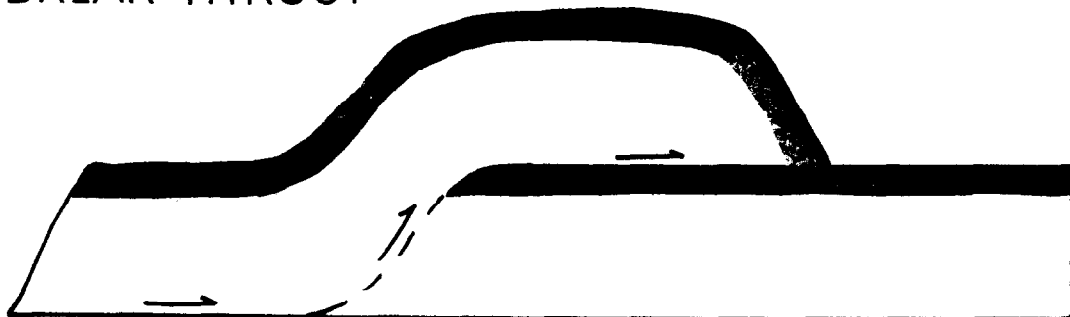
Assessing total shortening across the basin is further complicated by layer parallel shortening via solution **cleavage**. The press-solved material may fill intergranular void space, opening along joints and various types of fracture porosity associated with faults and the **discontinuities** mobile behavior of shales.

Three modes of shortening are illustrated by Marshak and Geiser (1980) (see **Figure 20**). In the fold thrust,

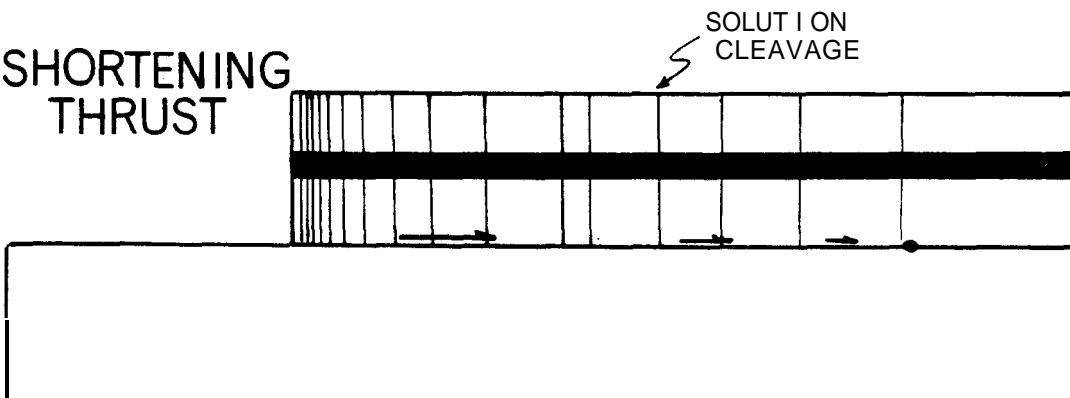
## FOLD THRUST



## BREAK THRUST



## SHORTENING THRUST



## METHODS OF THRUST PROPAGATION (FROM MARSHAK AND GEISER, 1980)

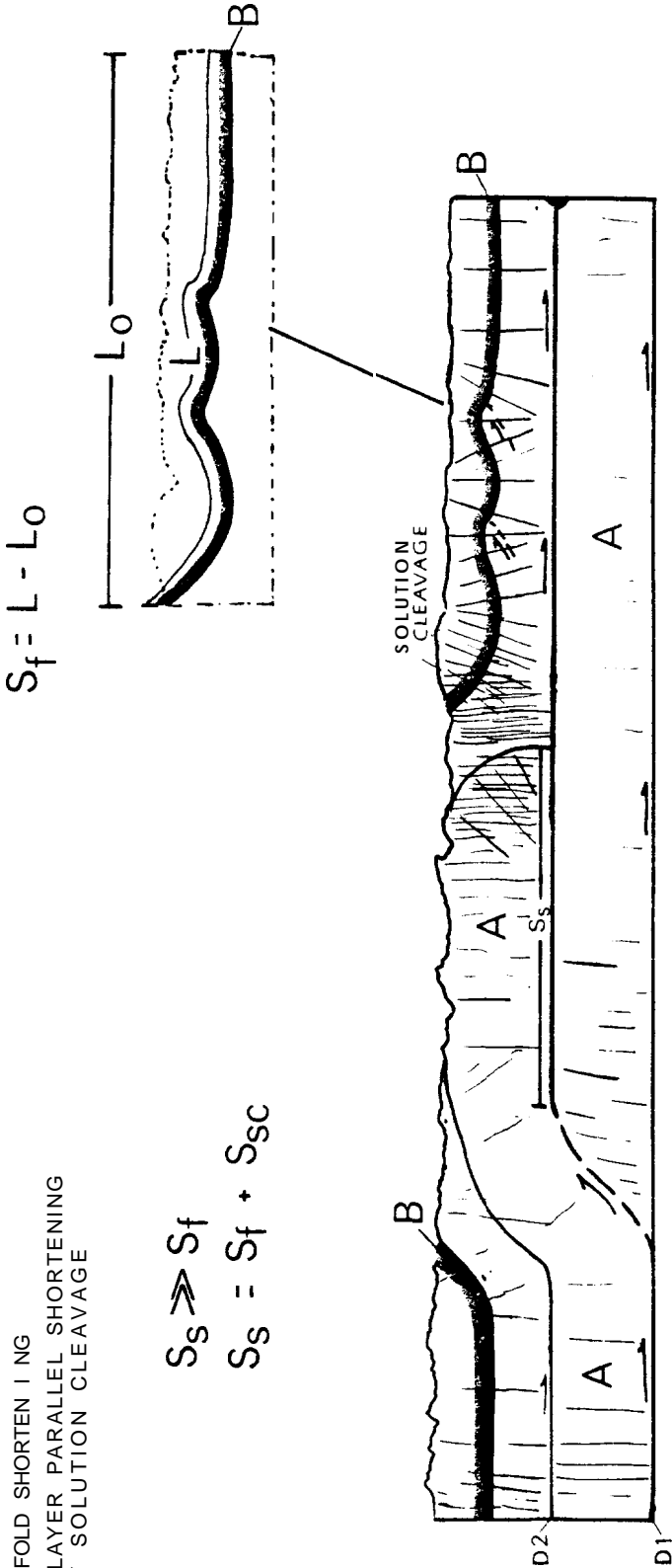
Figure 20

shortening within a sequence overlying a detachment interval is accomplished by folding of that sequence. In the break thrust, shortening above a detachment interval is produced by moving the overlying formations over a ramp through the sequence. Shortening of formations overlying a detachment interval by a shortening thrust occurs by solution cleavage. These methods of thrust propagation are combined to illustrate possible inter-relationships between the various mechanisms shortening a multilayer (Figure 21).

At the Allegheny Structural Front across sections SS' and NN' (Plate 1), the Cambrian-Ordovician sequence beneath the Wills Mountain anticline transfers approximately 2 mile net slip (Ss) into the Martinsburg detachment interval. Total shortening in the Plateau folds above the Martinsburg detachment interval is 1 to 1-1/2 miles. and, as discussed above, considerably more shortening can be inferred for the section above the Martinsburg detachment. This slight excess of shortening can be **accounted for** by movement along the Martinsburg detachment interval prior to the development of the Wills Mountain anticline (Sites, 1978). This movement could be related to transfer slip into the Martinsburg along ramps cutting the Cambrian-Ordovician sequence further southeast. **However**, to the north across Jacobeen's and **Kanes'** (1974) section (see JJ' Plate 2) 12 miles of slip have been transferred from the Cambrian Rome

- D1 LOWER DETACHMENT INTERVAL
- D2 UPPER DETACHMENT INTERVAL
- Ss NET SLIP TRANSFERRED FROM D1 TO D2
- Sf FOLD SHORTENING
- Ssc LAYER PARALLEL SHORTENING BY SOLUTION CLEAVAGE

$S_s \gg S_f$   
 $S_s = S_f + S_{sc}$



SHORTENING OF A MULTILAYER

Figure 21



Formation into the Ordovician Martinsburg Formation beneath the Plateau. Shortening measured from unpublished regional cross sections (Anonymous) along this line across the Plateau is approximately to miles--far short of the 12 miles required, even when considering the general nature of the section.

The role of layer-parallel shortening via solution cleavage may be an important factor to consider in accounting for total shortening beyond this thrust sheet. Engelder and Engelder (1977) have interpreted observed fossil distortion and solution cleavage in Upper Devonian shales of the New York Plateau to imply 5 km of shortening across 50 km of the Plateau. An earlier study by Nickelsen (1966) in the Plateau of northern Pennsylvania indicated an average 10% shortening normal to fold axis, from distorted brachiopods found in the Phillipsburg quadrangle. A comparison of observed amounts of pressure solution and fossil distortion northwest of this thrust sheet should be compared with amounts observed to the southwest on the Plateau where net slip transferred to the Martinsburg is considerably less.

It should be noted that directly northwest of Petersburg, along a line extending across strike through the Cambrian-Ordovician transfer zone, high amplitude **anticlines** of the High Plateau (see Gwinn, 1964, his Plate I) extend an additional 20 miles northwest along one of

Gwinn's (1964) lineaments (see Figure 22) to include the entire length of the Chestnut Ridge anticline. The folds of the High Plateau retreat southeast again, 100 miles to the northeast along strike near the Birmingham Window. The Birmingham Window occurs in the Cambrian-Ordovician sequence, is doubly plunging, exposing a second Cambrian-Ordovician slice beneath, and implying the presence of a ramp through an underlying third slice of Cambrian-Ordovician. R. Shumaker (1980, oral communication) indicates that the Salina of the Plateau pinches out to negligible thickness northwest of the Birmingham Window so that detachment in this interval is unlikely to be very extensive. R. Shumaker (1980, oral communication) also suggests that faulting of the Cambrian-Ordovician beneath the Birmingham Window does not transfer much slip into the Martinsburg Formation and that most of the shortening is taken up by imbrication of the Cambrian-Ordovician against an almost immovable wall at the structural front. This retreat of the High Plateau folds southeast across strike to the southwest-plunging nose of the Sinking Valley anticline coincides with the Tyrone-Mount Union lineament of Gold (1973) and Kowalik (1975) (see Figure 22 ).

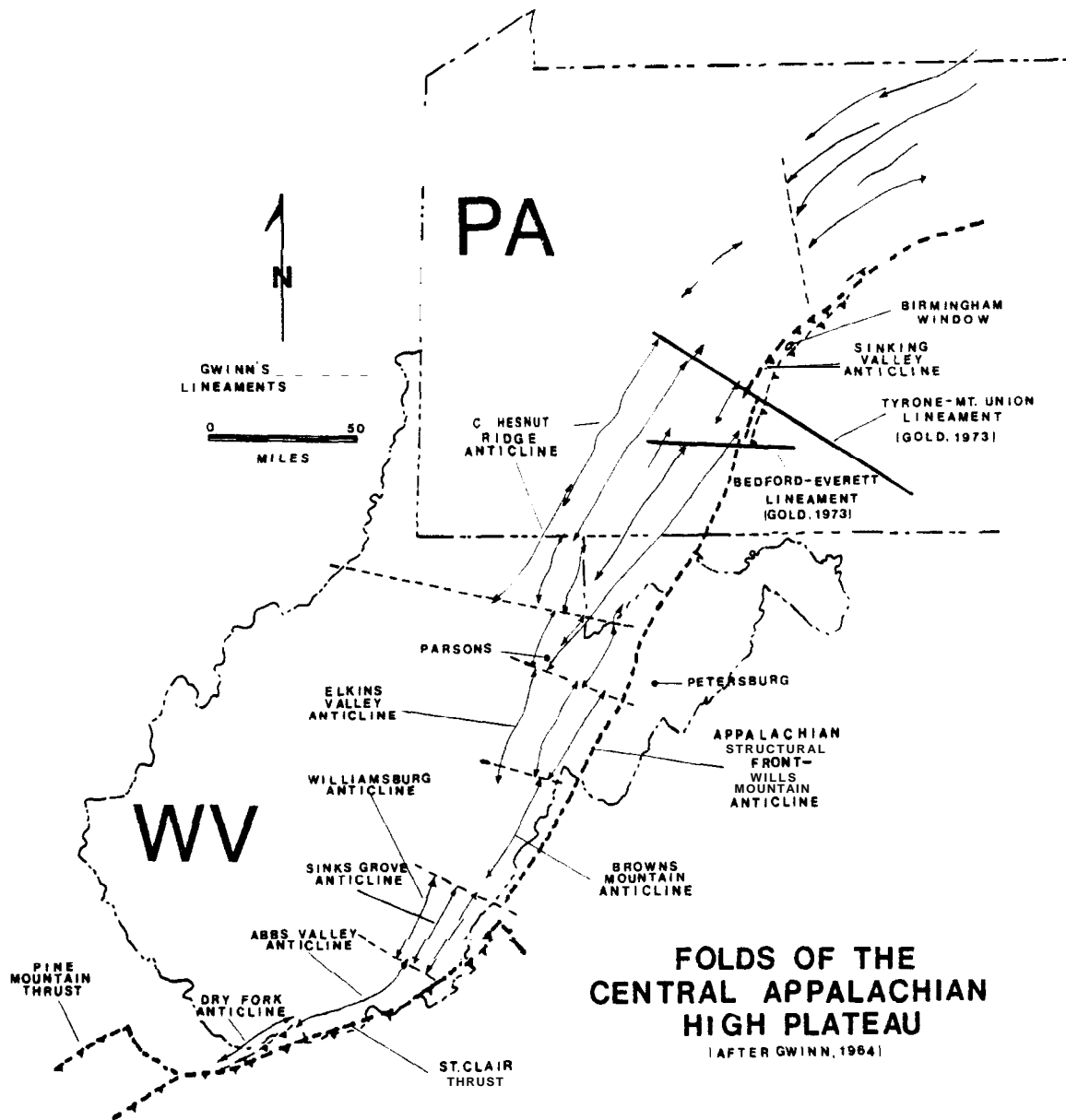


Figure 22 Folds of the Central Appalachian High Plateau and the Locations of Gwinn's Lineaments (after Gwinn, 1964)

#### IV. CENTRAL APPALACHIAN GRAVITY MODELS

##### A. Introduction

Previous use of observed gravity as an aid in unravelling details of Appalachian structure in West Virginia is limited. Kulander and Dean (1978) occupied 1,458 stations in central and eastern West Virginia, western Maryland, and Virginia. Their study is primarily regional in nature, with detailed coverage limited to a profile across the Warm Springs anticline in Bath County, Virginia. Byerly (1973) surveyed a detailed profile across the Massanutten Synclinorium in northern Berkeley County, West Virginia.

Calculated gravity for several generalized cross sections of the Appalachian Valley and Ridge and Plateau structures is discussed here and compared to contours of terrain-corrected residual Bouguer anomalies and, in some cases, to the terrain corrected Bouguer gravity from Kulander and Dean (1978). A new gravity profile surveyed across the Middle Mountain syncline is presented along with a subsurface model based on the terrain-corrected Bouguer gravity. Two interpretations of the section line of Jacobeen and Kanies (1974) through Mineral and Hampshire Counties, West Virginia, are also presented along with calculated gravity for both profiles.

Gravity profiles were calculated using a program

developed by Smith, Higgins, and Robertson (1970) of the Princeton University Department of Civil and Geological Engineering. The method of calculation was derived by **Hubbert** (1948) and evaluated by Talwani, et al (1959), and involves a line of integral which evaluates the vertical component of the gravitational field associated with unit thickness n-sided polygonal cylinders that are infinitely long in the horizontal direction perpendicular to the profile. A given polygonal cylinder represents a stratigraphic interval within the Paleozoic sedimentary cover. Average densities for stratigraphic intervals were calculated using individual formation densities taken from Kulander and Dean (1978, their Figure 5a) and weighted by thickness.

#### B. Causes of Disagreement

##### Between Observed and Calculated Gravity

Lack of agreement between observed and calculated gravity may result from: (1) the uncertainty in the observed gravity; (2) the removal of the regional gravity field; and (3) errors in the proposed structural model.

Terrain-corrected Bouguer gravity values are considered to have cumulative errors of no greater than 0.1 **milligal** (Byerly, 1973; Kulander and Dean, 1978). However, standard deviation in values of residual gravity projected onto the residual gravity profile along the Warm Springs

section line (Kulander and Dean, 1978, their Figure 6) is calculated by this author to be 1 milligal, and 1.3 milligals when compared to the calculated gravity for their model. Similarly, standard deviation in value about a curve visually fit to the Middle Mountain data of this report is calculated to be 0.65 milligals, and dispersion about the calculated gravity is 1 milligal (see Figure 20). Some uncertainty is introduced in projecting values along strike onto the profile line where the assumption of structural invariance perpendicular to the profile is incorrect. This uncertainty will be greatest for a regional survey such as Kulander and Dean's (1978) survey (see station locations, Figures 23 and 26), where few stations actually lie along the profile. In addition, near-surface density distributions are much more complex than represented by the generalized regional gravity models presented here. Such uncertainty may be related to near-surface lateral density contrasts produced by unrecognized structure, or ground water solutioning of near-surface limestones (Byerly, 1978). Byerly (1973) also related 1.5 to 1.8-milligal variations above the regional background to a subsurface zone of high-density dolomite. Thus, it appears that, in general, the uncertainty between observed and calculated gravity is of the order of one milligal.

Removal of the regional gravity from the observed Bouguer anomaly requires assumptions about deep seated

(basement) structure and lithology which may not be well supported. The regional gravity map (Kulander and Dean, 1978, their Figure 1) was constructed graphically from a series of orthogonal profiles of the terrain-corrected Bouguer gravity. Regional gradients were visually chosen for each profile. The regional gravity map was then compiled from the profile data. It would be impossible to anticipate the presence of smaller-scale features in the regional gravity without other sources of information on basement composition or structure. With gravity calculated for reasonable structural models of the Plateau and Valley and Ridge Paleozoic sedimentary cover, it may be possible to construct hypotheses about compositional variations in the basement that could be responsible for the disagreement between the observed and calculated gravity.

As mentioned in section B, the disagreement between calculated and observed gravity over the Blackwater anticline cannot be compensated for by Cambrian-Ordovician structure. Similarly, interpretations of the Ray-Sponaugle well in Pendleton County, West Virginia (Perry, 1964) of the Ray-Sponaugle and Greenland Lodge (Grant County, West Virginia) wells (Sites, 1978), and published seismic interpretation across the Wills Mountain anticline near Keyser, West Virginia (Bagnall, Beardsley, and Drabish, 1979), support duplication by faulting of the Cambrian-Ordovician carbonate sequence along the length of the Wills Mountain anticline. Yet, as we shall see, observed gravity differs by

more than a milligal (section C. this chapter) from calculated gravity for documented subsurface structure.

Where differences between observation and theory cannot be explained as errors of observation or measurement in the survey, and cannot be reconciled by adjustments of the model consistent with the assumed style of deformation, then the assumed structural style must be incorrect. It is possible that much of the disagreement between Kulander and Dean's (1978) residual Bouguer gravity and the calculated gravity lies in higher-order regional features (Wheeler, oral communication). Higher-order regional features in the earth's gravitational field could be produced by lateral density contrasts in the basement Grenvillian structural complex.

### C. Regional Gravity Profiles

Regional structural interpretations SS' and NN' were presented earlier in Chapter 111 (see Plate 1) for the Valley and Ridge and Plateau provinces of the central Appalachians of West Virginia and Virginia. Generalized segments of these cross sections covered by gravity observations are located on the residual Bouguer anomaly map (Figure 23 ) taken from Kulander and Dean (1978). Calculated gravity for those segments of sections SS' and NN' is compared to contours of residual Bouguer anomalies (Figures 24 and 25) and the terrain-corrected Bouguer gravity (Figure 26, 27 and 28) along these profiles. Profile intersections



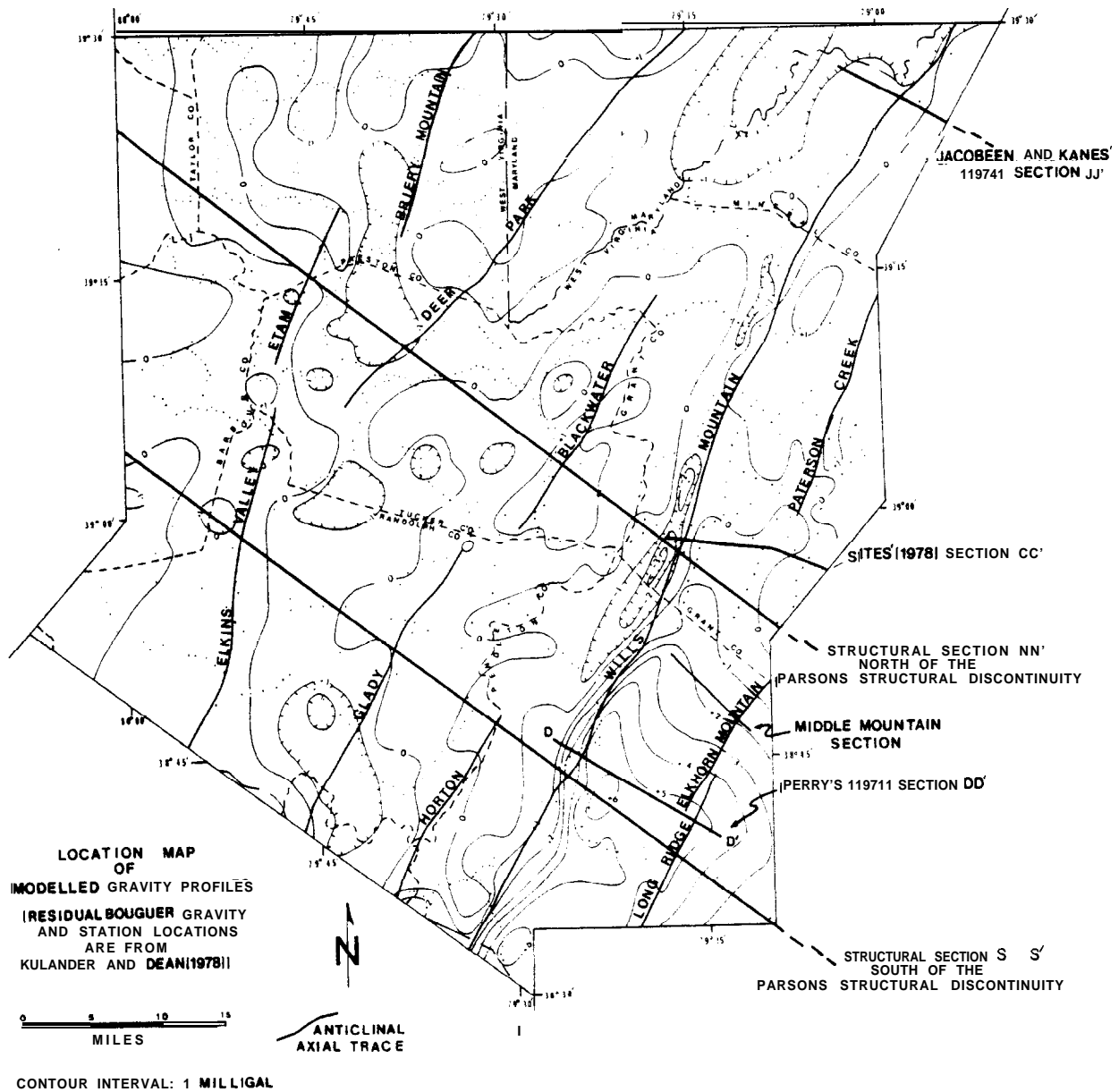


Figure 23

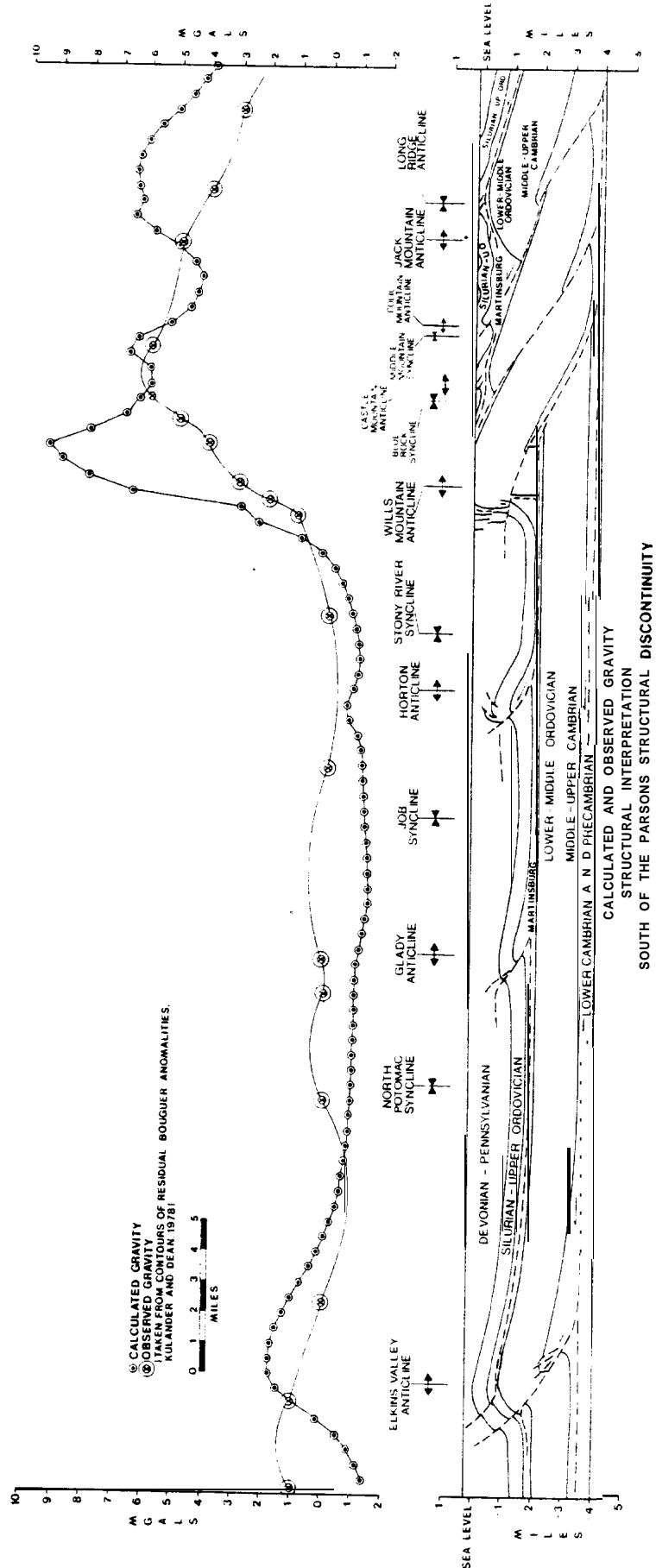


Figure 24 Calculated and Residual Bouguer Gravity Along Structural Interpretation SS' South of the Parsons

CSD are Plotted and Compared

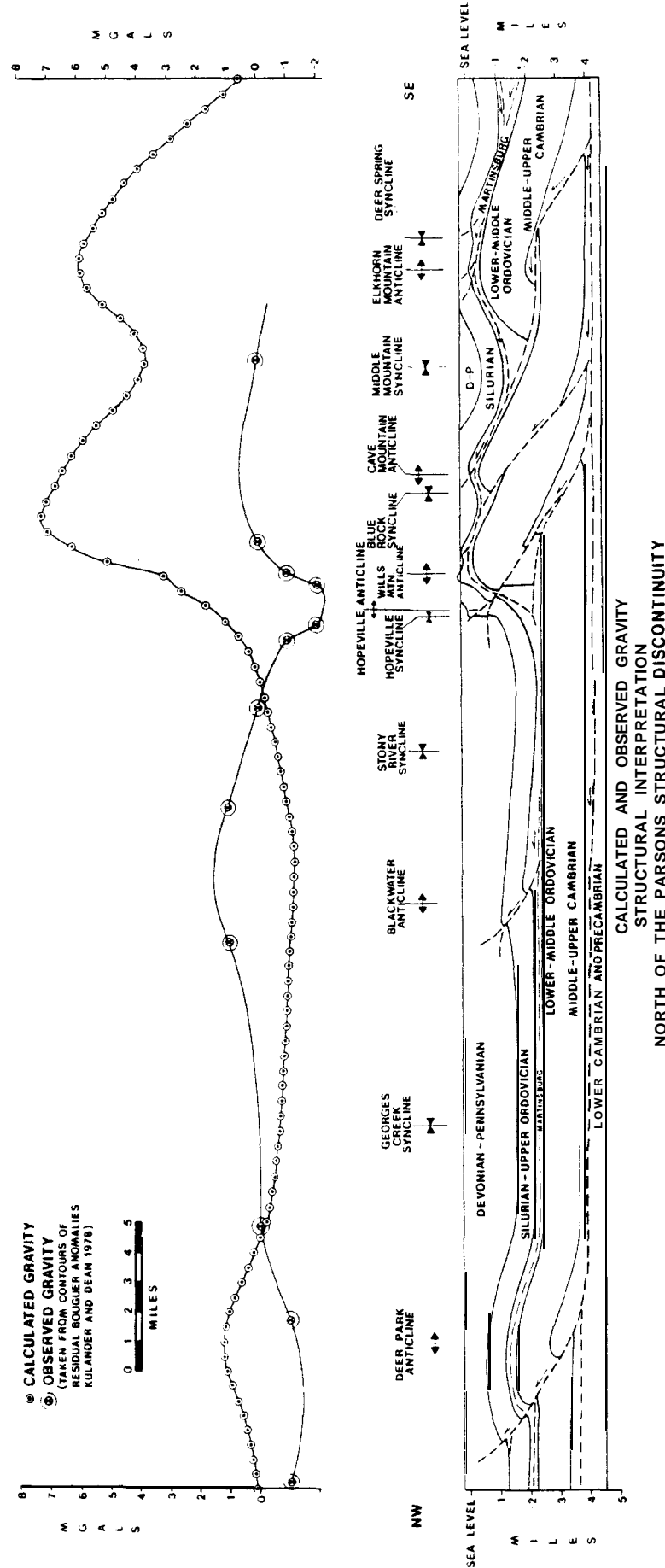


Figure 25 Calculated and Residual Bouguer Gravity Along the Structural Interpretation NN' North of the

Parsons CSD are Compared

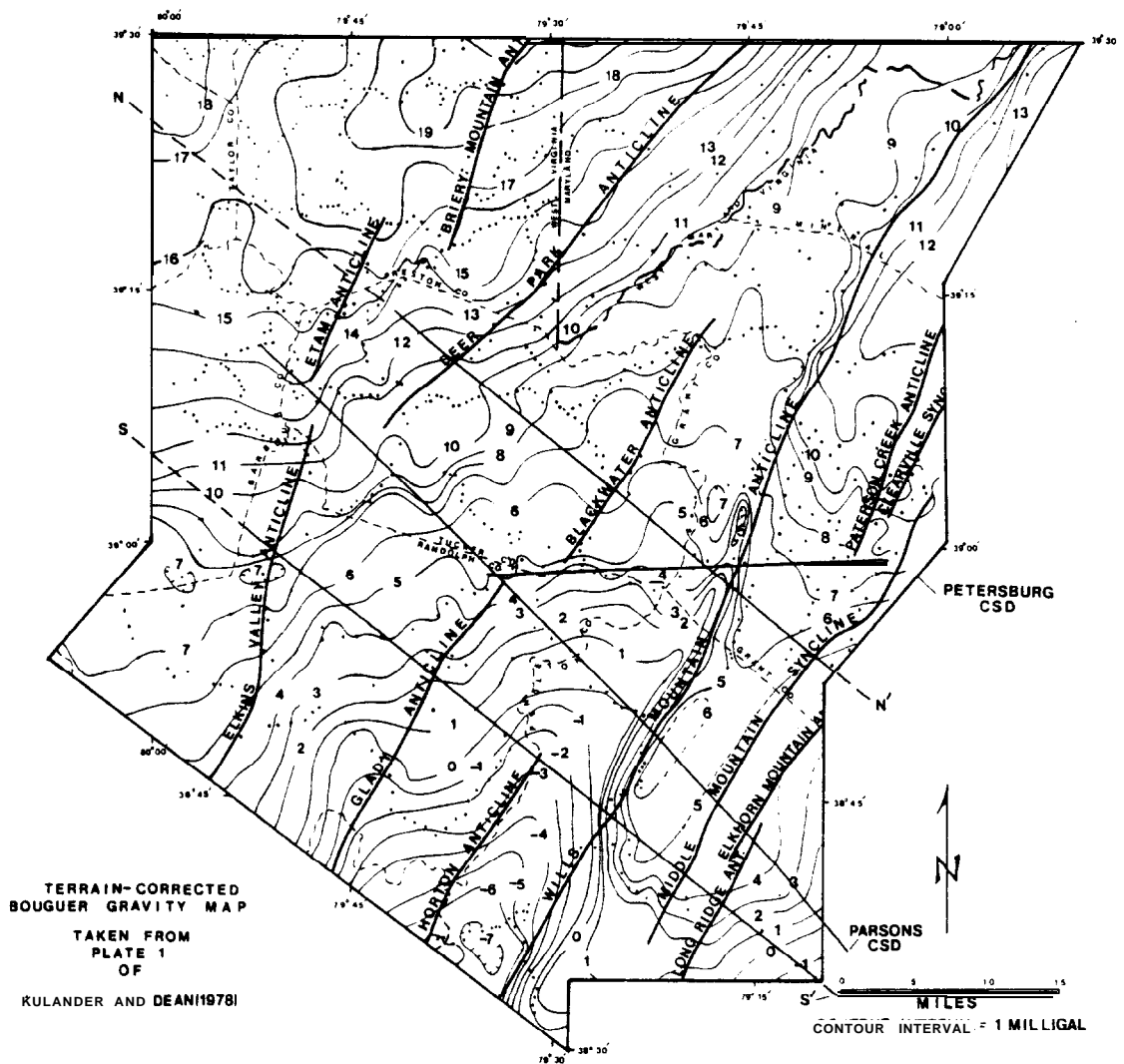
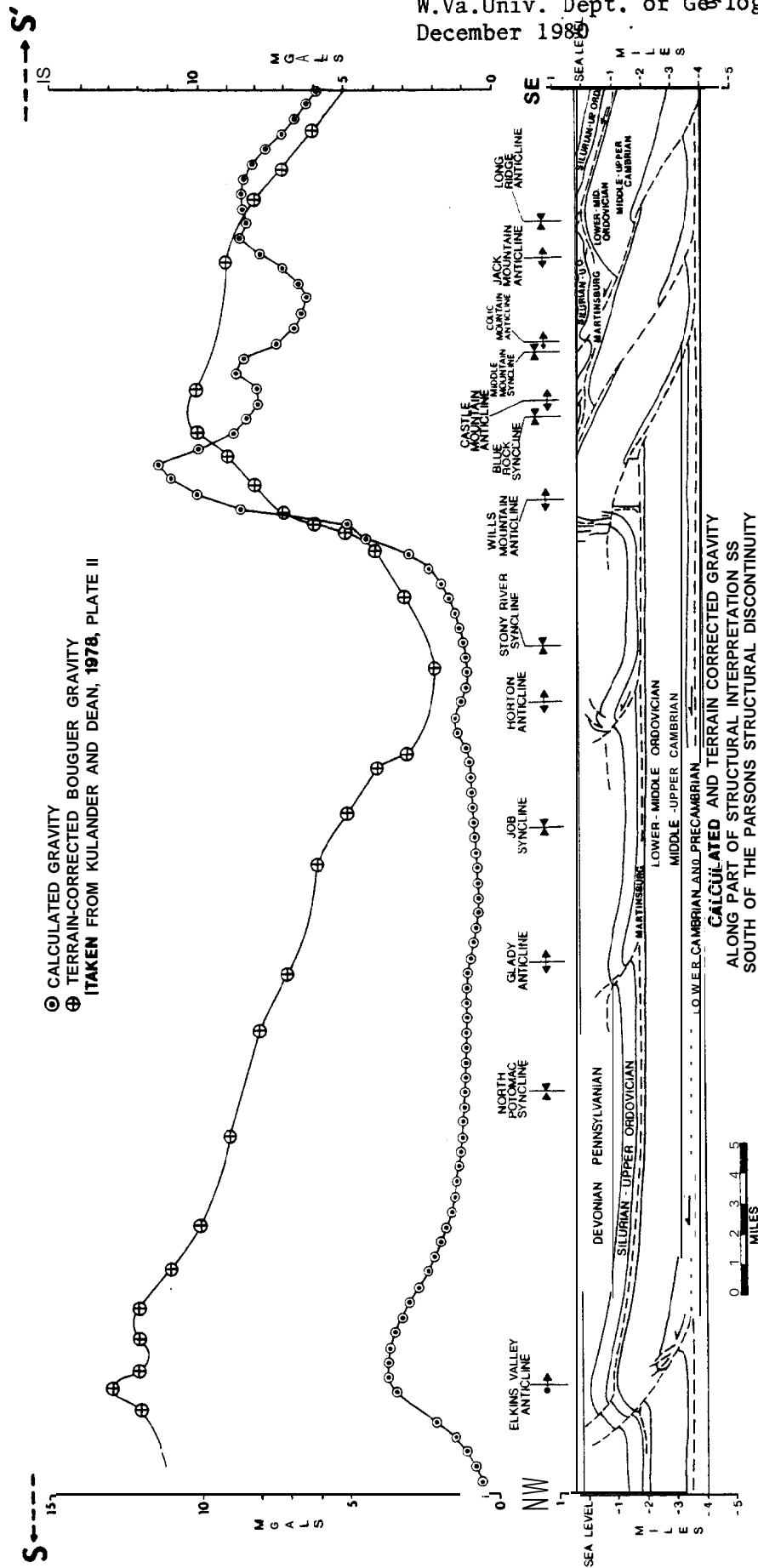


Figure 26 Structural Sections NN' and SS' are Located Along with the Petersburg and Parsons CSD's on Contours of Terrain-Corrected Bouguer Gravity Taken from Kulander and Dean, 1978.



**Figure 27** Calculated and Terrain-corrected Bouguer Gravity are Plotted and Compared for Structural Interpretation SS' South of the Parsons CSD

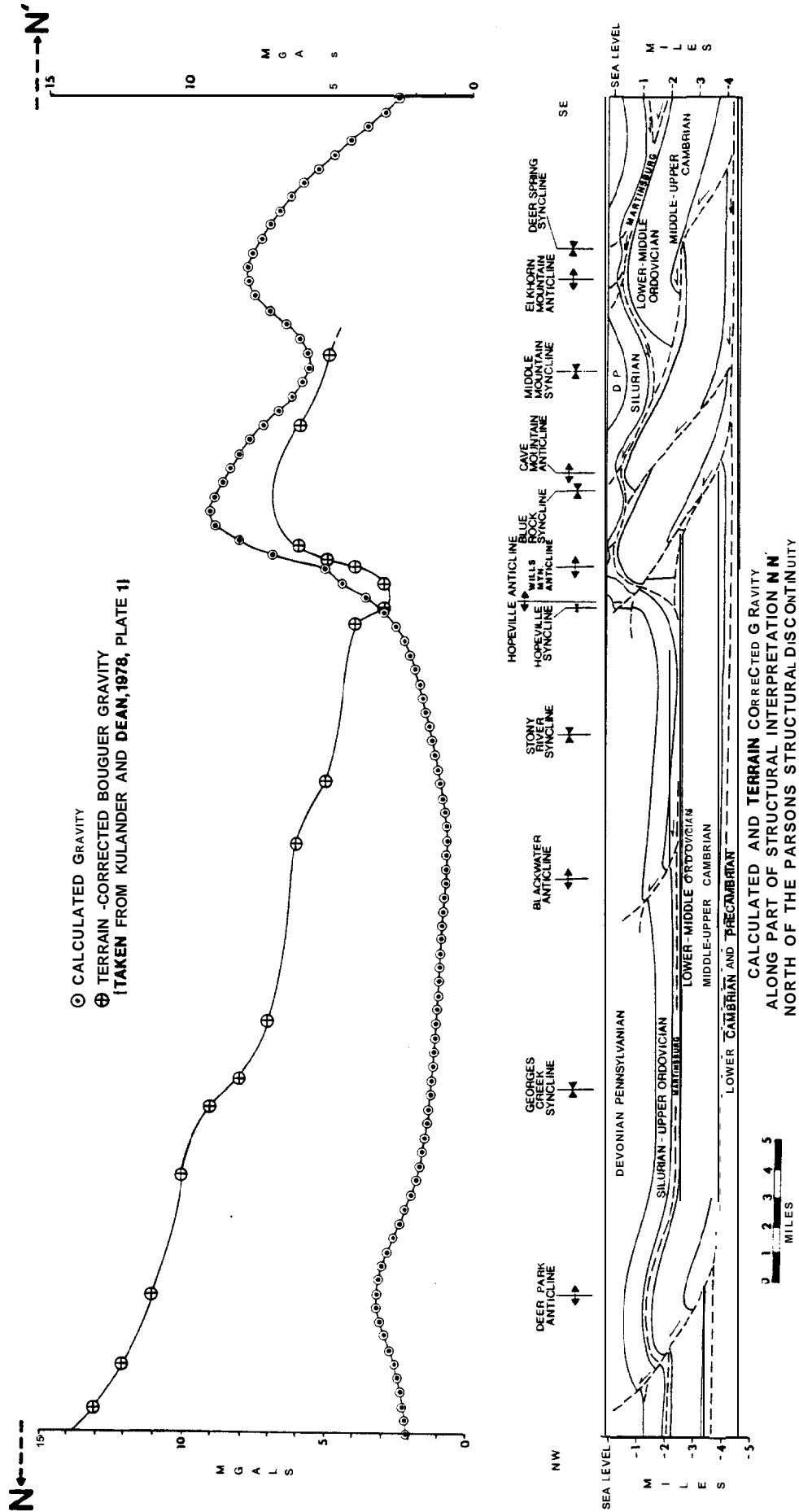


Figure 28 Calculated and Terrain-corrected Bouguer Gravity are Plotted and Compared for Structural

Interpretation NN' North of the Parsons CSD

with the contours were used. Density values used in the models are presented in Table 2.

Closest agreement between calculated and observed gravity occurs for section SS' (Figure 24). A two-milligal amplitude anomaly in observed gravity rises to a peak northwest of the **Elkins** Valley anticline. The calculated effect of the thrust faulted and folded high-density Cambrian and Ordovician carbonates is roughly a three-milligal anomaly rising to a peak just southeast of the crest of **Elkins** Valley anticline. There is rough correlation between the positions of the six-milligal high in observed gravity for structures between the Wills Mountain and **Elkins** Valley anticlines is uniformly less than the observed gravity.

Substantial disagreement is also found between observed and calculated gravity along section NN' (Figure 25 ). Much of this disagreement is less than 2 milligals. As noted earlier (section B), the error in the data is between 1 and 1-1/2 milligals so that this disagreement may not have structural significance. However, the low in observed gravity over the Deer Park anticline might imply that the Cambrian and Ordovician sequence is not thrust into the core of the anticline as shown in the cross section. In addition, Gwinn (1964) reports a 4,000-foot thickness of the Juniata Formation in the core of the Deer Park anti-

TABLE 4

Average Densities Assigned to  
Stratigraphic Intervals for  
Sections NN' and SS'  
(average calculated using densities  
taken from Kulander and Dean, 1978)

Stratigraphic Interval	Density	
	South	North
Pennsylvania through Devonian Oriskany Ss	2.61 gm cm <sup>-3</sup>	2.62 gm cm <sup>-3</sup>
Devonian Oriskany Ss through Ordovician Oswego Ss	2.64 gm cm <sup>-3</sup>	
Ordovician Martinsburg Fm	2.55 gm cm <sup>-3</sup>	2.55 gm cm <sup>-3</sup>
Ordovician Trenton Gp through Cambrian Elbrook Fm	2.71 gm cm <sup>-3</sup>	2.71 gm cm <sup>-3</sup>
Cambrian Waynesboro Fm into Precambrian	2.69 gm cm <sup>-3</sup>	2.69 gm cm <sup>-3</sup>



cline. However, the wavelength of the Deer Park fold is anomalously large for folds developed above a Martinsburg and/or higher level detachment. Martinsburg detachment produces folds of wavelengths similar to that for the Gladys and Horton anticlines (Figure 24). The numerous intermediate-scale folds observed at the surface in the Chemung Formation (Henderson, 1973; Wheeler, 1974; Mullenex, 1976; Trumbo, 1976) are probably developed above a Martinsburg, Juniata, and/or higher-level detachment. It seems likely, therefore, that considerably more shale is present than indicated in Figure 25, but that the Cambrian and Ordovician dolomites and limestones are faulted in the Deer Park core. Thus, the regional interpretation north of the Parsons structural discontinuity (see Plate 1) presented earlier (Chapter III) shows the presence of thickened Martinsburg shale in the core of the Deer Park anticline.

An uplift of 4,000 feet at the Trenton level would be required to produce the 1.5-milligal high over the Blackwater anticline. However, within the core of the Blackwater anticline, there is very little space available for the Cambrian and Ordovician carbonate sequence, so that if this sequence is thrust into the core of the Blackwater anticline, displacement along that thrust will have to be

small, and it certainly cannot be responsible for the observed anomaly.

As mentioned earlier, disagreement between the observed and calculated gravity may result from the removal of the regional gravity field. Contours of the terrain-corrected Bouguer gravity taken from Kulander and Dean (1978) are shown in Figure 26. Calculated gravity along segments of SS' and NN' are compared to the terrain-corrected Bouguer gravity in Figures 27 and 28. The terrain-corrected gravity increases steadily to the northwest of the Wills **Mountain** anticline along both sections SS' and NN'. If this almost linear rise to the northwest is chosen as the regional gravity field, then a somewhat different residual gravity field appears. Along section SS' (Figure 27 ) a positive one-to-two milligal anomaly occurs directly over the **Elkins** Valley anticline instead of further to the northwest as in Figure 24 for the residual Bouguer anomaly. In section NN' (Figure 28) the low over the Deer Park **anti-cline** would not be quite as low and the high over the **Black-water** anticline would disappear almost completely. The simple choice of a linear regional gradient in the Plateau would provide better agreement between calculated and observed or residual gravity. Likewise, in the Valley and Ridge southeast of the Wills Mountain anticline, better agreement can be produced by flattening the regional

gradient out to a constant value.

#### D. Valley and Ridge Models

##### 1. Perry's (1971) Section DD'.

Perry's (1971) section DD' (Figure 29) lies approximately two miles north of regional structural interpretations SS' (Figure 24). The model for DD' was extended several miles beyond the ends of the **calculated** profile to reduce edge effects. An average density assignment of  $2.64 \text{ gm cm}^{-3}$  (Table 3) to Silurian and Devonian rocks, when carried beyond the northwestern edge of the profile, has reduced the gravity high over the Wills Mountain anticline by 4 **milligals** from its value in section SS' (Figure 29 and Figure 24).

As discussed in the previous chapter (Chapter III, section e), Perry's (1971) section DD' (Figure 29) is different from the Valley and Ridge structure of SS' (Figure 24) in two respects: (1) there are four thrust slices in Perry's (1971) section, but only three in the southern section; and (2) the Martinsburg shale in Perry's (1971) section has not been thickened in front of the folded and thrust faulted Cambrian and Ordovician dolomites and limestones east of the Wills Mountain anticline, as is the case for section SS'. This ductile behavior of a shale at the leading edge of a brittle thrust sheet was documented for the Middle Devonian shales on the faulted southeast limb

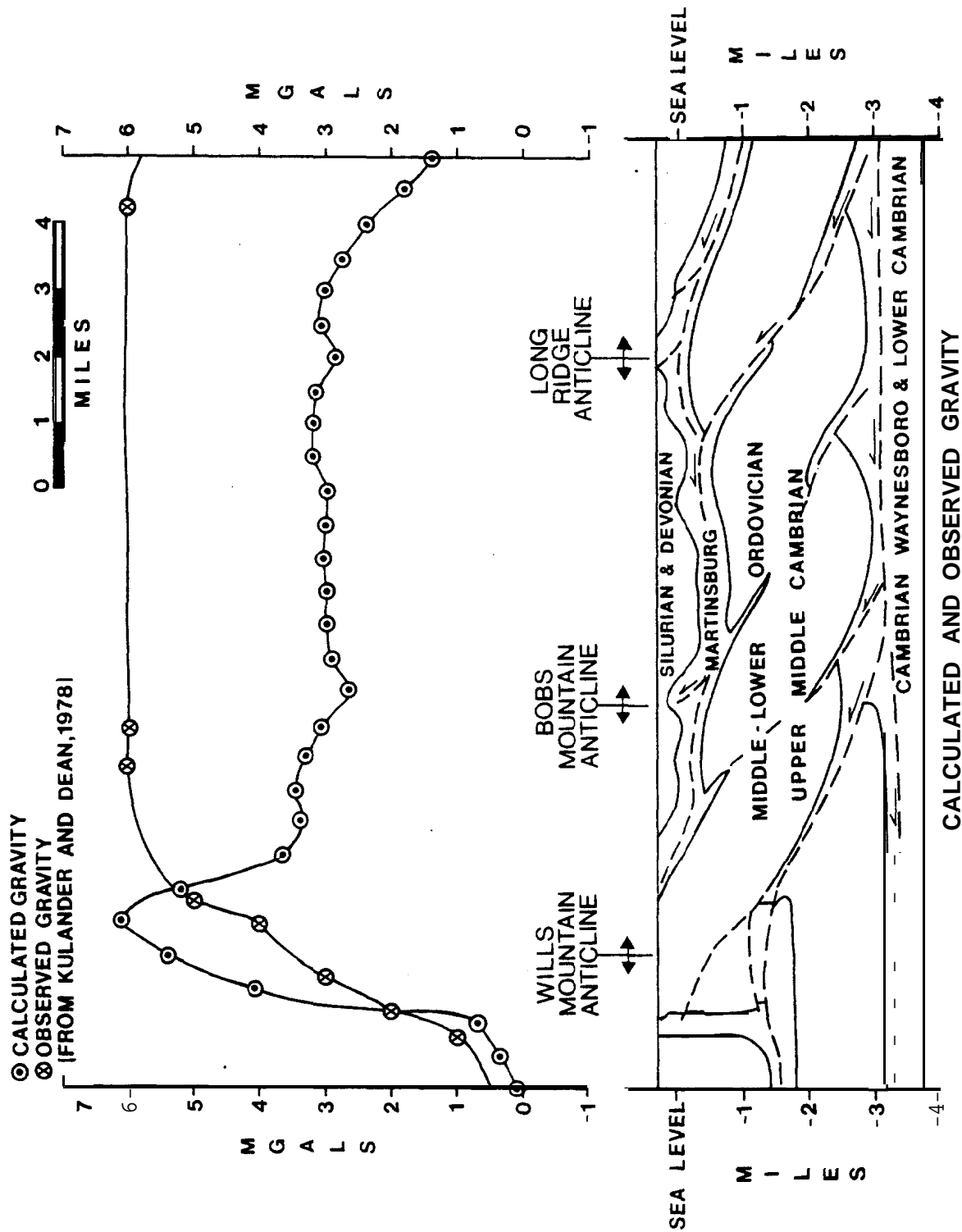


Figure 29 Calculated and Residual Bouguer Gravity are Plotted and Compared for Perry's (1971) Section DD'

TABLE 5

Average Densities Assigned to  
Stratigraphic Intervals for  
Perry's (1971) Section DD', Sites' (1978)  
Section CC", and the Corresponding  
Valley and Ridge Segment from SS'  
(averages calculated using densities  
taken from Kulander and Dean, 1978)

Stratigraphic Interval	Density
Devonian Oriskany Ss through Ordovician Oswego Ss	2.64 gm cm <sup>-3</sup>
Ordovician Martinsburg Fm	2.55 gm cm <sup>-3</sup>
Ordovician Trenton Gp through Cambrian Elbrook Fm	2.71 gm cm <sup>-3</sup>
Cambrian Waynesboro Fm into Precambrian	2.69 gm cm <sup>-3</sup>

of the Middle Mountain **syncline** (see Chapter II) and on the faulted northwest limb of the Wills Mountain anticline near Keyser, West Virginia (Bagnall, Beardsley, and Drabish, 1979). This thickened wedge of shale would produce a 2- to 3-milligal low in the observed gravity east of the Wills Mountain anticline, as shown in Figures 27 and 28. Kulander and Dean (1978) occupied very few stations in this area (Figure 23), so the existence of the low cannot be ruled out from the residual Bouguer anomalies profiled in Figures and .

## 2. The Middle Mountain Syncline.

A new gravity profile was surveyed across the Middle Mountain **syncline** to place constraints on the deep Ordovician and Cambrian structure. Twenty-eight stations were occupied at approximately four to five stations per mile. Where bench marks were not available, elevations were established with a precision barometric altimeter. Differences in elevation produced by fluctuations in barometric pressure were corrected for by using a continuous record of pressure changes recorded on a **baragraph** located in the field area. Errors in elevation were checked by periodically reoccupying a bench mark of known elevation. The error is from one to three feet, equivalent to 0.1 to 0.3 **milligals**. As mentioned above (section B of this chapter), standard deviation in value about a curve vis-

ually fit to the data is 0.65 milligals, and standard deviation about the calculated gravity for the proposed model is 1 milligal (Figure 30). Extension of the model layers horizontally to considerable distances from either end of the calculated profile has produced values of calculated gravity that are greater than the observed gravity near the edges of the profile. Average densities calculated for stratigraphic intervals used in the Middle Mountain model are listed in Table 4.

The structural model proposed for subsurface structure in Ordovician and Cambrian formations beneath the Middle Mountain **syncline** is shown in Figure 30. The observed gravity is consistent with the existence of a thickened wedge of the Ordovician Martinsburg Formation to the northwest of a thrust slice of Cambrian and Ordovician carbonates. In fact, the presence of observed gravity values lower than those calculated above the wedge suggests that the area of thickened shale may be more extensive than represented in the model.

Observed gravity values higher than those calculated for the model along the northwest flank of the **syncline** may imply that the Martinsburg Formation is abnormally thinned by **flexural** flow along the northwest limb of folded Cambrian and Ordovician carbonates beneath the southeast limb of the Cave Mountain anticline (see Figure 30). Similarly,

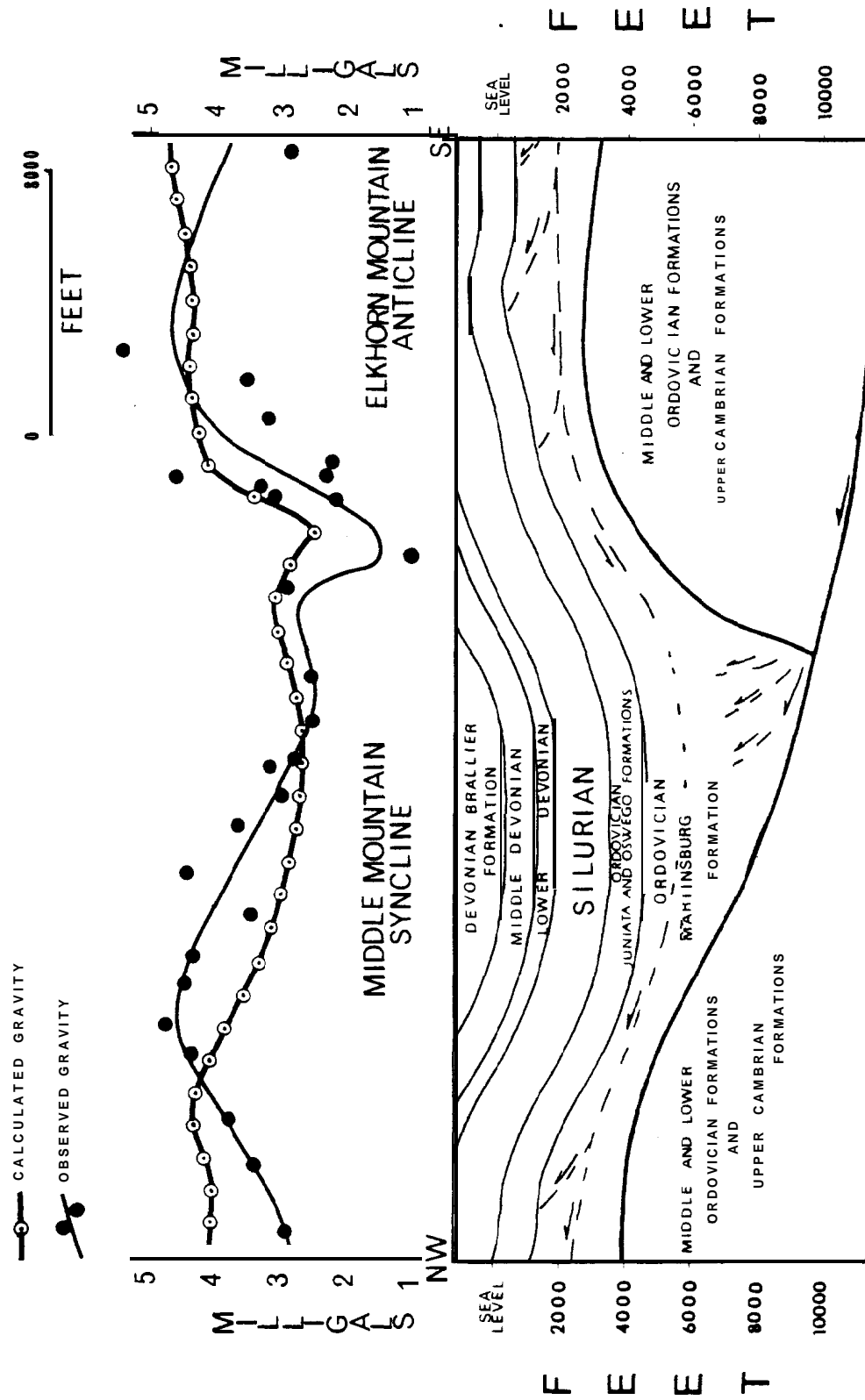


Figure 30 Calculated and Observed Gravity are Plotted and Compared for a Subsurface Structural Interpretation Across the Middle Mountain Syncline and Elkhorn Mountain Anticline



TABLE 6

Average Densities Assigned to  
Stratigraphic Intervals-in the  
Middle Mountain **Syncline**  
(averages calculated using densities  
taken from Kulander and Dean, 1978)

Stratigraphic Interval	Density
Devonian Brallier Fm	2.60 gm cm <sup>-3</sup>
Middle Devonian shales	2.63 gm cm <sup>-3</sup>
Lower Devonian Oriskany Ss and Helderberg Gp	2.69 gm cm <sup>-3</sup>
Silurian units	2.65 gm cm <sup>-3</sup>
Juniata Fm and Oswego Ss	2.63 gm cm <sup>-3</sup>
Martinsburg Fm	2.55 gm cm <sup>-3</sup>
Ordovician Trenton Gp and beneath	2.71 gm cm <sup>-3</sup>

the low observed values at the edges of the profile may result from decollement-related thickening in the cores of the Cave Mountain anticline to the northwest and Elkhom Mountain anticline to the southeast.

A list of pertinent gravity data is listed in Appendix IV for each station. A station location map is included as Plate 4.

### 3. Sites' (1978) Section CC'.

A theoretical gravity low over the Wills Mountain anticline (Figure 31) is produced by the thickening Martinsburg shale. Similar lows occur in the calculated gravity over the Cave Mountain and Elkhom Mountain anticlines.

The Cave Mountain and Elkhom Mountain anticlines in particular result entirely from Martinsburg detachment (Sites 1978). Whether the Cambrian and Ordovician involvement in these structures observed in the Middle Mountain gravity profile (Figure 30) dies out to the northeast as indicated by Sites (1978) is an interesting question that will require more detailed observation (see Chapter III, section e).

Average densities used in the model are listed in Table 4.

### 4. Jacobeen and Kanes' (1974) Section.

The Jacobeen and Kanes (1974) section located in Mineral and Hampshire Counties, West Virginia (Figure 23 and 32), shows a complete duplication of the Ordovician Edinburg through Cambrian Elbrook Formations. Net slip of the upper sheet of carbonates to the northwest over the

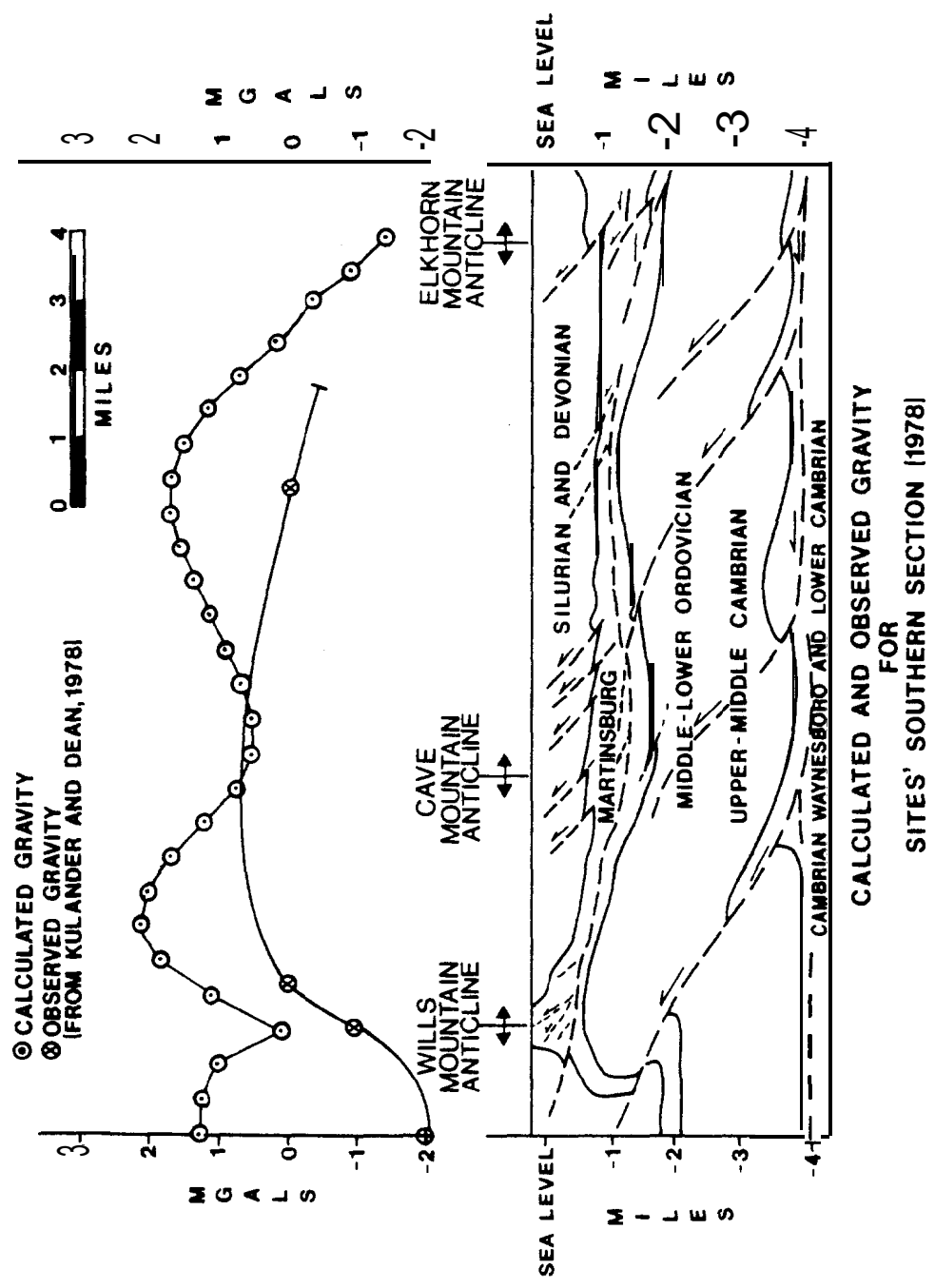


Figure 31 Calculated and Residual Bouguer Gravity are Plotted and Compared for Sites' (1978) Section CC'

TABLE 7

Average Densities Assigned to  
Stratigraphic Intervals for the  
**Jacobeen** and Kanes (1974) Section Line  
(averages calculated using densities  
taken from Kulander and Dean, 1978)

Stratigraphic Interval	Density
Devonian Hampshire Fm through Ordovician Oswego Ss	2.62 gm cm <sup>-3</sup>
Ordovician Martinsburg Fm	2.55 gm cm <sup>-3</sup>
Ordovician Trenton Gp through Cambrian Elbrook Fm	2.71 gm cm <sup>-3</sup>
Cambrian Waynesboro Fm into Precambrian	2.69 gm cm <sup>-3</sup>

lower sheet is approximately 12 miles. A double thickness interpretation is supported by seismic profiles across the **Broadtop** anticline (Jacobeen and Kanes, 1974, 1975: Zurgani, 1975) and on the northwest limb of the Wills Mountain anticline (Bagnall, Beardsley, and Drabish. 1979). Some question remains concerning the intervening Cambrian and Ordovician structure between the **Broadtop** anticline and the Wills Mountain **anticline**.

As mentioned previously (sections D.1 and D.2 of this chapter), thickening of ductile Middle Devonian shales is observed in the field and in the **subsurface** in front of splay-thrusts more brittle Lower Devonian and Silurian rocks. The gravity profile across the Middle Mountain **syncline** discussed in section D.2 supports the existence of a thickened wedge of Martinsburg shale in front of **splay-thrusts** Cambrian and Ordovician formations. If there are intervening thrust slices between the **Broadtop** and Wills Mountain anticlines, the shale wedges in front of these faults could be detected by observed gravity as done for the Middle Mountain syncline.

The deep Bedford **syncline** presents the greatest difficulty to drawing a complete duplication of the Cambrian and Ordovician formations. It is possible that the Bedford **syncline** is developed between two thrust slices (Figure 33 ). Gravity profiles are calculated for both

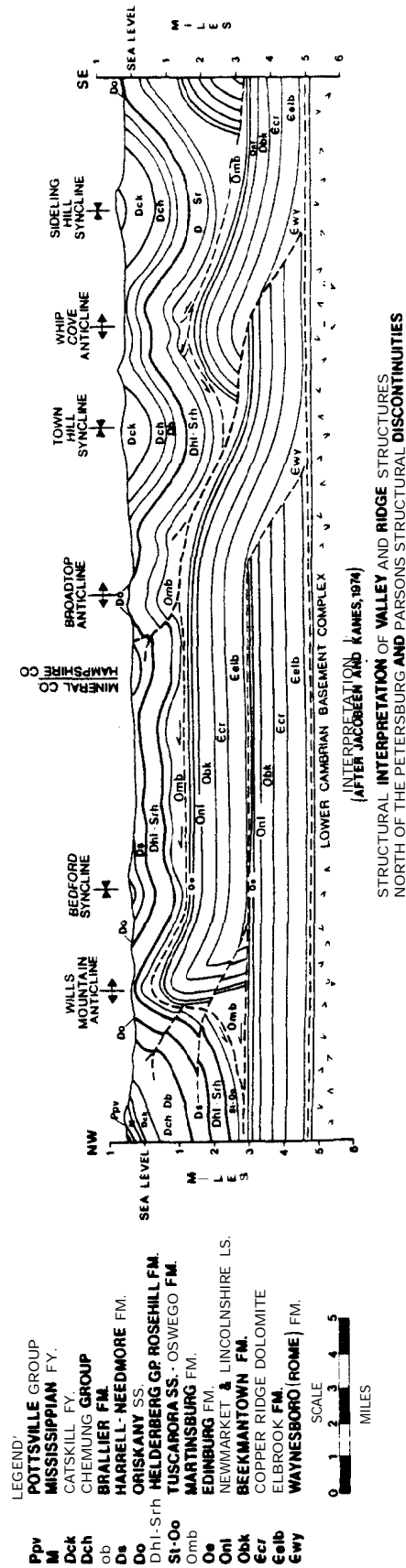


Figure 32

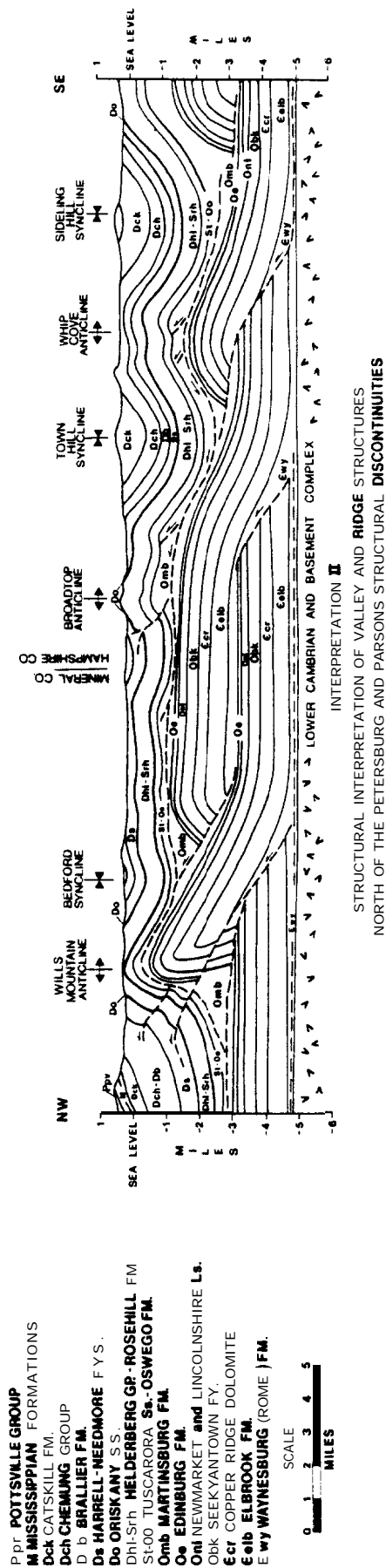


Figure 33

interpretations (Figures 34 and 35, respectively). Preliminary results of gravity profile surveyed across the Wills Mountain anticline and Bedford **syncline** along the **Jacobeen** and Kanes (1974) section line indicate that no thickened wedge of shale is present beneath the Bedford **syncline** (R. Perkey, oral communication, 1980). Thus, if Cambrian and Ordovician formations are faulted beneath the Bedford syncline, only minor amounts of displacement occur along the faults, and there is probably a complete duplication of these formations from the **Broadtop anticline** to the Wills Mountain syncline.

#### E. Conclusions

A useful subsurface structural model of the Cambrian-Ordovician structural **lithic** unit beneath the **Elkhorn** Mountain anticline and Middle Mountain **syncline** was obtained. The complexity of proposed subsurface structure required a station spacing of roughly 4 to 5 stations per mile and a constant regional gravity field was assumed.

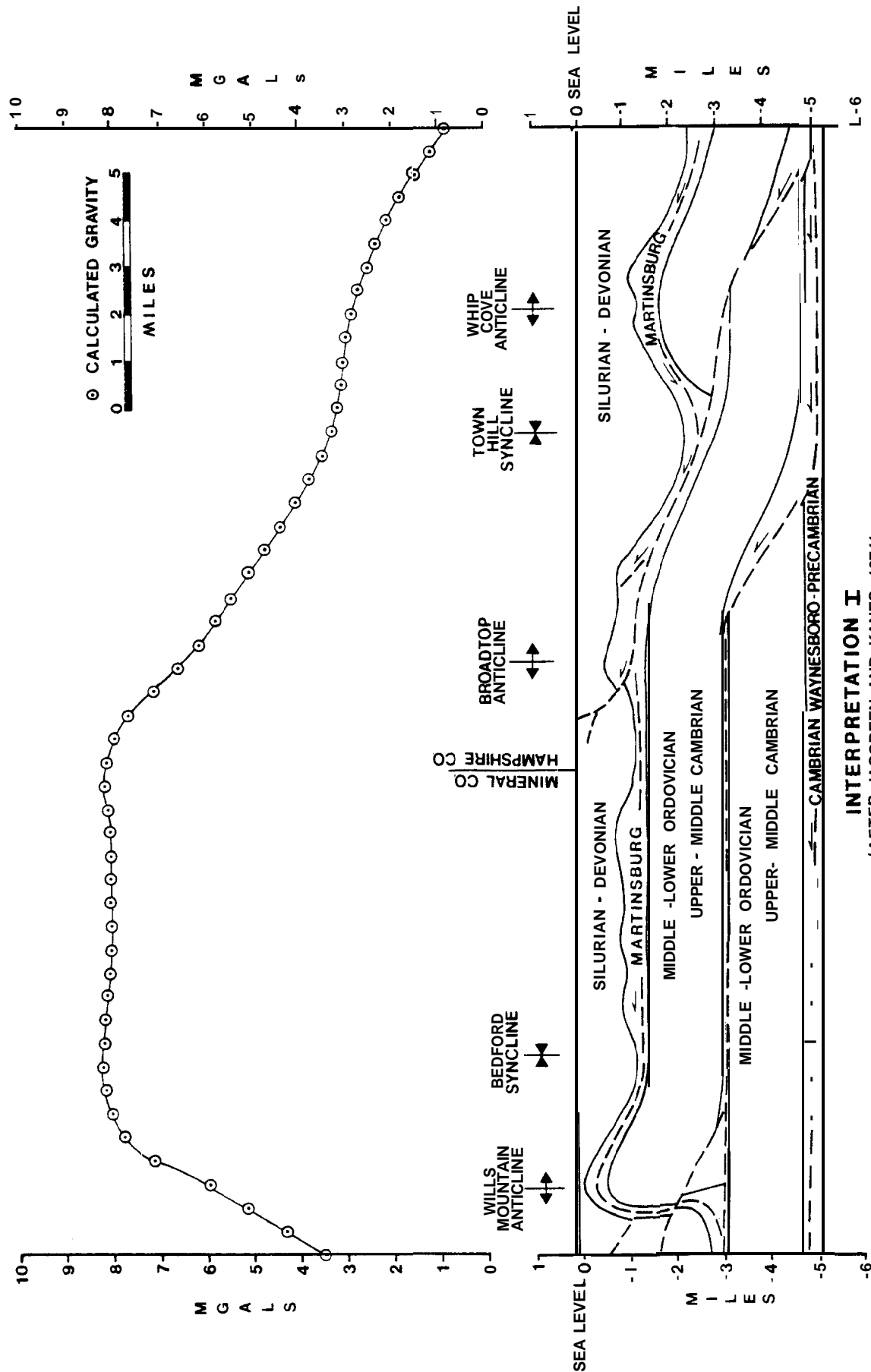
The presence of observed gravity values lower than those calculated above an inferred wedge of thickened Martinsburg shale suggests that thickening of the **shale** in response to thrust faults in the Cambrian-Ordovician sequence may be more extensive than represented in the model. Observed gravity values higher than those calculated for



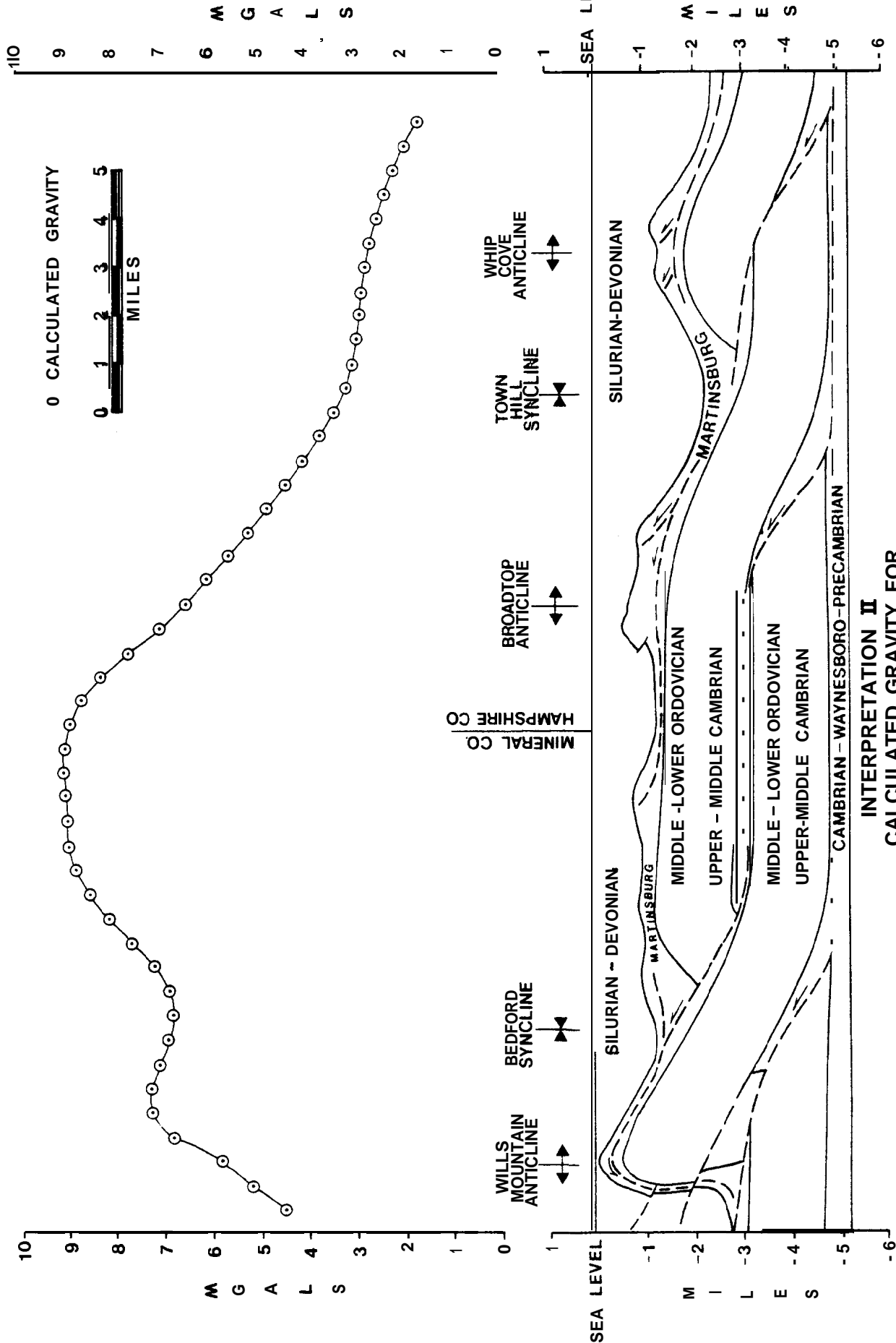
the model along the northwest flank of the **syncline** may imply that the Martinsburg Formation is abnormally thinned by **flexural** flow along the northwest limb of folded Cambrian and Ordovician carbonates beneath the southeast limb of the Cave Mountain anticline. Similarly, the low observed values at the edges of the profile may result from **decollement**-related thickening in the cores of the Cave Mountain anticline to the northwest and **Elkhorn** Mountain anticline to the southeast.

The use of observed gravity has the potential to be very useful in defining the characteristics of subsurface structure in the central Appalachians. The uncertainties in the observed gravity values in the Middle Mountain gravity profile are of the order of one **milligal**, so that useful data for subsurface **modelling** requires that appropriately detailed observations be made, particularly in structurally complex areas. The removal of the regional **gravity** field also presents problems in the interpretation of observed gravity. This problem is particularly apparent in the comparison of calculated gravity to the terrain-corrected residual Bouguer gravity of Kulander and Dean (1978). In this study, better results were obtained by making comparisons directly to the terrain-corrected **Bouguer** gravity and avoids making the regional gravity field unnecessarily complex. This also avoids making unnecessary assumptions about deep

basement structure -- structures which, for the most part, one knows even less about than **the** near surface structures being modelled. Thus, if attention is given to **potential sources of** disagreement between **the** observed and calculated gravity, one can be reasonably certain that differences between the observed and calculated gravity will be related to errors in the structural model.



INTERPRETATION I  
(AFTER JACOBSEN AND KANES, 1974)  
CALCULATED GRAVITY FOR  
STRUCTURAL INTERPRETATION OF VALLEY AND RIDGE STRUCTURES  
NORTH OF THE PETERSBURG AND PARSONS STRUCTURAL DISCONTINUITIES



**INTERPRETATION II**  
**CALCULATED GRAVITY FOR**  
**STRUCTURAL INTERPRETATION OF VALLEY AND RIDGE STRUCTURES**  
**NORTH OF THE PETERSBURG AND PARSONS STRUCTURAL DISCONTINUITIES**

## V. SUGGESTIONS TO FUTURE WORKERS

1. Additional detailed mapping and small scale structural studies of small structures along the Parsons discontinuity would be very useful in providing a more complete description of the structural characteristics of the discontinuity. Quickly acquired and useful results could be obtained by extending the area of detailed mapping completed by Henderson (1978), Mullenex (1974) and Trumbo (1976) in western Tucker County, West Virginia further south along the **Elkins** Valley anticline in western Randolph County. Results of such a study might lead to further implications concerning the nature of the tear fault suggested for the deep Cambrian-Ordovician sequence between the plunging noses of the Deer Park and **Elkins** Valley anticlines. A study of the relationship or lack of relationship between systematic joint intensity and local structures would also be useful.
2. Surveyed gravity profiles with station spacings on the order of 0.5 miles across the Deer Park and **Elkins** Valley anticlines would help define subsurface structure across these folds.
3. The Shenandoah **syncline** is apparently undeformed across the Parsons structural discontinuity.

There are excellent exposures of Middle Devonian shales in the **syncline** providing an opportunity to look for small structural effects of the discontinuity in this area.

4. The Bergton-Crab Run and Adams Run anticlines represent other structures where detailed structural studies would be quite informative. It may be possible to verify the presence of the inferred subsurface tear fault in the Cambrian-Ordovician sequence across the plunging noses of these structures.

Detailed gravity profiles surveyed across these structures would also provide a rapid means of evaluating the extent of subsurface Cambrian-Ordovician involvement in these two anticlines.

5. One area across which detailed gravity profiles must be surveyed is the Petersburg area, particularly to the north across the inferred transfer zone in Cambrian-Ordovician rocks. Such a study should be quite detailed and cover the area between the Allegheny structural front and the synclines southeast of the **Elkhorn** Mountain and **Broadtop** anticlines, extending north to the Grant-Mineral County border. This would include the area of two northerly (or left lateral) shifts in the trend of the **Wills** Mountain anticline. The southern trend change is at North Fork gap, and another is

further north at Greenland gap. These bends may in some way be related to the transfer zone across the Petersburg structural discontinuity.

Surface structural studies should be undertaken northeast of Sites' (1978) map area and McCullochs' (1977) map area in Grant, Hampshire and Mineral Counties, West Virginia. However, such studies should not proceed until detailed gravity studies have been completed.

An understanding of the regional and local expression of surface structures and their relationship to the underlying Cambrian-Ordovician structure will provide valuable information regarding the mechanisms of thin-skinned tectonics.

6. Several structural discontinuities have been noted in the central and southern Appalachians. The locations of several of these discontinuities along which field studies have been conducted are located in Figure 36 taken from Wheeler (1980). Restraint has been exercised to refrain from relating the mechanical origins of all or most structural discontinuities to vertically stacked transfer zones and/or tear faults. This chapter seems to be a fairly safe place to make that suggestion.

In Chapter III, section F, it was mentioned that the folds of the High Plateau plunge out along a **cross-strike** line that coincides with the Tyrone-Mount Union

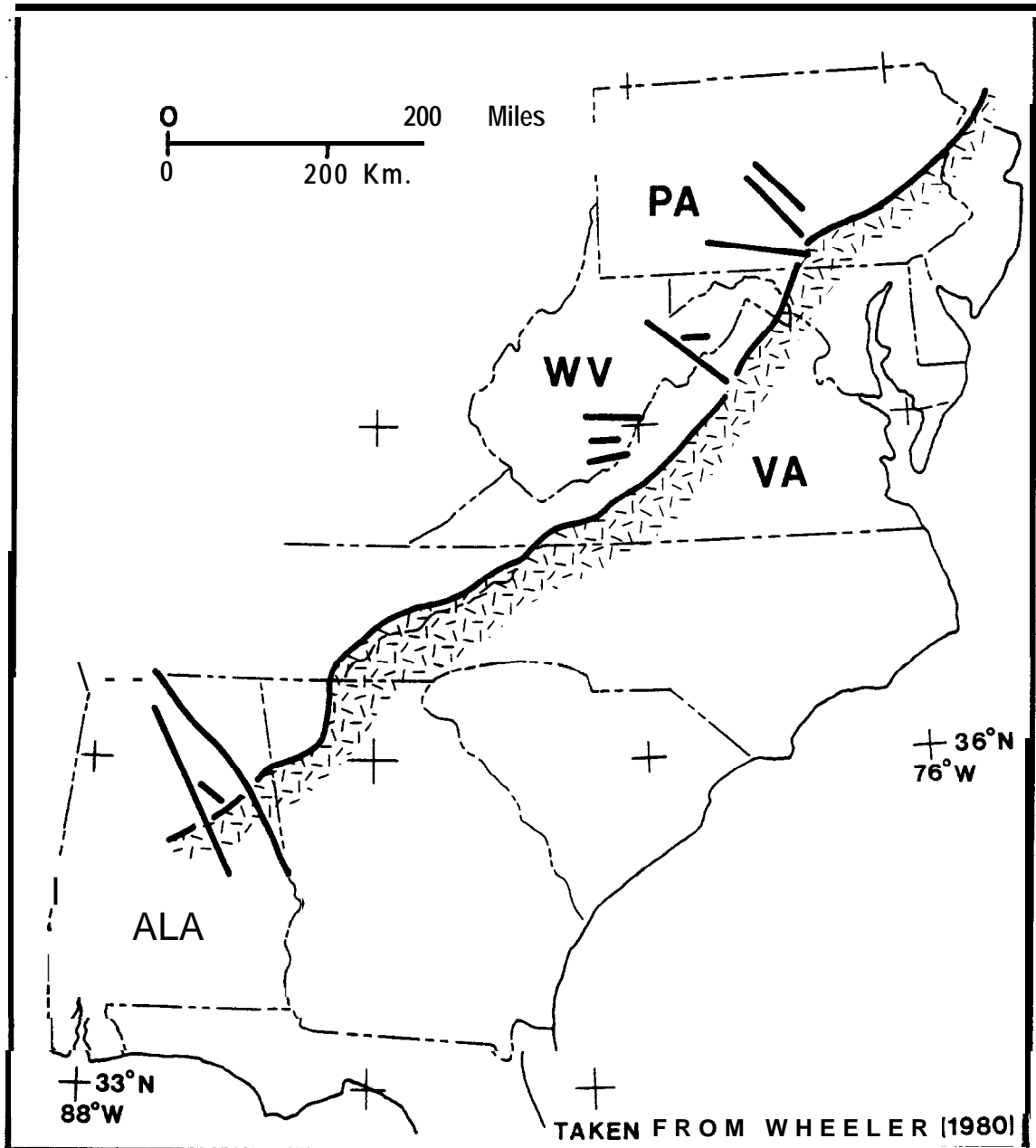


Figure 36 Location Map of Appalachian CSD's 'Taken from Wheeler, 1980



lineament. In addition to the alignment of noses in High Plateau folds, the Sinking Valley anticline and Wills Mountain anticlines terminate (Figure 22) along with terminations of faulting along the Little North Mountain thrust and other thrusts in the Cambrian-Ordovician of the Great Valley. Kowalik (1975) indicates that there is no evidence of tear faulting along the length of this lineament, but suggests that this and other "Gwinn-type" lineaments defined by:

abruptly plunging ends are due to formation within thrust blocks bounded by "stepped" tear faults or laterally restricted thrusts. (Kowalik, 1975, p. 13)

Although his model (Kowalik, 1975, his Figure 6) does not provide a compensating mechanism for shortening within and on either side of the "lineament", his descriptions of the Tyrone-Mount Union, the Bedford-Everett, and other "Gwinn-type" lineaments in Pennsylvania are very similar to those for the Parsons and Petersburg cross-strike structural discontinuities of West Virginia.

Wheeler (1978 and 1980) reports that traits most commonly shared among Appalachian cross-strike structural discontinuities are the alignment of bends, noses, and style changes of detached map-scale folds.

Re-evaluation of available surface structural information for individual discontinuities can test the hypo-

thesis that commonly observed traits are related to  
the presence of transfer zones in detached fold belts.

## VII. CONCLUSIONS

Surface structural studies along: the Middle Mountain **syncline** and **Elkhorn** Mountain anticline indicate that the Parsons structural discontinuity crossing these structures is a zone across which displacement along a Martinsburg detachment is transferred to Juniata, Wills Creek and Middle Devonian detachment horizons southwest of the discontinuity, but is confined to the **Martinsburg** northeast of the discontinuity. The structural relationships across the discontinuity can be explained by representing the discontinuity as a transfer zone (Dahlstrom, 1969) within which shortening is taken up by small displacements along more numerous faults and by increased numbers of small folds. Shortening across the Middle Mountain **syncline** and **Elkhorn** Mountain anticline is discontinuous northeast along strike across the **discontinuity**, however, displacement along the Martinsburg detachment northeast of the discontinuity ramps up to higher structural levels producing an equivalent amount of shortening northwest across the resultant Cave Mountain **anticline**. Instead of tear faults across the structure, constant shortening is accommodated mechanically by a transfer zone.

In the Silurian-Devonian formations of the Plateau, the transfer is seen to oscillate northeast to southwest,

back and forth to the northwest across the Plateau producing the Horton, Blackwater, and Glady anticlines and, in part, the Deer Park and **Elkins** Valley anticlines.

The expression of the Parsons discontinuity, however, is not confined to detachment in the **Ordovician Martinsburg** Formation and higher level detachment intervals. Detached structures in the Cambrian-Ordovician dolomite and limestones sequence are also related to the expression and development of the structural discontinuity. The Deer Park and **Elkins** Valley anticlines are related in part to ramping through the Cambrian-Ordovician sequence. A north-easterly swing in fold trends along the plunging nose of the Deer Park anticline (**Wheeler**, 1976) is related to a tear fault in the Cambrian-Ordovician sequence beneath the plunging noses of the **Elkins** Valley and Deer Park anticlines. The required right-lateral tear could be produced if slip along the Rome beneath the **Elkins** Valley anticline continued over a longer period of time or at a greater rate than clip beneath the Deer Park anticline.

Cambrian-Ordovician involvement is not confined to the Plateau segment of the Parsons discontinuity. The Bergton-Crab Run and Adams Run anticlines of the Valley and Ridge in Rockingham County, Virginia, are related to ramping of the Cambrian-Ordovician sequence and both **anticlines** plunge out southwest across the Parsons discontinuity.

A tear fault in the Cambrian-Ordovician sequence has been proposed across the plunging noses of these two folds on the basis of an abrupt change in shortening in that sequence across the discontinuity and a substantial left lateral swing in surface fold traces across the discontinuity.

The transfer zone mechanism also explains the surface expression of the Petersburg discontinuity. In addition, subsurface information indicates that a broad transfer zone occurs in the Cambrian-Ordovician sequence across the Petersburg discontinuity.

Reported characteristics (Wheeler, 1978) suggests that most central and southern Appalachian cross-strike structural discontinuities may actually be transfer zones.

A study of systematic joint intensity in the Parsons discontinuity across the Middle Mountain syncline indicates that increased folding and faulting in the transfer zone produces intensely jointed rock.

REFERENCES CITED

- Allen, R. M., Jr., 1967, Geology and mineral resources of Page County: Virginia Division of Minerals Resources Bulletin 81, 78p, 1 Plate.
- Anderson, E. M., 1951, The dynamics of faulting and dyke formation, with applications to Britain, Oliver and Boyd, London, 206 p.
- Bagnall, W. D., Beardsley, R. W., Drabish, R. A., 1979, The Keyser gas field Mineral County, West Virginia, In Avary, K. L., ed., Devonian clastics in West Virginia and Maryland: AAPG field trips, Oct. 1-4, 1979, Morgantown, W. Va., pp. 69-76.
- Bally, A. W., Gordy, P. L., and Stewart, G. A., 1966, Structure, seismic data, and orogenic evolution of southern Canadian Rocky Mountains: Bull. Canadian Petrol. Geol., v. 14, pp. 337-381.
- Benvenuto, G. L. and Price, R. A., 1979, Structural evolution of the Hosner thrust sheet, southeastern British Columbia: Bull. of Canadian Petroleum Geology, v. 27, pp. 360-394.
- Berger, P., and Johnson, A. M., 1980, First-order analysis of deformation of a thrust sheet moving over a ramp: in review Tectonophysics, 23 pp.
- Brent, W. B., 1960, Geology and mineral resources of Rockingham County: Bulletin 76 of the Virginia Division of Mineral Resources, 174 p., 1 Plate.
- Byerly, J. R., 1973, Gravity profile across Massanutten Syndinorium at Bedington, West Virginia: a study in gravity modeling of near-surface structure in the central Appalachians (abstract): Proceedings of the West Virginia Academy of Science, 45: 283-284.
- Cardwell, D. H., Erwin, R. B., and Woodward, H. P., Compilers, 1968, Geologic map of West Virginia: Morgantown, W. Va., West Virginia Geol. and Econ. Survey, scale 1:250,000, 2 sheets.
- Cardwell, D. H., 1974, Oriskany and Huntersville gas fields of West Virginia: West Virginia Geol. and Econ. Survey Mineral Resources Series; No. 5, 151 p. 1 Plate.

- Cardwell, D. H., 1977, West Virginia gas development in Tuscarora and deeper formations: West Virginia Geol. and **Econ.** Survey Mineral Resources Series No. 8, 34 p. 1 Plate.
- Cardwell, D. H., 1978, Oil and gas report and maps of Marshall, Wetzel and Tyler Counties in W. Va.: **Morgan-**town, W. Va., West Virginia Geol. and **Econ.** Survey Bulletin 12 A, 39 p, 1 Plate.
- Chopple, W. M., and Spang, J. H., 1974, Significance of layer-parallel slip during folding of layered sedimentary rocks: Geol. **Soc.** Amer. Bull. v. 85, pp. 1523-1534.
- Chen, Ping-fan, 1977, Lower Paleozoic stratigraphy, tectonics, paleogeography, and oil/gas possibilities in the Central Appalachians (West Virginia and adjacent states) Part 1. Stratigraphic maps: West Virginia Geol. and **Econ.** Survey, Report of Inv. RI-26-1.
- Chinnery, M. A., 1966, Secondary faulting: Canadian Journal of Earth Science, v. 3, pp. 163-190.
- Cook, F. A., Dennis, S. A., Brown, L. D., Kaufman, S., Oliver, J. E., and Hatcher, R. D., 1979, Thin-skinned tectonics in the crystalline southern Appalachians; **COCORP seismic**--reflection profiling of the Blue Ridge and Piedmont: Geology, v. 7, pp. 563-567.
- Currie, J. B., **Patnode**, H.W., and Trump, R. P., 1962, Development of folds in sedimentary strata: Geol. **Soc.** Amer. Bull., v. 73, pp. 655-674.
- Dahlstrom, C. D. A., 1969, Balanced cross sections: Canadian Jour. Earth Sci., v. 6, pp. 743-757.
- Dahlstrom, C. D. A., 1970, Structural geology in the eastern margin of the Canadian Rocky Mountains: Bull. **Canad.** Petrol. Geol., v. 18, pp. 332-406.
- Dennison, J. M., 1961, Stratigraphy of the Onesquethaw stage of Devonian in West Virginia and bordering **states**. West Virginia Geological and Economic Survey Bulletin 22, 87 pp.
- Dennison, J. M., and Naegle, O. D., 1963, Structure of Devonian strata along the Allegheny Front from **Cor-**riganville, Maryland, to Spruce Knob, West Virginia. West Virginia Geological and Economic Survey Bulletin 24, 42 p.

- Dennison, J. M., and Hasson, K. O., 1974, Lithostratigraphic nomenclature recommendations for Devonian Hamilton Group in Southern Pennsylvania, Maryland, and the Virginias. Talk presented at annual meeting Northeastern Section of the Geological Society of America. Abstract published in Abstract with Programs, GSA, vol. 5, No. 1, p. 18.
- Dennison, J. M., and Johnson, R. Y., Jr., 1971, Tertiary intrusions and associated phenomena near the thirty-eighth parallel fracture zone in Virginia and West Virginia: Geol. Soc. America Bull., v. 82, pp. 501-508.
- Dietrich, J. H., 1969, Computer experiments on mechanics of finite amplitude folds. Canadian Jour. Earth Sci., v. 7, pp. 467-476.
- Dixon, J. M., 1979, Techniques and Tests for measuring joint intensity, Ph.D. dissertation, West Virginia Univ., 144 pp.
- Donath, F. A., and Parker, R. B., 1964, Folds and folding: Geol. Soc. Amer. Bull., v. 75, pp. 45-62.
- Drahovzal, J. A., Neathery, T. L., and Wielchowsky C. C. 1974, Significance of selected lineaments in Alabama: in 3rd Earth Resources Technology Satellite - 1 Symposium Proc.: Natl. Aeronautics and Space Adm. SP351, v. 1, pp. 897-918.
- Engelder, T., and Engelder, R., 1977, Fossil distortion and decollement tectonics of the Appalachian plateau: Geology, v. 5, pp. 457-460.
- Evans, M. A., ms. 1980, Fractures in Oriented Devonian Shales cores from the Appalachian Basin Masters Thesis, Dept. Geology, West Virginia University, 276 pp.
- Girdler, R. talk, 1979, Go stop go sea floor spreading, talk given at the NATO conference on Plate Tectonics and Continental Drift, Univ. Newcastle-upon-Tyne Newcastle-upon-Tyne, England, March-April, 1979.
- Gold, D. P., Parizek, R. R., and Alexander, S. S., 1973, Analysis and applications of ERTS-1 data for regional geologic mapping, in Symposium on significant results obtained from the Earth Resources Technology Satellite -1, v. I, Technical Presentations, Section A: U. S.



- Natl. Aeronautics and Space Adm., Spec. Pub. 327,  
p. 231-245.
- Gwinn, V. E., 1964, Thin skinned tectonics in the Plateau and Northwestern Valley and Ridge provinces of the central Appalachians. *Geol. Soc. Amer. Bull.*, vol. 75, pp. 863-900.
- Hafner, W., 1951, Stress distributions and faulting: *Geol. Soc. Amer. Bull.*, v. 62, pp. 373-398.
- Harris, L. D., 1970, Details of thin-skinned tectonics in parts of Valley and Ridge and Cumberland plateau provinces of southern Appalachians: in Fisher, G. W., et al, eds., *Studies in Appalachian geology, central and southern*, Interscience Pub., N.Y., pp. 161-173.
- Harris, L. D., and Bayer, K. C., 1979, Sequential development of the Appalachian orogen above a master decollement--A hypothesis: *Geology*, v. 7, pp. 568-572.
- Hasson, K. O., 1972, Stratigraphy and structure of the Harrell Shale and part of the Mahantango Formation between Bedford, Pa., and Scherr, West Virginia. *Guidebook, Thirty-Seventh Annual Field Conference of Pennsylvania Geologists*, pp. 81-89.
- Hasson, K. O., and Dennison J. M., 1974, The Pokejoy Member, a new subdivision of the Mahantango Formation (Middle Devonian) in West Virginia, Maryland, and Pennsylvania. *Proceedings of the West Virginia Academy of Science*, v. 46, No. 1, pp. 78-86.
- Henderson, C. D., ms, 1973, minor structures of the High Plateau, northeastern Tucker Co., West Virginia: M.S. thesis, West Virginia Univ., 43 pp.
- Hennen, R. V., and White, I. C., 1909, Marshall! Wetzel, and Tyler Counties, West Virginia: *West Virginia Geol. and Econ. Survey County Geologic Report*, 654 pp.
- Hennen, R. V., Reger, D. B., and White, I. C., 1913, Marion, Monongalia, and Taylor Counties, West Virginia: *West Virginia Geol. and Econ. Survey County Report*, 844 op.
- Hennen, R. V., White, I. C., 1912, Doddridge and Harrison County Report: *West Virginia Geol. and Econ. Survey County Report*, 712 pp.

- Holland, S., and Wheeler, R. L., 1977, Parsons structural lineaments, a cross-strike zone of more intense jointing in West Virginia (abs): Geol. Soc. America Abs. with Programs, v. 9, pp. 147-148.
- Horne, R. R., 1974, Transverse fault control of base metal mineralization in the Irish and British Caledonides (abs): Geol. Soc. America Abs. with Programs, v. 6, pp. 800-801.
- Horne, R. R., 1975a, Possible transverse fault control of base metal mineralization in Ireland and Britain: Irish Naturalists' Jour., v. 18, pp. 140-144.
- Horne, R. R., 1975b. Transverse fault systems in fold belts and oceanic fracture zones: Nature, v. 255, pp. 620-621.
- Horne, R. R., 1976a, Transverse fault zones in the Irish Caledonides and other fold belts (abs.): Abs. of the 2d Internat. Conf. on the New Basement Tectonics, Newark, Del., Univ. of Delaware, p. 27.
- Hubbart, M. K., 1948, Line-integral method of computing gravity, Geophysics, v. 7, pp. 293-310.
- Hunter, C. D., and Young, D. M., 1953, Relationship of natural gas occurrence and production in eastern Kentucky (Big Sandy gas field) to joints and fractures in Devonian bituminous shale: American Assoc. Pet. Geol., Bull., vol. 37, no. 2, pp. 282-299.
- Jacobeen, F., Jr., and Kanes, W. H., 1974, Structure of the Broadtop synclinorium and its implications for Appalachian structural style. Amer. Assoc. Petrol. Geol. Bull., 58: 362-375.
- Jacobeen, F., Jr., and Kanes, W. H., 1975, Structure of Broadtop synclinorium, Wills Mountain anticlinorium and Allegheny Frontal zone. Amer. Assoc. Petrol. Geol. Bull., 59: 1136-1150.
- Johnson, A. M., 1977, Styles of folding: Elsevier, 406 p.
- Johnson, A. M., and Page, B. M., 1976, Part VII, Development of folds within Huasna syncline, San Luis Obispo County, California: Tectonophysics, v. 33, pp. 97-143.

- Kowalik, W. S., 1975, Use of LANDSAT-1 Imagery in the analysis of lineaments in Pennsylvania: M.S. Thesis, Pennsylvania State University, 93 pp.
- Kowalik, W. S., and Gold, D. P., 1976, The use of LANDSAT-1 imagery in mapping lineaments in Pennsylvania, in Hodgson, R. A., and others eds., 1st Internat. Conf. on the New Basement Tectonics Proc.: Salt Lake City, Utah, Utah Geol. Assoc. Pub. No. 5, p. 236-249.
- Kulander, B. R., and Dean, S. L., 1978, Gravity, magnetics and structure of the Allegheny Plateau--Western Valley and Ridge in West Virginia Geological and Economic Survey Report of Investigation R.I. - 27, 91 pp.
- Kulander, B. R., Dean, S. L., and Barton, C. C., 1977 Fractographic logging for determination of pre-core and core-induced fractures...Nicholas Combs No. 7239 well, Hazard, Kentucky, U. S. Energy research and Development Administration, Morgantown Energy Research Center, MERC/CR-77/3, 44 pp.
- Kulander, B. R., Dean, S. L., and Barton, C. C., 1977, The application of fractography to core and outcrop fracture investigations: United States Department of Energy, Morgantown Energy Technology Center, Morgantown, West Virginia, special publication METC/SP-79/3.
- LaCaze, J. A., ms, 1978. Structural analysis of the Petersburg structural lineament in the eastern Appalachian Plateau province, Tucker Co., West Virginia: M.S. Thesis, West Virginia Univ., 69 pp.
- Larese, E., and Heald, M. I., 1977, Petrography of selected Devonian shale core samples from CGTC 20403 and CGSC 11940 wells, Lincoln and Jackson Counties, West Virginia: USERDA-Morgantown Energy Research Center Technical Report, MERC/CR-77/6, 27 pp.
- Lis, M. G., and Price, R. A., 1976, Large-scale faulting during deposition of the Windermere Supergroup (hadrynian) in southwestern British Columbia: Geol. Soc. Canada Paper 76-1A, pp. 135-136.
- Marshak, S., and Geiser, P., 1980, Guidebook to pressure solution phenomena in the Hudson Valley: Prepared for the Geological Society of America Penrose Conference entitled "The Role of Pressure Solution and Dissolution phenomena in Geology--May 18-23, 1980" 49 pp.

- McColloch, G. H., Jr., ms 1976, Structural analysis in the central Appalachian Valley and Ridge, Grant and Hardy Counties, West Virginia Univ., 62 pp.
- Mosteller, F., and Tukey, J. W., 1977, Data analysis and Regression, Addison Wesley Publishing Co., Reading, Mass., 588 pp.
- Mullennex, R. H., ms., 1976, Surface expression of the Parsons lineament, southwestern Tucker County, West Virginia: M.S. Thesis, West Virginia Univ., 62 pp.
- Nickelsen, R. P., 1966, Fossil distortion and penetrative rock deformation in the Appalachian plateau, Pennsylvania: Jour. Geol. v.74, pp. 924-931.
- Patchen, D. G., 1977, Subsurface stratigraphy and gas production of the Devonian Shales in West Virginia, U. S. Energy Research and Development Administration, Morgantown Energy Research Center, MERC/CR-77/5, 35 pp.
- Perry, W. J., Jr., 1964, Geology of Ray Sponaugle well Pendleton County, West Virginia: AAPG Bull., v. 48, pp. 659-669.
- Perry, W. J., Jr., 1971, Structural development of the Nittany anticlinorium, Pendleton County, West Virginia, Ph.D. dissertation, Yale Univ., 227 pp.
- Perry, W. J., Jr., 1978, Sequential deformation in the central Appalachians. Amer. Jour. Sci., v. 278: pp. 518-542.
- Price, R. A., and Kluwer, H. M., 1974, Structure of the Rocky Mountains of the Glacier-Waterton Lakes National Park area, in Voight, B., and Voight, M. A., eds. Rock Mechanics: the American Northwest: Expedition Guide, 3d Cong. of the Internat. Soc. for Rock Mechanics: University Park, Pa., The Pennsylvania State Univ. pp. 213-216.
- Price, R. A., and Lis, M. G., 1975, Recurrent displacements on Basement-controlled faults across the cordilleran miogeocline in southern Canada (abs.): Geol. Soc. America Abs. with Programs, v.7, p. 1234.
- Rader, E. K., and Perry, W. J., Jr., 1976a, Reinterpretation of the geology of Brocks Gap, Rockingham County, Virginia: Virginia Minerals, v. 22, no. 4, pp. 37-45.

- Rader, E. K., and Perry, W. J., Jr., 1976b, Stratigraphy as key to arch-related origin of Little North Mountain structural front, Virginia and West Virginia (abs.): Am. Assoc. Petroleum Geologists Bull., v. 60, p. 1632.
- Ramberg, H., 1963, Evolution of drag folds: Geol. Mag., v. 100, pp. 97-106.
- Reger, D. B., 1931, Randolph County, West Virginia: West Virginia Geol. and Econ. Survey County Geologic Report, 989 pp.
- Reger, D. B., Price, W. A., Tucker, R. C., 1923, Tucker County, West Virginia: West Virginia Geol. and Econ. Survey County Geologic Report, 542 pp.
- Reger, D. B. and Teets, D. D., 1918, Barbour and Upshur Counties and the Western portion of Randolph County, West Virginia: West Virginia Geol. and Econ. Survey County Geologic Report, 867 pp.
- Reger, D. B., and Tucker, R. B., 1924, Grant and Mineral Counties, West Virginia: West Virginia Geol. and Econ. Survey, County Geologic Report, 866 pp.
- Rodgers, D. A., and Rizer, W. G., 1979a, Deformation and secondary faulting near the leading edge of a thrust fault (abs): Thrust and Nappes Tectonic Symposium, Imperial College, London, Abstracts, v. p. 6.
- Rodgers, D. A., and Rizer, W. G., 1979b, Deformation and secondary faulting near the leading edge of a thrust fault (preprint): Proceedings Volume, Thrust and Nappes Tectonics Symposium, Imperial College, London.
- Rodgers, J., 1963, Mechanics of Appalachian foreland folding in Pennsylvania and West Virginia: Amer. Assoc. Petrol. Geol. Bull., v. 47, pp. 1527-1536.
- Schaefer, W. W., ms., 1979, Geology and producing characteristics of certain Devonian Brown shales in the Midway--Extra field, Putnam County, West Virginia: M.S. Thesis, West Virginia Univ., 67 pp.
- Shumaker, R. C., 1976, Kentucky--West Virginia Gas Company final reports--well no. 7239, Perry County, Kentucky: Text of U. S. Energy Research and Development Administration contract No. E (46-1) 8000.

- Shumaker, R. C., 1978, Porous fracture facies in the Devonian shales of West Virginia and eastern Kentucky: Second Eastern Gas Shales Symposium, Morgantown Energy Technology Center, Morgantown, West Virginia, v. 1, **METC/SP-78/6**, pp. 360-369.
- Sites, R. S., 1971, Geology of the Smoke Hole region in Grant and Pendleton Counties, West Virginia: M.S. Thesis, West Virginia Univ., 2 vols., 106 pp.
- Sites, R. S., 1978, Structural analysis of the Petersburg lineament, Central Appalachians: Ph.D. Dissertation, West Virginia Univ., 274 pp. (Ann Arbor, Michigan, Univ. Microfilms).
- Sites, R. S., 1973, Geology of the Smoke Hole region of West Virginia: Southeastern Geology, v. 15, pp. 153-168.
- Sites, R. S., and Wheeler, R. L., 1977, Structural geology of Smoke Holes area. Valley and Ridge, West Virginia --exposed model for complex subsurface structures (abs.): American Association of Petroleum Geologists Bulletin, 61:830.
- Smith, A. G., Higgins, E., and Robertson, J. D., 1970, Polygon V, a computer program for the computation of the gravitational attraction of two dimensional structures: Dept. of Civil and Geological Engineering, Princeton Univ., Princeton, N.J., 19 pp.
- Spencer, E. W., 1969, Introduction to the structure of the Earth, McGraw Hill Pub., 630 pp.
- Staub, W., ms., 1979, The tectonic significance of faults in the Pennsylvanian Conemaugh Group in the Appalachian Plateau of West Virginia: Masters project (Alan C. Donaldson, supervisor), West Virginia Univ., Dept. Geol. and Geog.
- Talwani, M., Worzel, J. L., and Landisman, M. G., 1959, Rapid gravity computation for two-dimensional bodies with application to the Mendocino submarine fracture zone: Jour. Geophys. Research, v. 65, no. 1, pp. 49-59.
- Tilton, J. L., Prouty, W. F., and Price, P. H., 1927, Pendleton County, West Virginia: West Virginia Geol. and Econ. Survey County Geologic Report, 384 pp.

- Trumbo, D. B., ms., 1976, the Parsons lineament, Tucker County, West Virginia: M.S. Thesis, West Virginia University, 81 pp.
- Vialon, P., Ruland, M., and Grolier J., 1976, Elements de tectonique analytique: Paris, Masson, 118 pp.
- Wheeler, R. L., 1980, Cross-strike structural discontinuities: possible exploration tool for natural gas in Appalachian overthrust belt: In press, Dec. 1980, for Bulletin of Am. Assoc. Petr. Geol.
- Wheeler, R. L., Mullenex, R. H., Henderson, C. D., and Wilson, T. H., 1974, Major, cross-strike structures of the central sedimentary Appalachian: Progress Report: **Proc. of West Virginia Acad. Sci.**, v. 46, pp. 196-203.
- Wheeler, R. L., Mullenex, R. H., Henderson, C. D., and Wilson, T. H., 1974, Cross-strike structural discontinuities, possible exploration tool in detached forelands (abs.): **Geol. Soc. America Abs. with Programs**, v. 8, p. 298.
- Wheeler, R., Trumbo, D., Mullenex, R., Henderson, C. D., and Moore, R., 1976b. Field study of the Parsons lineament, Tucker County, West Virginia (abs.): **Geological Society of America Abstracts with Programs**: v. 8, no. 2, p. 298.
- Wheeler, R. L., 1978, Fracture intensity predictions for eastern gas shales: Eastern Gas Shales Open-File Report 137, 78 pp; available from U. S. Department of Energy, Morgantown Energy Technology Center, Morgantown, West Virginia.
- Wheeler, R. L., Winslow, M., Horne, R. R., Dean, S., Kulander, B.; Drahovzal, J. A.; Gold D. P.; Gilbert, O. E., Jr.; Werner, E.; Sites, R., and Perry, W. J., Jr., 1979, Cross-strike structural discontinuities in thrust belts, mostly Appalachian: **Southeastern Geology**, v. 20, pp. 193-203.
- Wheeler, R. L., and Dixon, J. M., 1980, Intensity of Systematic Joints: Methods and Applications: **Geology**, v. 8, pp. 230-233.
- Wilson, C. W., Jr., and Sterns, R. G., 1958, Structure of the Cumberland Plateau, Tennessee: **Geol. Soc. Amer. Bull.**, v. 69, pp. 1283-1296.

Wilson, T. H., and Wheeler, R. L., 1974, Structural geology of the Plateau-Valley and Ridge transition Grant County, West Virginia: **Proc. of West Virginia Acad. Sci.**, v. 46, pp. 204-216.

Wilson, T. H., 1979a, Bedding orientation contours of Middle Devonian shales in the **Middle Mountain syncline**, Valley and Ridge Province, West Virginia (abs.): **Geol. Soc. Amer. Abs. with Programs North-eastern Section of the Geol. Soc. of Amer.**, 14th Annual Meeting, v. 11, no. 1, p. 60.

Wilson, T. H., 1979b, Bedding orientation contours of Middle Devonian shales exposed in the Middle Mountain syncline, Valley and Ridge Province, West Virginia: Morgantown Energy Technology Center Open-File Report, Morgantown, West Virginia, 39 pp.

Wilson, T. H., Dixon, J. M., Shumaker, R. C., Wheeler, R. L., 1980, Fracture patterns observed in cores from **the Appalachian Basin**: in **Preprints of the 3rd Annual Eastern Gas Shales Symposium**, Morgantown, West Virginia.

Woodward, H. P., 1959, Structural interpretations of the Burning Springs anticline: in, Woodward, H. P., ed., **Symposium on Sandhill Deep Well**, Wood County, West Virginia, West Virginia Geol. and Econ. Survey Inv. Rept. 18, pp. 159-168.

Zurgani, M.-R., 1975, Petroleum and structural geology of the northern portion of the **Broadtop** anticline Hampshire County, West Virginia, M.S. Thesis, West Virginia Univ.



## APPENDIX I

### Rotated and Unrotated Joints

A. Joint Strike and Dip In Rotated and Unrotated Bedding.

STATION NUMBER: 1

Bedding Strike and Dip: N25E/18SE

Joint Strike and Dip

<u>Rotated</u>	<u>Unrotated</u>
N34W/89SW	N36W/80SW
N49W/87NE	N48W/89SW
N40W/89SW	N41W/81SW
N40W/88NE	N41W/84SW
N40W/90NE	N42W/83SW
N06W/62SW	N14W/47SW
N06W/69SW	N11W/54SW
N04W/80SW	N07W/63SW
N10E/78NW	N07E/50NW
N09E/68NW	N05E/43NW
N10E/78NW	N09E/60NW
N17E/86NW	N17E/66NW
N16E/85NW	N16E/65NW
N48E/84NW	N50E/67NW
N41E/84SE	N43E/76NW
N41E/78SE	N42E/83NW
N42E/78SE	N43E/83NW
N36E/86NW	N38E/67NW
N76E/84NW	N80E/72NW
N72E/84NW	N77E/71NW
N74E/84NW	N78E/71NW
N70E/90NW	N72E/77NW

STATION NUMBER: 2

Bedding Strike and Dip: N39E/25SE

Joint Strike and Dip

<u>Rotated</u>	<u>Unrotated</u>
N33W/90SW	N35W/82SW
N42W/90NE	N43W/86SW
N46W/89SW	N47W/86SW
N38W/88NE	N38W/86SW
N40W/88NE	N41W/87SW

<u>Rotated</u>	<u>Unrotated</u>
N54E/85NW	N56E/63NW
N58E/88SE	N59E/69NW
N59E/88SE	N60E/69NW
N54E/83NW	N57E/60NW
N48E/80SE	N47E/77NW
N54E/85NW	N56E/63NW
N30W/88NE	N31W/83SW

STATION NUMBER: 3

Bedding Strike and Dip: N35E/34SE

Joint Strike and Dip

<u>Rotated</u>	<u>Unrotated</u>
N87W/86SW	N85W/77NE
N85W/78NW	N86W/86NE
N78W/74SW	N82W/88SW
N73W/70SW	N80W/83SW
N85W/86SW	N83W/78NE
N11W/88SW	N17W/65SW
N15W/88SW	N22W/67SW
N30W/87NE	N31W/79SW
N45E/75SE	N45E/73NW
N49E/74SE	N50E/72NW
N47E/76SE	N46E/71NW
N52E/82SE	N53E/65NW
N43E/77SE	N43E/70NW

STATION NUMBER: 4

Bedding Strike and Dip: N15E/25SE

Joint Strike and Dip

<u>Rotated</u>	<u>Unrotated</u>
N67W/85NE	N66W/89NE
N87E/84SE	N57W/89SW
N18W/76SW	N25W/56SW
N19W/88SW	N22W/68SW
N13W/80SW	N18W/60SW

<u>Rotated</u>	<u>Unrotated</u>
N28E/87SE	N28E/68NW
N36E/86SE	N17E/70NW
N11E/77NW	N11E/70NW
N14E/82SE	N14E/74NW
N29E/74SE	N29E/81NW
N32E/87NW	N34E/64NW
N17E/84SE	N38E/70NW
N68E/80NW	N75E/66NW
N63E/76NW	N72E/60NW
N72E/89NW	N75E/75NW
N74E/89NW	N77E/76NW

STATION NUMBER: 5

Bedding Strike and Dip: N38E/20SE

Joint Strike and Dip

<u>Rotated</u>	<u>Unrotated</u>
N76W/82NE	N78W/90NE
N61W/87NE	N63W/90NE
N69W/84NE	N70W/90NE
N46W/88NE	N45W/90NE
N53W/90NE	N53W/90NE
N25E/62NW	N20E/43NW
N29E/88NW	N28E/67NW
N25E/88NW	N24E/68NW
N24E/88NW	N23E/68NW
N50E/86SE	N25E/76NW
N24E/84NW	N23E/65NW

STATION NUMBER: 6

Bedding Strike and Dip: N10E/30SE

Joint Strike and Dip

<u>Rotated</u>	<u>Unrotated</u>
N44W/72NE	N40W/90NE
N43W/71NE	N39W/90NE
N49W/79NE	N47W/85SW
N53W/76NE	N50W/90NE
N53W/76NE	N50W/90NE

<u>Rotated</u>	<u>Unrotated</u>
N19E/88NW	N20E/59NW
N19E/87NW	N20E/58NW
N18E/84NW	N20E/55NW
N28E/88NW	N31E/60NW
N24E/84SE	N25E/64NW
N24E/80SE	N25E/71NW
N24E/80SE	N25E/71NW
N31E/84SE	N33E/68NW
N32E/79SE	N33E/74NW
N23E/80SE	N24E/70NW
N14W/72NE	N12W/81SW
N00E/24SE	N02E/76NW
N07E/70SE	N08E/80NW
N00E/88SE	N00E/62NW
N31E/74SE	N10W/78SW
N10W/80NE	N10W/72SW
N60E/87NW	N65E/68NW
N51E/84SE	N53E/74NW
N61E/90NW	N65E/71NW
N54E/90NW	N58E/68NW
N10W/75NE	N50E/66NW
N85E/67SE	N76E/78SE
N87E/82SE	N85E/90NW
N86E/87SE	N86E/86NW
N72E/89SE	N75E/78NW
N68E/89NW	N72E/73NW
N62E/57SE	N52E/78SE

STATION NUMBER: 7

Bedding Strike and Dip: N20E/21SE

Joint Strike and Dip

<u>Rotated</u>	<u>Unrotated</u>
N11E/89SE	N10E/70NW
N11E/89SE	N10E/70NW
N09E/89SE	N08E/70NW
N12E/87SE	N12E/72NW
N83E/76SE	N80E/86SE
N83E/74SE	N80E/84SE
N78E/76SE	N75E/86SE
N79E/78SE	N77E/89SE
N78E/74SE	N75E/85SE

STATION NUMBER: 8

Bedding Strike and Dip: N25E/21SE

Joint Strike and Dip

<u>Rotated</u>	<u>Unrotated</u>
N66W/84SW	N68W/85SW
N79E/88SE	N80E/80NW
N80W/82SW	N82W/89SW
N80W/80SW	N82W/86SW
N41W/82NE	N87E/90NW
N69W/88SW	N70W/90NE
N72W/87NE	N70W/85NE
N83W/80SW	N85W/88SW
N69W/90SW	N68W/89NE
N13E/85SE	N12E/75NW
N07E/82SE	N06E/78NW
N28E/87SE	N18E/72NW
N11E/84SE	N10E/76NW
N26E/83SE	N26E/77NW
N57W/78NE	N53W/82NE
N52W/88NE	N52W/89SW

STATION NUMBER: 9

Bedding Strike and Dip: N36W/08NE

Joint Strike and Dip

<u>Rotated</u>	<u>Unrotated</u>
N79W/86NE	N79W/89SW
N78W/89SW	N79W/84SW
N74W/82SW	N85W/77SW
N44W/80NE	N43W/88NE
N47W/86NE	N47W/87SW
N40W/86NE	N40W/87SW
N39W/88NE	N40W/86SW
N42W/83NE	N44W/89SW
N44W/76NE	N43W/85NE
N49W/82NE	N49W/89NE
N48W/80NE	N48W/88NE
N48W/80NE	N48W/84NE
N47W/76NE	N47W/84NE

<u>Rotated</u>	<u>Unrotated</u>
N12W/82SW	N11W/75SW
N49W/88NE	N09W/85SW
N05W/81SW	N04W/73SW
N04W/82SW	N03W/75SW
N09W/87SW	N08W/80SW
N43E/90SE	N43E/89NW
N41E/90SE	N41E/89NW
N34E/90SE	N33E/88NW
N35E/89SE	N35E/29SE
N40E/88SE	N39E/90NW
N67E/74SE	N65E/73SE
N75E/77SE	N73E/73SE
N71E/68SE	N68E/66SE
N70E/67SE	N68E/76SE
N65E/82SE	N64E/81SE

STATION NUMBER: 10

Bedding Strike and Dip: N38E/28SE  
N07W/66NE

## Joint Strike and Dip

<u>Rotated</u>	<u>Unrotated</u>
N73E/59NW	N70W/70NE
N86E/76NW	N82W/88NE
N79E/76NW	N85W/82NE
N86E/56NW	N63W/81NE
N83E/78NW	N85W/86NE
N04E/88NW	N00E/56NW
N03E/83NW	N00E/60NW
N06W/88SW	N10W/66SW
N11E/80NW	N08E/55NW
N22E/90NW	N21E/64NW
N34E/83NW	N34E/55NW
N47E/90NW	N48E/62NW
N56E/96NW	N59E/60NW
N67E/79NW	N74E/55NW
N45E/76NW	N47E/48NW
N62E/81NW	N66E/56NW
N54E/72NW	N60E/53NW
N55E/85NW	N59E/65NW
N61E/82NW	N66E/63NW
N04W/86NE	N58E/74NW



STATION NUMBER: 11

Bedding Strike and Dip: N25E/15SE

Joint Strike and Dip

<u>Rotated</u>	<u>Unrotated</u>
N86W/85NE	N84W/80NE
N76W/88NE	N75W/85NE
N78W/90NE	N78W/87NE
N51W/86NE	N50W/90NE
N48W/89NE	N48W/87SW
N59W/85NE	N58W/87NE
N62W/86NE	N61W/88NE
N49W/87NE	N49W/90NE
N63E/89NW	N64E/78NW
N57E/90NW	N58E/78NW
N60E/83NW	N62E/71NW
N55E/86NW	N56E/74NW
N56E/88SE	N57E/81NW
N71E/88SE	N72E/81NW
N70E/85NW	N72E/75NW
N67E/84NW	N69E/72NW
N61E/86NW	N63E/74NW

STATION NUMBER: 13

Bedding Strike and Dip: N03E/15SE

Joint Strike and Dip

<u>Rotated</u>	<u>Unrotated</u>
N19E/86NW	N20E/72NW
N18E/90NW	N18E/76NW
N22E/88SE	N22E/78NW
N20E/86SE	N20E/81NW
N03E/89SE	N03E/76NW
N70E/71SE	N66E/78SE
N61E/78SE	N59E/87SE
N64E/76SE	N62E/83SE
N64E/68SE	N60E/77SE
N55E/84SE	N65E/88NW

STATION NUMBER: 14

Bedding Strike and Dip: N23W/15NE

Joint Strike and Dip

<u>Rotated</u>	<u>Unrotated</u>
N48E/63NW	N56E/60NW
N45E/85NW	N47E/80NW
N52E/79NW	N56E/76NW
N59E/78NW	N63E/77NW
N60E/81NW	N63E/80NW

STATION NUMBER: 16

Bedding Strike and Dip: N22E/12SE

Joint Strike and Dip

<u>Rotated</u>	<u>Unrotated</u>
N81E/78SE	N80E/84SE
N82E/79SE	N81E/85SE
N85E/86SE	N83E/88NW
N85E/86SE	N83E/88NW
N84E/85SE	N83E/90NW
N85W/85SW	N85W/89SW
N84E/80SE	N85E/88NW
N82W/90NE	N80W/88NE
N51W/88NE	N50W/89SW
N48W/88NE	N47W/89SW
N53W/89NE	N53W/89SW
N49W/86SW	N50W/84SW
N49W/90NE	N50W/86SW
N30E/88NW	N29E/75NW
N27E/86NW	N27E/73NW
N28E/82NW	N27E/68NW
N25E/84NW	N26E/72NW
N30E/82NW	N30E/69NW

STATION NUMBER: 17

Bedding Strike and Dip: N04W/04NE

Joint Strike and Dip

<u>Rotated</u>	<u>Unrotated</u>
N06W/86NE	N06W/90NE
N20W/86NE	N20W/90NE
N26W/86NE	N25W/90NE
N18W/86NE	N17W/90NE
N27W/86NE	N26W/71NE
N32E/89NW	N33E/86NW
N37E/84NW	N37E/81NW
N32E/84NW	N33E/82NW
N32E/89NW	N34E/86NW
N32E/84NW	N33E/81NW
N74E/88NW	N74E/86NW
N74E/90SE	N73E/90NW
N70E/89SE	N70E/90NW
N70E/89SE	N70E/90NW
N67E/88SE	N67E/90NW

STATION NUMBER: 18

Bedding Strike and Dip: N75E/09NW

Joint Strike and Dip

<u>Rotated</u>	<u>Unrotated</u>
N03E/88SE	N02E/85SE
N04W/82SW	N04W/85SW
N07E/83NW	N07E/87NW
N10W/84SW	N09W/85SW
N01W/88SW	N00E/90NW
N02E/82NW	N02E/86NW
N00W/82SW	N01E/86NW
N06W/85SW	N05W/87SW
N10W/80SW	N09W/82SW
N00W/86SW	N00E/90NW

STATION NUMBER: 19

Bedding Strike and Dip: N13W/10NE

## Joint Strike and Dip

<u>Rotated</u>	<u>Unrotated</u>
N30E/82SE	N30E/90NW
N36E/83SE	N35E/90NW
N30E/82SE	N30E/90NW
N25E/82SE	N25E/90NW
N17E/81SE	N17E/90NW
N84E/88NW	N84E/90NW
N82E/90NW	N82E/90NW
N86E/88NW	N87E/90NW
N84E/81NW	N86E/82NW
N82E/90NW	N82E/90NW

STATION NUMBER: 20

Bedding Strike and Dip: N12W/14NE

## Joint Strike and Dip

<u>Rotated</u>	<u>Unrotated</u>
N45E/83SE	N68W/88SW
N80W/82NE	N78W/88NE
N87W/82NE	N85W/85NE
N77W/83NE	N76W/89NE
N85W/85NE	N84W/89NE
N38W/87NE	N39W/81SW
N40W/83NE	N40W/85SW
N37W/83NE	N37W/84SW
N39W/86NE	N40W/82SW
N41W/83NE	N41W/84SW
N29E/80NW	N32E/69NW
N28E/80NW	N31E/68NW
N44E/81NW	N47E/72NW
N38E/82NW	N41E/72NW
N26E/83NW	N28E/71NW

STATION NUMBER: 23

Bedding Strike and Dip: N75W/12NE

Joint Strike and Dip

<u>Rotated</u>	<u>Unrotated</u>
N03E/90NW	N03E/90NW
N00W/89SW	N00E/87NW
N12W/89SW	N11W/84SW
N06E/88NW	N06E/86NW
N02E/89NW	N02W/86SW
N74E/76NW	N75E/86NW
N75E/76SE	N73E/66SE
N86E/82SE	N85E/70SE
N80E/86NW	N80E/84SE
N69E/86SE	N68E/78SE

STATION NUMBER: 24

Bedding Strike and Dip: N20E/90NW

Joint Strike and Dip

<u>Rotated</u>	<u>Unrotated</u>
N74W/80SW	N79W/87NE
N74W/74SW	N86W/87NE
N70W/90SW	N90E/88SE
N75W/74SW	N83W/87NE
N76W/80SW	N79W/86NE
N76W/87SW	N72W/84NE
N76W/79NE	N58W/85NE
N75W/75NE	N54W/86NE
N71W/67NE	N46W/90NE
N71W/65NE	N44W/90NE
N57W/68NE	N37W/74SW

STATION NUMBER: 25

Bedding Strike and Dip: N30E/87SE

Joint Strike and Dip

<u>Rotated</u>	<u>Unrotated</u>
N36W/72SW	N78W/66SW
N45W/83SW	N66W/74SW
N42W/84SW	N65W/71SW
N61W/76SW	N75W/90NE
N61W/87SW	N58W/90NE
N73W/82NE	N52W/77NE
N73W/82NE	N52W/77NE
N70W/89NE	N58W/81NE
N70W/78NE	N47W/81NE
N62W/92NE	N51W/89NE
N70E/52NW	N10W/52NE
N77E/58NW	N21W/54NE
N60E/64NW	N18W/38NE
N59E/68NW	N23W/35NE
N66E/66NW	N25W/40NE

STATION NUMBER: 26

Bedding Strike and Dip: N30E/90NW

Joint Strike and Dip

<u>Rotated</u>	<u>Unrotated</u>
N69W/79NE	N47W/82NE
N65W/87NE	N56W/86NE
N65W/88NE	N58W/86NE
N64W/89NE	N57W/86NE
N73W/84NE	N53W/78NE
N54W/79SW	N71W/83SW
N55W/82SW	N67W/84SW
N54W/82SW	N68W/83SW
N50W/79SW	N71W/79SW
N51W/82SW	N68W/80SW
N21E/71NW	N53E/21SE
N23E/60NW	N40E/31SE
N19E/69NW	N55E/23SE
N21E/83NW	N55E/20SE

STATION NUMBER: 27

Bedding Strike and Dip: N20E/78NW  
 N33E/68NW  
 N26E/58SE  
 N35E/70NW

## Joint Strike and Dip

<u>Rotated</u>	<u>Unrotated</u>
N72W/88SW	N68W/88SW
N60W/88SW	N67W/82NE
N60W/86SW	N65W/82NE
N68W/84SW	N66W/90NE
N69W/88SW	N68W/90NE
N82W/86NE	N78W/79SW
N74W/83NE	N79W/88SW
N55W/84SW	N64W/79SW
N45W/89NE	N53W/79NE
N52W/89NE	N56W/86NE
N55W/86SW	N56W/86SW
N48W/87SW	N50W/83NE
N49W/89SW	N52W/83NE
N45W/82NE	N47W/78SW
N61W/76NE	N50W/85NE
N61W/74NE	N49W/85NE
N55W/77NE	N48W/90NE
N55E/86NW	N75E/30SE
N52E/67NW	N58E/47SE
N55E/75NW	N65E/40SE
N55E/64NW	N54E/50SE
N86E/82NW	N87E/43SE

STATION NUMBER: 28

Bedding Strike and Dip: N63E/24NW

## Joint Strike and Dip

<u>Rotated</u>	<u>Unrotated</u>
N52W/80SW	N52W/88NE
N46W/84SW	N46W/88NE
N47W/82SW	N48W/88NE
N49W/82SW	N50W/88NE
N50W/82SW	N50W/86NE

RotatedUnrotated

N29E/82NW  
 N31E/80NW  
 N30E/78NW  
 N25E/77NW  
 N27E/72NW

N27E/79SE  
 N24E/81SE  
 N25E/83SE  
 N30E/84SE  
 N27E/90NW

STATION NUMBER: 29

Bedding Strike and Dip: N19E/48NW

## Joint Strike and Dip

RotatedUnrotated

N72W/80SW  
 N68W/78SW  
 N71W/85SW  
 N75W/90NE  
 N74W/89NE  
 N87W/86SW  
 N87W/86SW

N65W/82SW  
 N61W/84SW  
 N68W/87SW  
 N75W/87SW  
 N75W/88SW  
 N80W/76SW  
 N80W/75SW

N50W/74SW  
 N49W/77SW  
 N55W/78SW

N45W/86NE  
 N46W/83NE  
 N51W/88NE

STATION NUMBER: 32

Bedding Strike and Dip: N63E/24NW

## Joint Strike and Dip

RotatedUnrotated

N40W/88NE  
 N34W/90NE  
 N33W/90NE  
 N38W/89NE  
 N38W/89NE

N41W/90NE  
 N34W/90NE  
 N33W/90NE  
 N40W/90NE  
 N40W/90NE

N11E/86NW  
 N09W/80SW  
 N02W/84SW  
 N10E/74NW  
 N09W/76SW  
 N04E/86NE

N11E/85SE  
 N07W/86SW  
 N00W/87NE  
 N11E/85NW  
 N07W/86SW  
 N02E/76SE



<u>Rotated</u>	<u>Unrotated</u>
N29E/76NW	N30E/90NW
N32E/76NW	N33E/90NW
N34E/76NW	N35E/90NW
N29E/76NW	N30E/90NW
N37E/76NW	N37E/90NW
N29E/90NW	N80E/78SE
N79E/89NW	N80E/78SE
N80E/86NW	N80E/84SE
N86E/79NW	N86E/90NW
N81E/90NW	N82E/79NW

STATION NUMBER: 33

Bedding Strike and Dip: N41E/11NW

Joint Strike and Dip

<u>Rotated</u>	<u>Unrotated</u>
N85E/80NW	N84E/87NW
N87E/70NW	N88E/78NW
N89E/83NW	N89E/88NW
N77W/82NE	N80W/87NE
N81W/86NE	N82W/88SW
N30W/87SW	N30W/90NE
N30W/87SW	N30W/90NE
N33W/89SW	N33W/90NE
N31W/88SW	N31W/90NE
N32W/87SW	N32W/90NE
N14E/80NW	N15E/90NW
N16E/80NW	N17E/90NW
N18E/80NW	N18E/90NW
N20E/80NW	N20E/90NW
N22E/80NW	N21E/90NW
N47E/80NW	N47E/90NW
N52E/80NW	N52E/90NW
N50E/80NW	N50E/90NW
N60E/80NW	N60E/90NW
N45E/80NW	N46E/90NW

STATION NUMBER: 34

Bedding Strike and Dip: N19W/04NE

Joint Strike and Dip

<u>Rotated</u>	<u>Unrotated</u>
N25W/86NE	N25W/90NE
N23W/86NE	N23W/90NE
N24W/86NE	N24W/90NE
N39W/86NE	N38W/90NE
N35W/86NE	N35W/90NE
N36E/88NW	N36E/86NW
N48E/82NW	N49E/80NW
N55E/88SE	N55E/90NW
N42E/84NW	N42E/82NW
N65E/90NW	N65E/90NW
N69E/90NW	N69E/90NW
N70E/90NW	N70E/90NW
N80E/90NW	N80E/90NW
N75E/90NW	N75E/90NW
N64E/80SE	N63E/81SE
N59E/74SE	N58E/75SE
N64E/80SE	N63E/83SE
N62E/82SE	N62E/83SE
N68E/81SE	N68E/82SE

STATION NUMBER: 35

Bedding Strike and Dip: N39E/20NW

Joint Strike and Dip

<u>Rotated</u>	<u>Unrotated</u>
N40W/85SW	N39W/90NE
N39W/82SW	N38W/87NE
N35W/90NE	N36W/86NE
N38W/85NE	N40W/80NE
N09W/78NE	N14W/65NE
N10W/83NE	N15W/70NE
N15W/80NE	N20W/68NE
N12W/82NE	N17W/70NE
N06W/86NE	N09W/71NE

<u>Rotated</u>	<u>Unrotated</u>
N25E/82SE	N23E/62SE
N21E/84SE	N20E/65SE
N27E/86SE	N26E/67SE
N52E/82NW	N52E/79SE
N57E/82NW	N57E/79SE
N55E/79NW	N55E/82SE
N88W/72NE	N88E/85NW

STATION NUMBER: 36

Bedding Strike and Dip: N47E/19NW

Joint Strike and Dip

<u>Rotated</u>	<u>Unrotated</u>
N11W/80SW	N09W/90NE
N02W/90NE	N03W/79NE
N16W/84SW	N15W/89NE
N21W/68SW	N16W/76SW
N21W/83SW	N20W/90NE
N46E/86NW	N46E/75SE
N42E/84NW	N42E/77SE
N57E/89NW	N58E/72SE
N51E/87SE	N52E/68SE

STATION NUMBER: 37

Bedding Strike and Dip: N43E/17NW

Joint Strike and Dip

<u>Rotated</u>	<u>Unrotated</u>
N34W/83SW	N33W/87SW
N31W/84SW	N30W/89SW
N34W/86SW	N33W/90NE
N46W/86SW	N45W/86SW
N33W/81SW	N32W/85SW

<u>Rotated</u>	<u>Unrotated</u>
N12E/78NW	N13E/88SE
N02W/84NW	N02W/85NE
N06W/80SW	N05W/89NE
N00E/80NW	N01E/88SE
N03W/88SW	N02W/90NE
N12E/84NW	N11E/81SE
N04W/88SW	N03W/90NE

STATION NUMBER: 38

Bedding Strike and Dip: N60E/13NW

Joint Strike and Dip

<u>Rotated</u>	<u>Unrotated</u>
N81W/88NE	N82W/82SW
N82W/87NE	N83W/83SW
N83W/85NE	N83W/83SW
N72W/88NE	N73W/83SW
N70W/86SW	N69W/78SW
N81W/81NE	N82W/90NE
N76W/76SW	N78W/84SW
N70W/80NE	N71W/88NE
N84W/90SW	N83W/80SW
N86E/74NW	N86E/86NW
N69E/82SE	N45W/88NE
N69E/80SE	N45W/89SW
N26E/84SE	N25E/75SE
N39E/82NW	N40E/86SE
N35E/86SE	N34E/74SE
N06W/78SW	N07W/81SW
N06W/76SW	N07W/80SW
N06E/89NW	N06E/90NW
N06W/83SW	N07W/87SW

STATION NUMBER: 39

Bedding Strike and Dip: N27E/25NW

Joint Strike and Dip

<u>Rotated</u>	<u>Unrotated</u>
N34E/86NW	N34E/70SE
N57E/68NW	N55E/90SE
N34E/83NW	N34E/72SE
N30E/86NW	N30E/67SE
N48E/78NW	N47E/89SE
N53E/70NW	N52E/88SE
N55E/69NW	N52E/89SE
N53E/82NW	N52E/86SE
N58E/79NW	N57E/80SE
N53E/70NW	N52E/89SE

STATION NUMBER: 40

Bedding Strike and Dip: N37E/52NW

Joint Strike and Dip

<u>Rotated</u>	<u>Unrotated</u>
N80E/78NW	N85E/66SE
N78E/80NW	N86E/62SE
N81E/78NW	N86E/66SE
N86W/75NE	N86W/75SW
N84E/74SE	N68W/47SW
N53W/84SW	N47W/90NE
N53W/86SW	N49W/90NE
N50W/83SW	N48W/86NE
N52W/83SW	N50W/87NE
N50W/80SW	N45W/87NE
N19E/86SE	N06E/35SE
N20E/82SE	N05E/33SE
N20E/88SE	N07E/38SE
N19E/86SE	N06E/37SE
N26E/82SE	N15E/32SE

STATION NUMBER: 41

Bedding Strike and Dip: N40E/21NW

Joint Strike and Dip

<u>Rotated</u>	<u>Unrotated</u>
N81W/90NE	N80W/80SW
N80W/86NE	N80W/84SW
N88W/88NE	N87W/80SW
N73W/88NE	N73W/84SW
N38W/89NE	N39W/85NE
N42W/84NE	N45W/81NE
N42W/84NE	N45W/81NE
N49W/90NE	N50W/88NE
N44W/90NE	N45W/88NE
N10E/90NW	N10E/73SE
N14E/72NW	N16E/90NW
N16E/85NW	N15E/76SE
N05E/89NW	N09E/57SE
N72E/88NW	N10E/75SE

B. Equal area projections of rotated and unrotated joints.

Tables 8 through 16 list the trend and plunge of cluster poles, the standard deviation of poles in each cluster and the number n of poles in each cluster for the rotated and unrotated systematic joints of group 1. Stations included in each group are listed below each table, and the stations within each group and the group boundaries are located on Figure 10 of Chapter II.

Group 1\*

Rotated			Unrotated		
Cluster Pole	Standard Deviation (degrees)	<u>n</u>	Cluster Pole	Standard Deviation (degrees)	<u>n</u>
N51E/07SW	2	5	N12E/02SW	9	5
N07E/10SW	6	4	N57W/23SE	12	5
N58W/06SE	10	5	N50E/05NE	3	5

Table 8

\*The systematic joints of group 1 were measured in the upper part of the Devonian Harrell formation at station 20. Station 20 is located in the plunging nose of the Middle Mountain syncline. The stations comprising groups 1-9 are located on Figure 10.



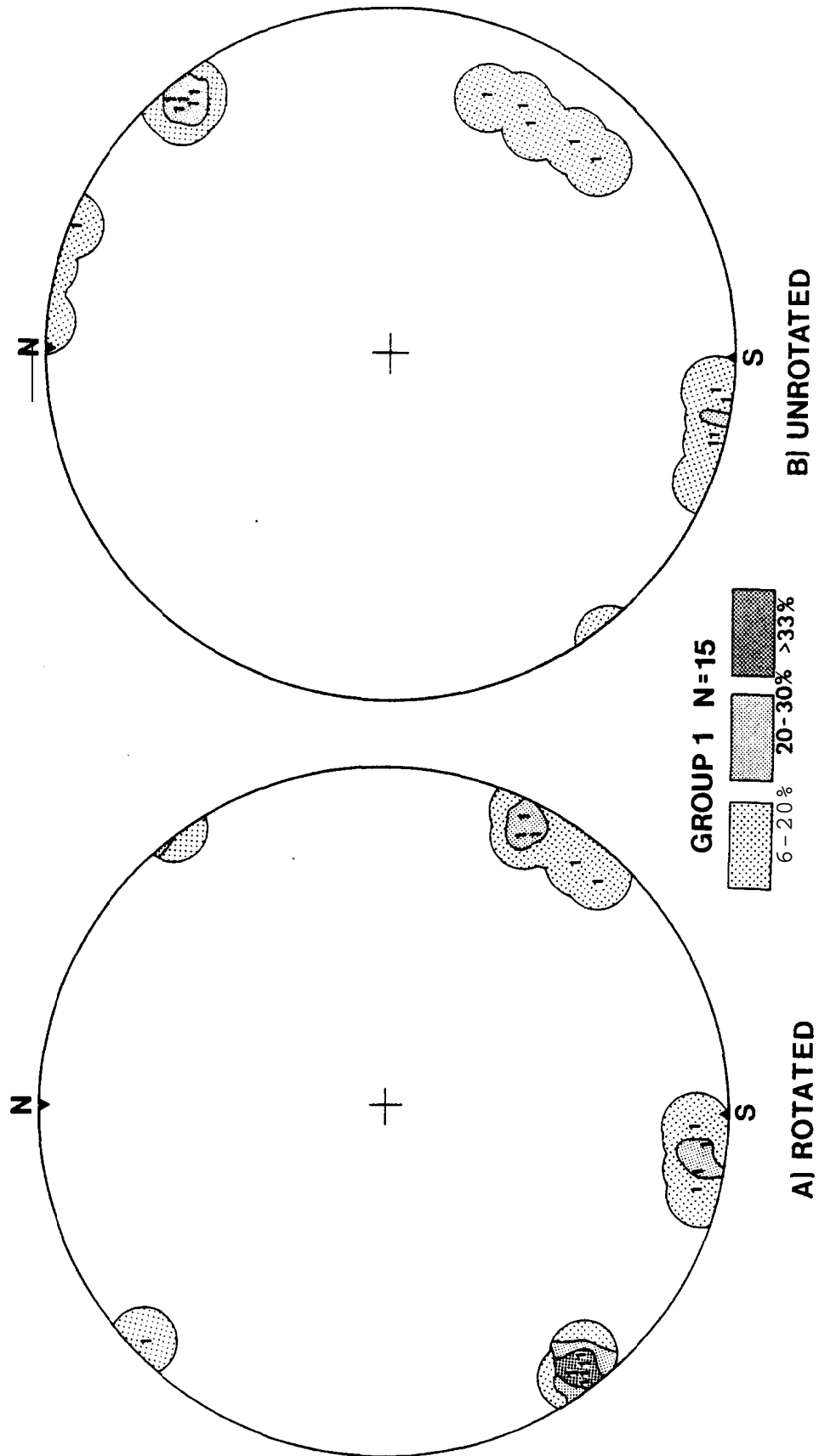


Figure 37 Equal Area Projections of Poles to Rotated and Unrotated Systematic Joints from Group 1

Group 2\*

Rotated			Unrotated		
Cluster Pole	Standard Deviation (degrees)	n	Cluster Pole	Standard Deviation (degrees)	n
N11W/00NW	11	14	N12W/00NW	12	15
N60W/06SE	12	13	N65W/00SE	10	15
N88E/06NE	12	20	N87E/00NE	12	19
N42E/07NE	14	5	N42E/04SW	3	5

Table 9

\*Group 2 systematic joints were measured in the Devonian Brallier formation at stations located in the plunging nose of the Middle Mountain syncline. The following stations comprise group 2: 13, 14, 17, 18, 19, 23, and 28.

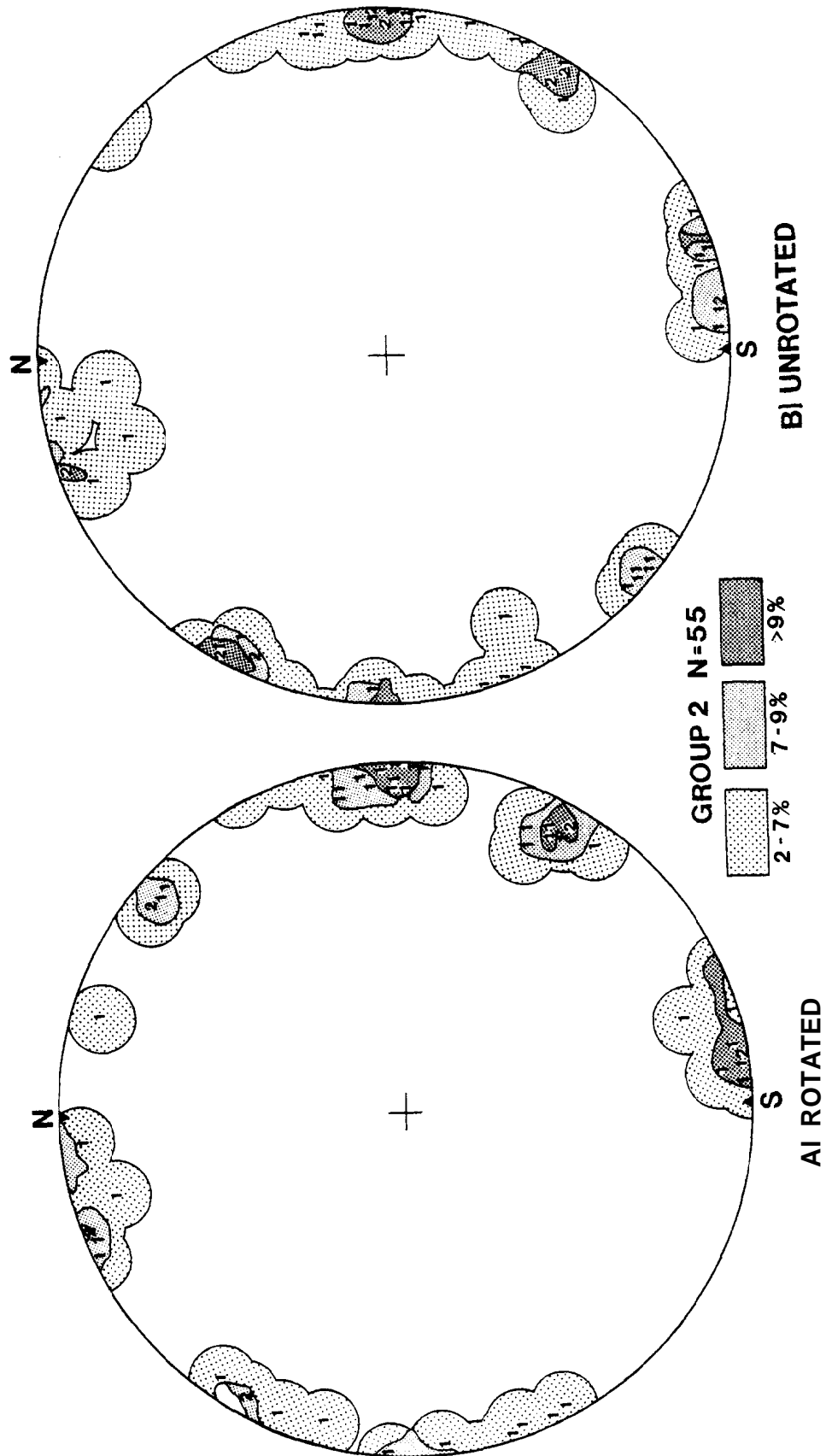


Figure 38 Equal Area Projections of Poles to Rotated and Unrotated Systematic Joints from Group 2

Group 3\*

Rotated			Unrotated		
Cluster Pole	Standard Deviation (degrees)	<u>n</u>	Cluster Pole	Standard Deviation (degrees)	<u>n</u>
N72W/08SE	10	13	N75W/04NW	13	13
N88W/09SE	11	22	N84E/04SW	12	20
N24W/04NW	8	11	N33W/04NW	9	22
N46W/06SE	11	22	N56W/00NW	8	9
N12E/04SW	10	12	N10E/04NE	8	11
N08W/08SE	9	11	N06W/06SE	10	13
N57E/00NE	9	26	N56E/00NE	8	29

Table 10

\*Systematic joints included in group 3 were measured at stations 32, 33, 34, 35, 36, 37, and 38. These stations are located on the southeast limb of the Middle Mountain **syncline** in the Devonian Brallier formation. These stations are also northwest of the adjacent more faulted and folded Middle Devonian shales.

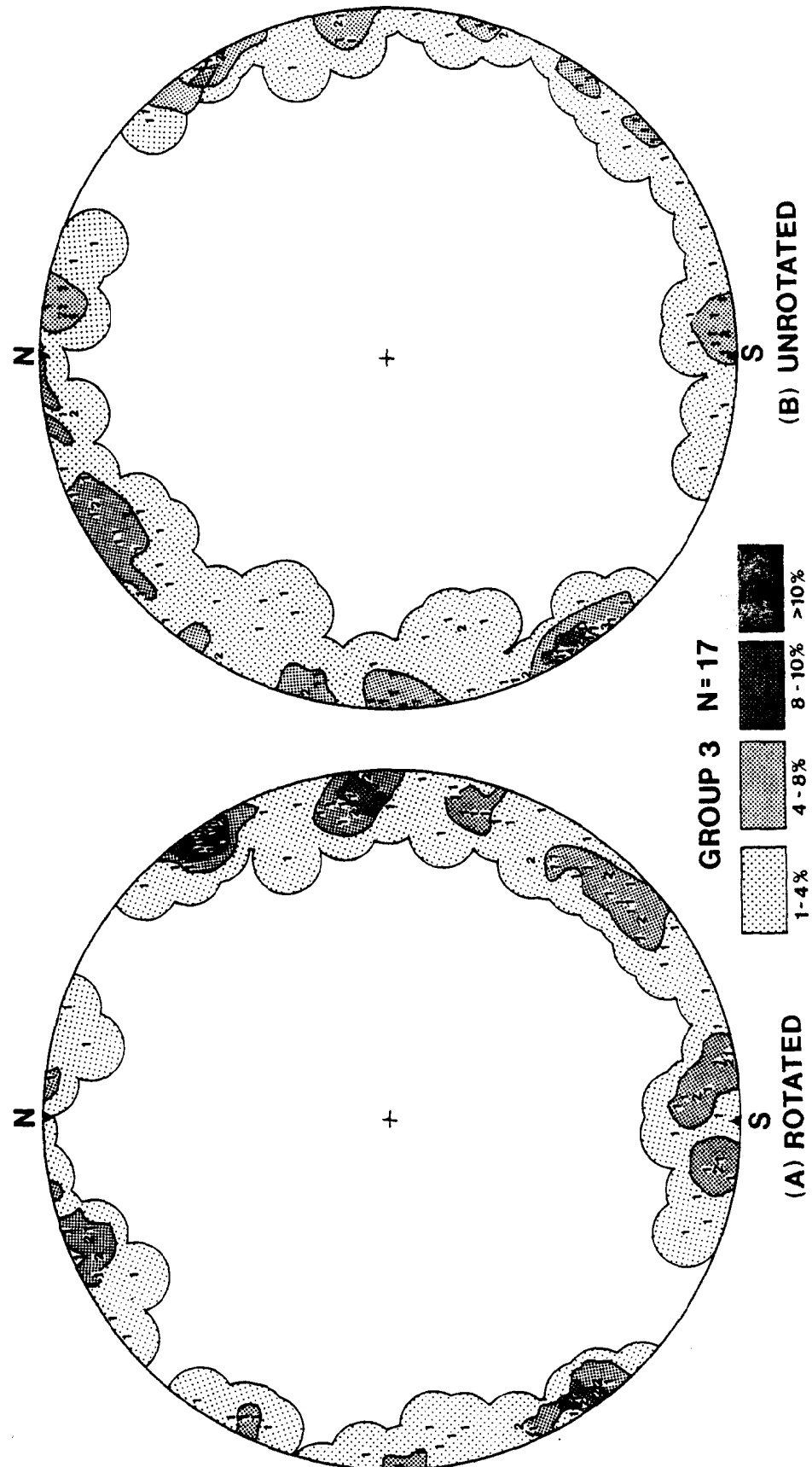


Figure 34 Equal Area Projections of Poles to Rotated and Unrotated Systematic Joints from Group 3

Group 4\*

Rotated			Unrotated		
Cluster Pole	Standard Deviation (degrees)	<u>n</u>	Cluster Pole	Standard Deviation (degrees)	<u>n</u>
N14E/00NE	9	3	N09E/04NE	8	3
N20W/15NW	8	5	N23W/14NW	8	5
N48W/00NW	6	4	N51W/00SE	6	4
N82E/06NE	5	4	N82E/13NE	8	5
N45E/10SW	7	11	N45E/04SW	6	10

Table 11

\*Group 4 is comprised of station 9. Station 9 is in the upper part of the Devonian Brallier formation. A low-angle thrust fault with 80 to 100 feet of displacement is exposed at this station along the axis of the Middle Mountain syncline.

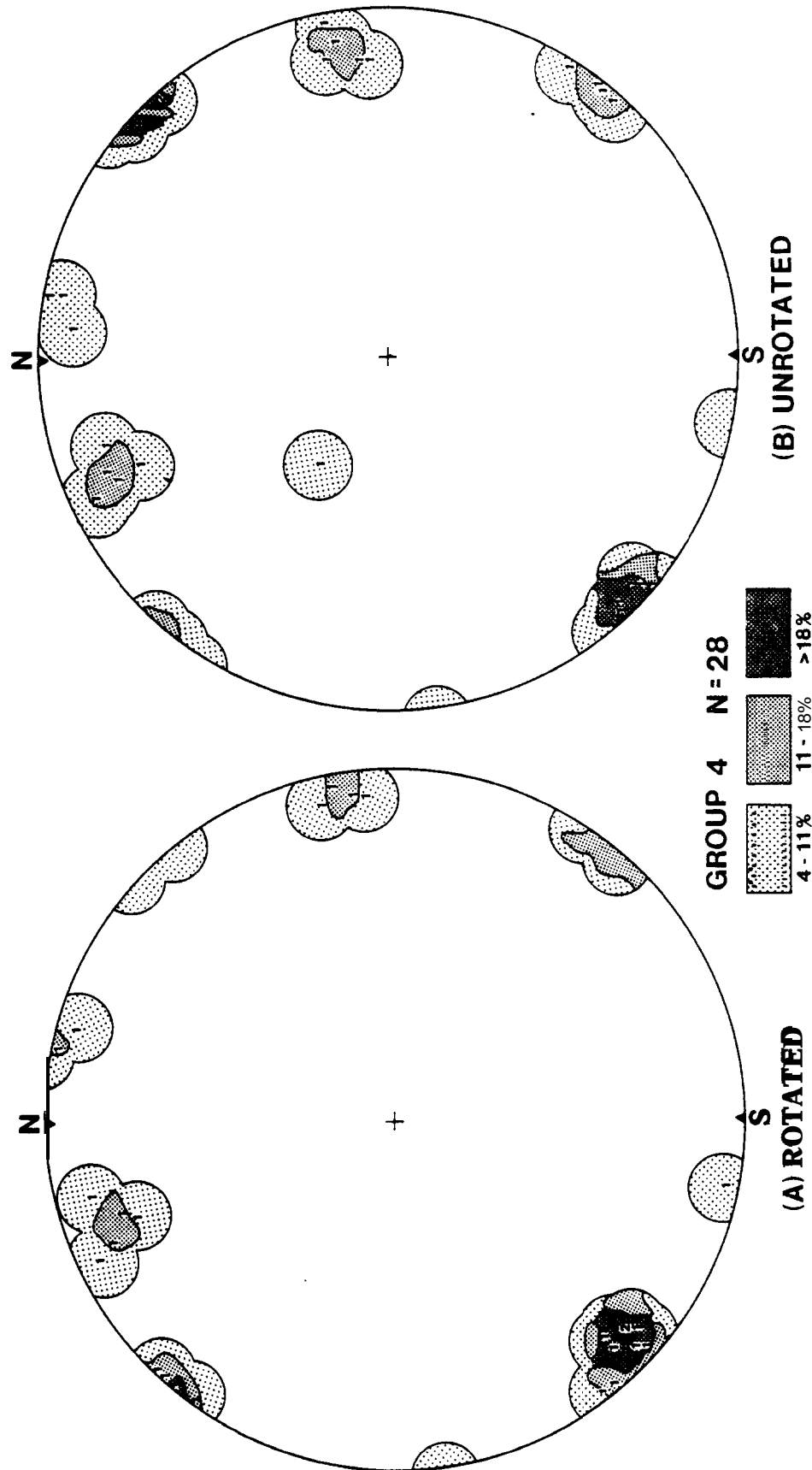


Figure 40 Equal Area Projections of Poles to Rotated and Unrotated Systematic Joints from Group 4

G r o u p 5\*

Rotated			Unrotated		
Cluster Pole	Standard Deviation (degrees)	<u>n</u>	Cluster Pole	Standard Deviation (degrees)	<u>n</u>
N29W/00NW	17	39	N26W/14SE	18	41
N70W/00NW	16	40	N68W/20SE	12	39
N75E/00NE	16	6	N76E/20NE	13	6
N31E/00NE	16	27	N31E/00NE	16	24

Table 12

\*Stations of this group are located in the Brallier formation exposed on the northwest limb of the Middle Mountain **syncline** opposite the intensely deformed area on the syncline's southeast limb. stations included in this group are 4, 5, 6, 7, 8, and 11.



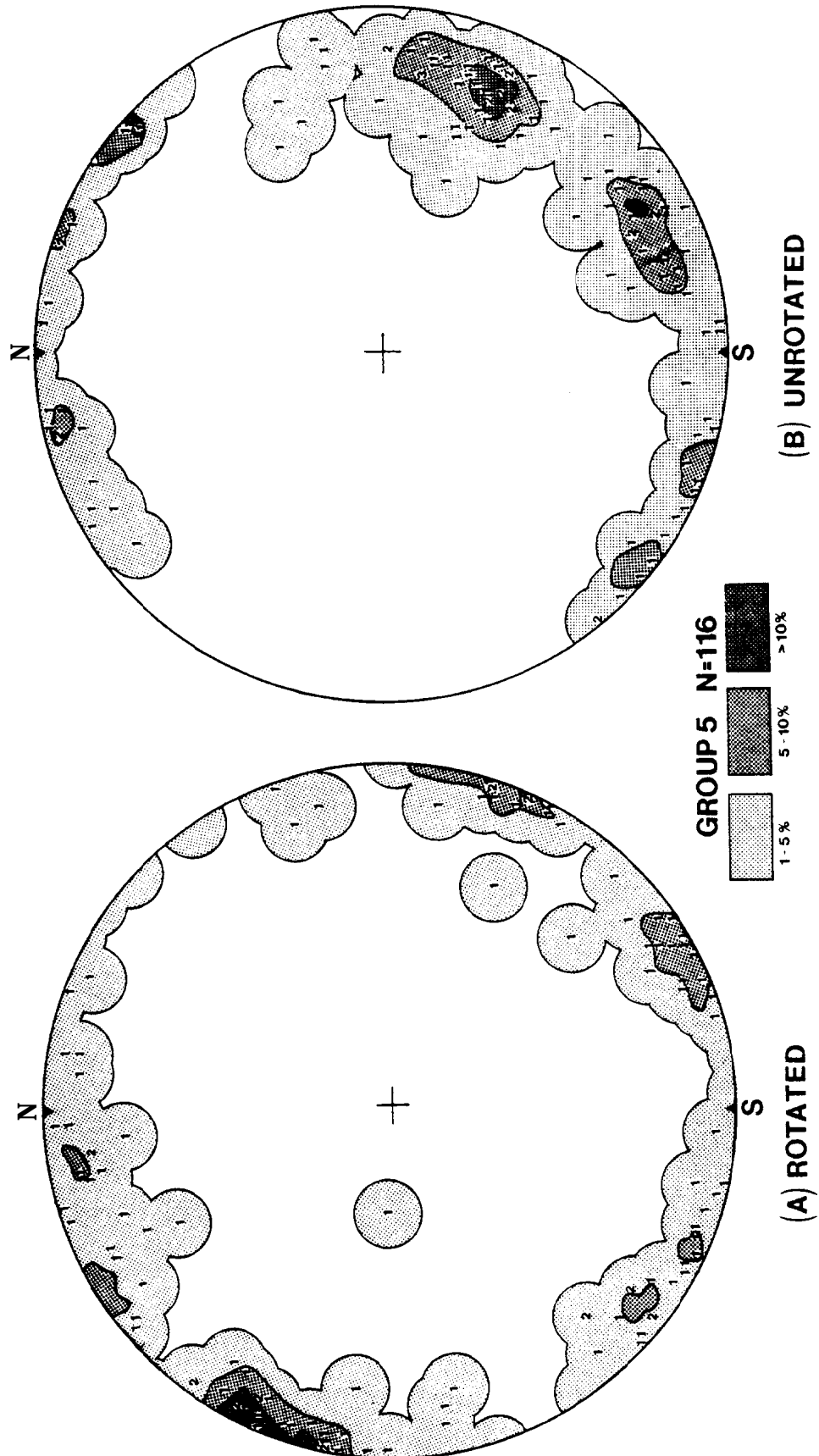


Figure 41 Equal Area Projections of Poles to Rotated and Unrotated Systematic Joints from Group 5

Group 6\*

Rotated			Unrotated		
Cluster Pole	Standard Deviation (degrees)	n	Cluster Pole	Standard Deviation (degrees)	n
N64W/16SE	14	7	N27W/57NW	15	9
			N73E/47SW	11	5
			N37W/04NW	5	7
N35W/24SE	11	16	N56W/20NW	7	3
N18E/00NE	14	35	N22E/03NE	13	29
N38E/02NE	12	23	N39E/06SW	9	28

Table 13

\*Systematic joints measured at stations within the intensely folded and faulted Middle Devonian shales exposed on the southeast limb of the Middle Mountain **syncline** comprise this group. Group 6 contains stations 24, 25, 26, 27, 29, 30, 31, and 39.

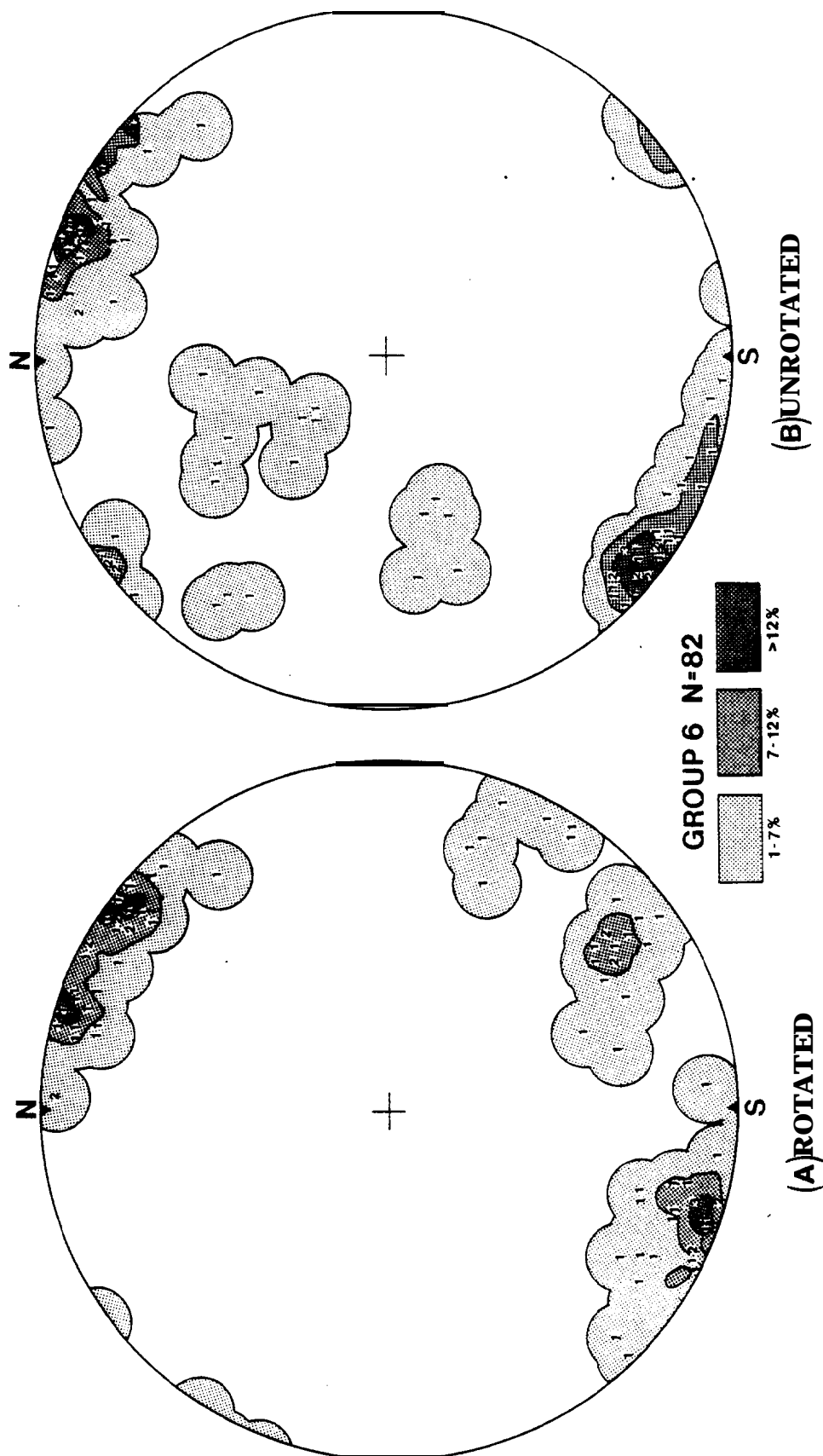


Figure 42 Equal Area Projections of Poles to Rotated and Unrotated Systematic Joints from Group 6

Group 7\*

Rotated			Unrotated		
Cluster Pole	Standard Deviation (degrees)	n	Cluster Pole	Standard Deviation (degrees)	n
N06W/10SE	19	12	N02E/00NE	11	10
N32W/08SE	10	7	N28W/32SE	11	9
N62W/05SE	9	7	N63W/21SE	8	7
N89W/04SE	10	5	N88E/32NE	9	4
N40E/00NE	5	5	N33E/03SW	17	5

Table 14

\*Stations contained in group 7 have the same structural position as those of group 5, including the Middle Devonian shales exposed on the northwest limb of the Middle Mountain **syncline** across strike from the folded and faulted shales on the southeast limb. Stations 10, 12, 15, 16, 21, and 22 are included in this group.

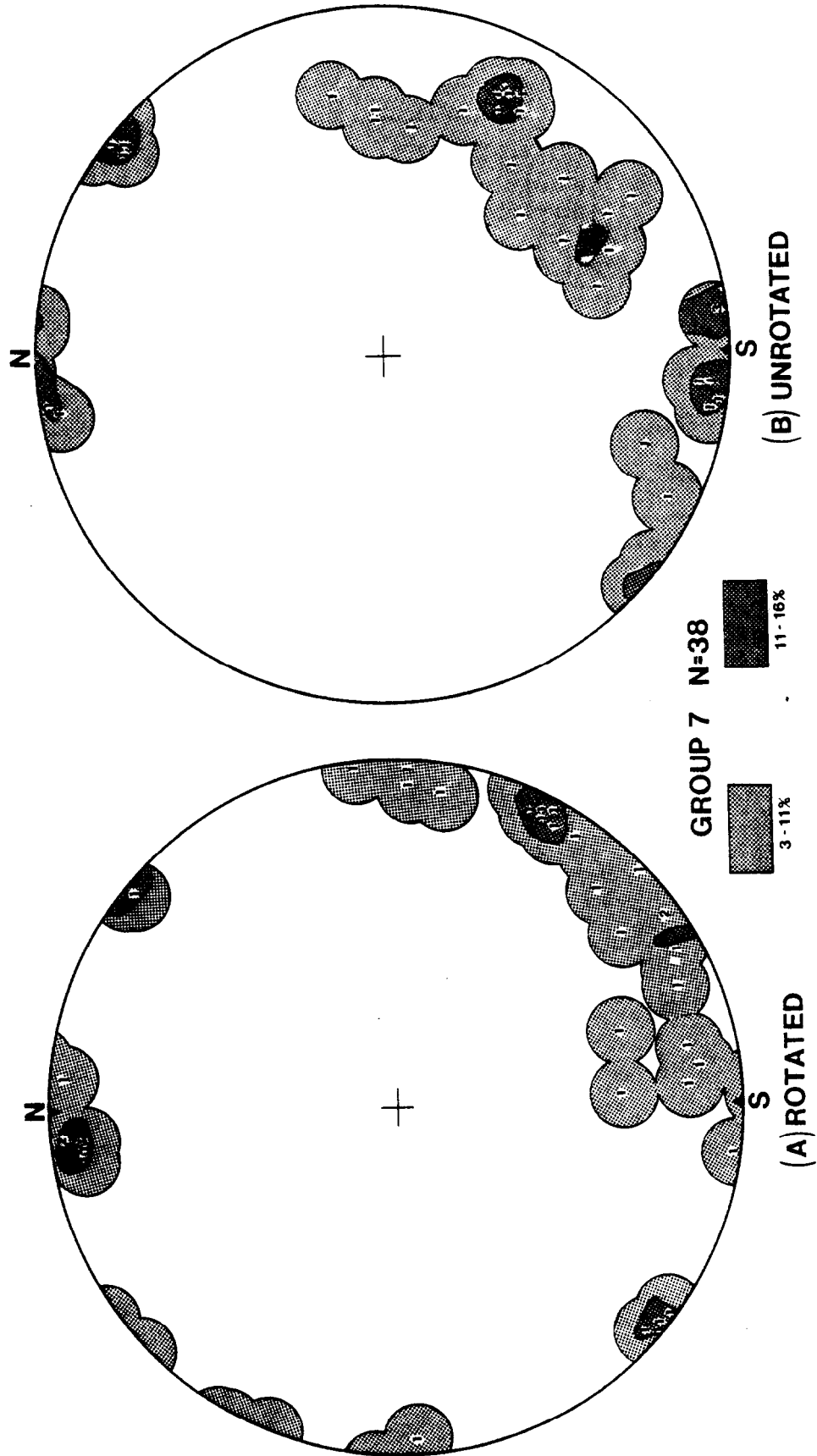


Figure 43 Equal Area Projections of Poles to Rotated and Unrotated Systematic Joints from Group 7

Group 8\*

Rotated			Unrotated		
Cluster Pole	Standard Deviation (degrees)	n	Cluster Pole	Standard Deviation (degrees)	n
N07E/10NE	11	5	N07E/08SW	11	5
N18W/06SE	5	5	N12W/18SE	6	5
N43W/06NW	11	17	N44W/18SE	11	15
N86W/13SE	15	10	N88E/34NE	16	10
N51E/00NE	8	11	N50E/06NE	9	13

Table 15

\*The systematic joints of group 8 include those stations on the northwest limb of the Middle Mountain **syncline** in the exposed Brallier formation north of the region covered by group 5 and across strike from the area covered by group 9. This group includes stations 1, 2, and 3.

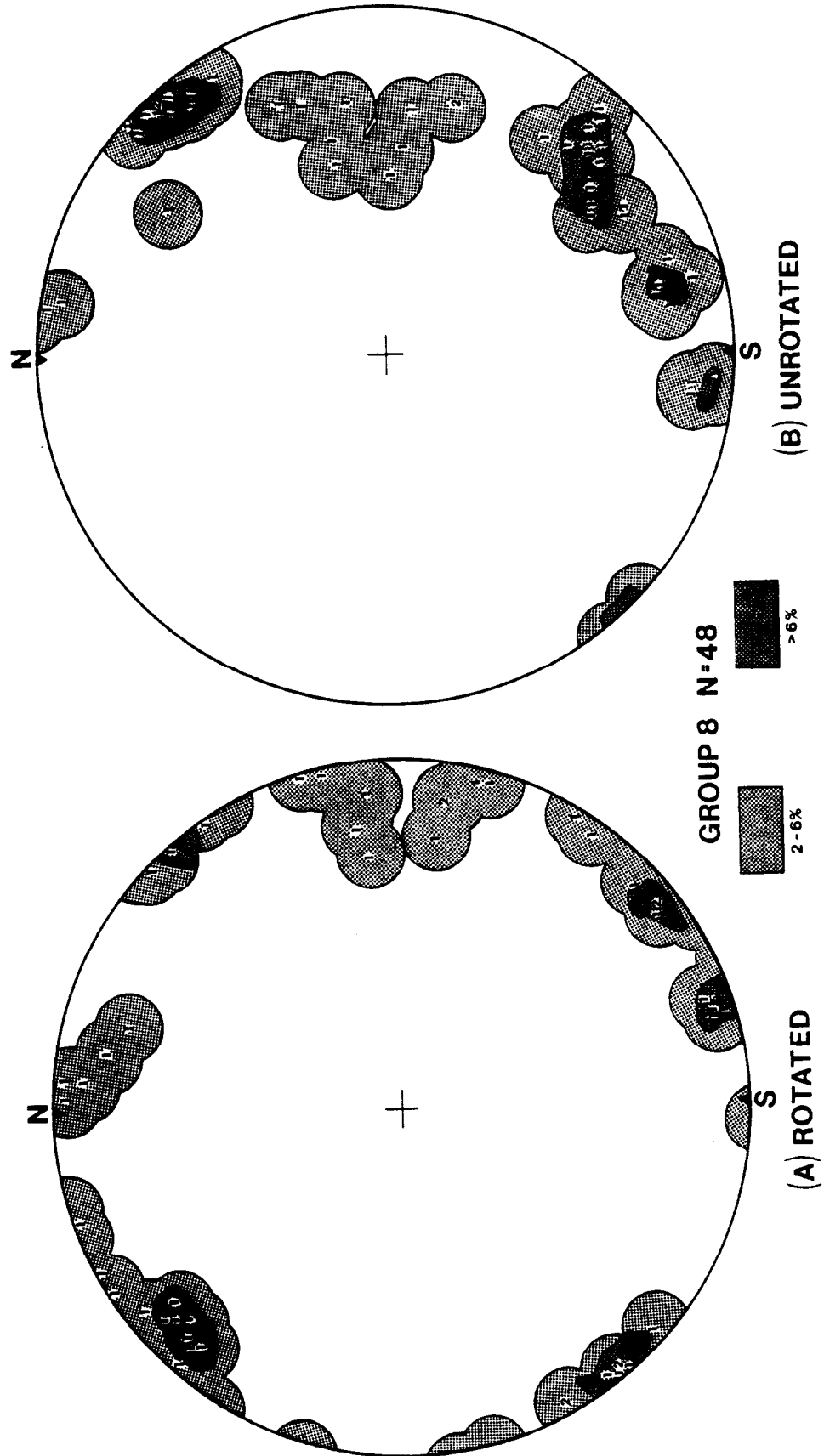


Figure 44 Equal Area Projections of Poles to Rotated and Unrotated Systematic Joints from Group 8

Group 9\*

Rotated			Unrotated		
Cluster Pole	Standard Deviation (degrees)	<u>n</u>	Cluster Pole	Standard Deviation (degrees)	<u>n</u>
N02W/10SE	16	10	N04E/12NE	18	9
			N80W/55NW	5	5
N72W/00NW	12	9			
			N76W/13NW	14	5
N41E/00NE	9	10	N43E/03SW	6	10

Table 16

\*Stations in the Middle Devonian shales on the southeast limb of the Middle Mountain **syncline** just north of the deformed area covered by group 6 were examined separately in group 9. Stations included in this group were 40, 41, and 42.



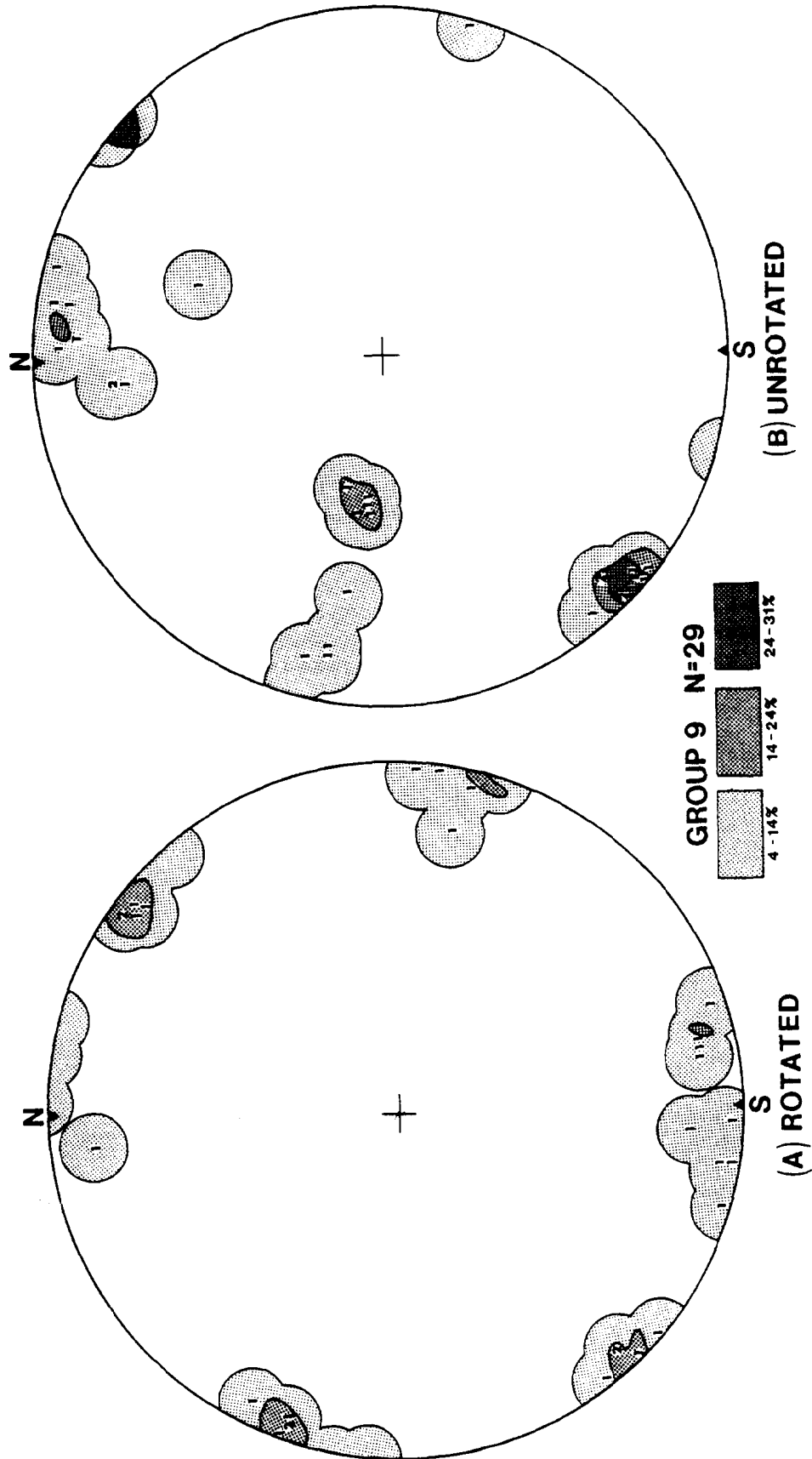


Figure 45 Equal Area Projections of Poles to Rotated and Unrotated Systematic Joints from Group 9

## APPENDIX II

### Joint Spacings and Intensities

## A. Introduction

Spacing is the distance between adjacent joints within the same set, measured along a line that is normal (or near normal) to both joint surfades. Formula 1 (below), used to calculate intensity, was developed by Vialon and others (1970) and applied to joints by Wheeler (1979); Dixon (1979) and Wheeler and Dixon (1980) and is used in this study.

$$I_E = \sum_{i=1}^n \frac{1}{\bar{S}_i} \quad (1)$$

$I_E$  = intensity of jointing in exposure E

n = total number of sets present in exposure E

$\bar{S}_i$  = average spacing of joints in the ith set in exposure E

Joint intensity is an estimate of total joint surface area per unit volume of rock at a given exposure. Because calculation of intensity uses all joint spacings measured at an exposure, only one value of intensity is obtained for an exposure. Additional estimates of intensity require remeasurement of the exposure. This would not only be time-consuming but would introduce a bias through the observer's prior recollection of the exposure.

A method to place confidence limits on a value of intensity is suggested by Wheeler (oral communication,

(1979). The method involves the calculation of pseudo-values in a procedure called jack knifing (Mosteller and Tukey, 1977, pp. 133 ff.). A pseudovalue  $I_{jm}^*$  is calculated using Formula (2).

$$I_{jm}^* = KI_E - (K-1) I_{jm} \quad (2)$$

$I_{jm}$  is calculated the same as  $I_E$  of equation (1) except that the inverse mean spacing from set  $j$  is omitted and replaced by the inverse mean spacing from set  $j$  minus spacing value  $m$  of set  $j$ . In this way, only  $N_j-1$  spacing values are used as indicated in equation (3).

$$I_{jm}^* = KI_E - [(K-1) \times \left( \sum_{\substack{i,j=k \\ i,j,m=1 \\ i \neq j}}^{m-N_j} \frac{1}{\bar{S}_i} + \frac{N_j-1}{N_{JJ}\bar{S}_j - s_m} \right)] \quad (3)$$

$I_E$  = intensity of jointing in exposure  $E$

$I_{(jm)}$  = intensity calculated by equation (1) but omitting spacing  $\underline{m}$  of set  $\underline{j}$

$K$  = total number of spacings from all measured sets at an exposure

$k$  = total number of sets present in an exposure

$\bar{S}_i$  = average spacing of joints in the  $i$ th set

$N_j$  = number of spacings measured from the  $j$ th set

$S_m$  =  $\underline{m}$ th spacing in the  $\underline{j}$ th set

$j$  takes on values 1 through  $k$ . and indentifies the sets

$m$  takes on values 1 through  $N_j$  and identifies the spacing values in the  $j$ th set

If we calculate a pseudovalue for each spacing, we will have a sample of  $K$  pseudovalues whose mean,  $\overline{I_{jm}^*}$ , is an estimate of intensity for which we can calculate confidence limits. The standard error of the mean pseudovalue,  $\frac{1.96\sigma}{\sqrt{K}}$ , provides us with 95 percent confidence limits on the estimate of the mean pseudovalue, that is, on the estimate of  $I_E$ .  $\sigma$  is the standard deviation.

#### B. Joint Spacing and Pseudovalue

The following tables provide a complete listing of spacings measured for each station in the Middle Mountain study area. The stratigraphic unit is also identified, and brief comments are made concerning lithology, bed thickness, and other characteristics of the site. Each set is identified by the average strike and standard deviation of strike of the measured joints. In a few instances, a rapid check of joint spacings was made, but joint orientations were not measured. The number ( $N$ ) of spacing measurements made for the joints within a set is also indicated. Pseudovalues are listed for corresponding values of spacing. The dimension of spacing is centimeters. The pseudovalue is representative of area per unit volume, and its dimension is inverse centimeters. Best estimates of station intensities (means of pseudovalues) and 95 percent

confidence limits are plotted at station locations in Figure 9 of Chapter 11.

Joints present in interbedded siltstones and shales were measured in both the siltstones and the shales, although measurable joints were often more numerous in the siltstones. No study has been made of differences in orientations, numbers of sets, or spacings, between joints in the shales and joints in the siltstones.

B. Joint spacing and pseudovalues

STATION NUMBER: 1

Stratigraphic Unit: **Brallier** Formation (lower)

Comments: Dark, thickly laminated shale with  
occasional siltstones 5 cm to 10 cm thick

<u>Set</u>	<u>N</u>	<u>Spacing (cm)</u>	<u>Pseudovalue (cm<sup>-1</sup>)</u>
N42W±4	8	11	.434
		18	.365
		22	.323
		12	.424
		29	.246
		50	-.035
		40	.108
		8	.461
N03E±12	1 9	7	.283
		3	.495
		1	.596
		11	.057
		16	-.249
		13	-.062
		3	.495
		9	.172
		3	.495
		1	.596
		3	.495
		1	.596
		4	.443
		4	.443
		9	.172
		10	.115
		4	.443
		5	.391
		19	-.447
N43E±4	8	32	-.516
		4	.600
		4	.600
		21	.010
		6	.541
		8	.480
		4	.60
		27	-.259



<u>Set</u>	<u>N</u>	<u>Spacing (cm)</u>	<u>Pseudovalue (cm<sup>-1</sup>)</u>
N77E±3	9	53	.107
		14	.395
		18	.370
		55	.089
		15	.389
		17	.377
		20	.357
		18	.370
		40	.215

STATION NUMBER: 2

Stratigraphic Unit: **Brallier** Formation

Comments: Thinly laminated to **chippy** shales  
**interbedded** with siltstones, each 5 cm  
to 20 cm thick

<u>Set</u>	<u>N</u>	<u>Spacing (cm)</u>	<u>Pseudovalue (cm<sup>-1</sup>)</u>
N39W±6	14	55	-.014
		43	.037
		27	.099
		23	.114
		8	.165
		25	.106
		25	.106
		20	.124
		13	.148
		35	.069
		3	.181
		14	.145
		19	.128
		15	.141
N56E±5	12	13	.128
		10	.160
		16	.094
		5	.210
		49	-.379
		16	.094
		32	-.107
		8	.180
		12	.138
		2	.240
		4	.220
		5	.210

STATION NUMBER: 3

Stratigraphic Unit: **Harrell** Formation

Comments: Thickly laminated shale, platy weathering

<u>Set</u>	<u>N</u>	<u>Spacing (cm)</u>	<u>Pseudovalue (cm<sup>-1</sup>)</u>
N83W±2	6	21	-.277
		9	.308
		20	-.217
		3	.519
		13	.141
		2	.550
N02W±7	8	20	.196
		26	.122
		45	-.168
		37	-.034
		4	.363
		2	.381
		8	.325
		5	.353
N47E±4	14	32	-.007
		2	.336
		40	-.121
		23	.109
		27	.059
		3	.326
		3	.326
		6	.296
		10	.255
		8	.276
		6	.296
		20	.144
		7	.286
		6	.296

STATION NUMBER: 4

Stratigraphic Unit: Brallier Formation

Comments: Shales weathering to chips, occasional  
siltstones 5 cm to 20 cm thick, cleavage  
present in shales, cleavage planes  
oriented N40E/61SE . . .

<u>Set</u>	<u>N</u>	<u>Spacing (cm)</u>	<u>Pseudovalue (cm<sup>-1</sup>)</u>
N62W±6	2	73	.18
		73	.18
N22W±4	2	30	.177
		30	.177
N24E±10	7	5	.262
		12	.224
		15	.206
		29	.110
		37	.043
		18	.187
		17	.194
N75E±2	4	13	.157
		1	.449
		18	-.031
		17	.011

STATION NUMBER: 5

Stratigraphic Unit: Brallier Formation

Comments: Interbedded siltstones and shales,  
siltstones 7 cm to 27 cm thick, N24E set  
has quartz glaze on joint surfaces,  
very large crystals found (10 cm C-axis),  
bedding slightly folded

<u>Set</u>	<u>N</u>	<u>Spacing (cm)</u>	<u>Pseudovalue (cm<sup>-1</sup>)</u>
N62W±13	5	9	.156
		13	.146
		15	.140
		35	.073
		45	.026
N24E±3	3	5	.24
		18	.02
		18	.02

STATION NUMBER: 6

Stratigraphic Unit: **Brallier** Formation

Comments: Predominantly shales, some siltstones  
up to 21 cm thick

Set	<u>N</u>	<u>Spacing (cm)</u>	<u>Pseudovalue (cm<sup>-1</sup>)</u>
N45W±5	4	23	.27
		35	.144
		18	.313
		36	.132
N26E±5	10	15	.143
		3	.374
		10	.246
		3	.374
		7	.303
		8	.284
		8	.284
		15	.143
		9	.265
		37	-.466
N04W±8	3	80	.009
		29	.298
		41	.255
N66E±13	8	12	.133
		8	.208
		8	.208
		9	.189
		20	-.038
		14	.093
		19	-.015
		21	-.062

STATION NUMBER: 7

Stratigraphic Unit: Brallier Formation

Comments: Predominantly shale; some siltstones  
(3 cm to 5 cm) have very closely spaced  
(.5 cm to 2 cm) fractures, possibly  
cleavage **N60E**; these fractures were not  
included as a joint set

Set	<u>N</u>	<u>Spacing (cm)</u>	<u>Pseudovalue (cm<sup>-1</sup>)</u>
N77E±3	5	8	.169
		6	.196
		7	.183
		15	.056
		20	-.053
N10E±2	4	18	.153
		86	-.296
		6	.177
		13	.163

STATION NUMBER: 8

Stratigraphic Unit: Brallier Formation

Comments: Interbedded shales and siltstones,  
siltstones 2 cm to 47 cm thick

<u>Set</u>	<u>N</u>	<u>Spacing (cm)</u>	<u>Pseudovalue (cm<sup>-1</sup>)</u>
N52W±1	2	360	.06
		600	.044
N80W±12	9	13	.084
		23	.07
		2	.098
		28	.062
		33	.055
		87	-.05
		25	.067
		54	.02
		37	.049
N14E±8	4	64	.006
		40	.066
		22	.099
		56	.029

STATION NUMBER: 9

Stratigraphic Unit: Brallier Formation

Comments: Siltstones (1 cm-27 cm) interbedded  
with shales, faulted, fault displacement  
approximately 30 m, fault orientation  
**N30W/22NE, discon** folds (Wheeler, 1978)  
and cleavage present in shales, cleavage  
orientation **N32E/28SE**

Set	<u>N</u>	<u>Spacing (cm)</u>	<u>Pseudovalue (cm<sup>-1</sup>)</u>
N81W±4	2	5	1.55
		11	-1.21
N45W±3	10	35	.683
		27	.689
		118	.609
		30	.687
		46	.674
		44	.676
		50	.671
		44	.676
		97	.63
		100	.627
N07W±3	5	11	.519
		7	.824
		4	1.014
		9	.68
		15	.136
N32E±14	5	3	.264
		3	.264
		2	1.21
		2	1.21
		3	.264
N68E±4	5	78	.314
		40	.633
		24	.718
		8	.787
		22	.728

STATION NUMBER: 10

Stratigraphic Unit: Mahantango Formation

Comments: Shale, folds and faults present, yellowish  
white residue and black residue **present** in  
some areas, fold wavelength approximately 10 m

<u>Set</u>	<u>N</u>	<u>Spacing (cm)</u>	<u>Pseudovalue (cm<sup>-1</sup>)</u>
N57E±11	1 8	8	.202
		5	.311
		11	.088
		2	.414
		7	.239
		5	.311
		5	.311
		4	.346
		3	.380
		12	.049
		9	.165
		6	.275
		16	-.115
		12	.049
		3	.380
		10	.127
		2	.414
		13	.009
N04E±12	1 1	7	.356
		13	.235
		25	-.044
		21	.055
		15	.193
		18	.126
		18	.126
		12	.256
		4	.413
		4	.413
N77W±10	6	3	.431
		7	.409
		13	.360
		9	.393
		33	.164
		10	.385
		83	-.804

STATION NUMBER: 11

Stratigraphic Unit: **Brallier** Formation

Comments: 2 m to 3 m thick sequence of fine  
**grained** sandstones, individual beds  
from 12 cm to 50 cm interbedded with  
shale, **N64E** set has fine coating of  
quartz crystals mm size

<u>Set</u>	<u>N.</u>	<u>Spacing (cm)</u>	<u>Pseudovalue (cm<sup>-1</sup>)</u>
N53W±6	5	21	.034
		12	.249
		12	.249
		14	.207
		14	.207
N64E±6	15	22	-.146
		18	-.039
		4	.275
		17	-.014
		9	.172
		11	.128
		4	.275
		2	.314
		3	.295
N64E±6	15	9	.172
		5	.255
		5	.255
		4	.275
		2	.314
		5	.255



STATION NUMBER: 12

Stratigraphic Unit: Mahantango Formation

Comments: Shale, one joint set present N25E/56NW,  
spacings in upper beds larger than those  
below

<u>Set</u>	<u>N</u>	<u>Spacing (cm)</u>	<u>Pseudovalve (cm<sup>-1</sup>)</u>
N25E	7	54	-.073
		35	.004
		6	.079
		12	.067
		10	.071
		15	.06
		7	.077

STATION NUMBER: 13

Stratigraphic Unit: Brallier Formation

Comments: 9 cm to 22 cm thick siltstones  
interbedded with shale, N17E set has  
coatings of fine quartz crystals

<u>Set</u>	<u>N</u>	<u>Spacing (cm)</u>	<u>Pseudovalve (cm<sup>-1</sup>)</u>
N17E±8	4	11	.19
		22	.076
		20	.101
		12	.182
N62E±3	5	9	.184
		20	.026
		6	.217
		14	.121
		13	.135

STATION NUMBER: 14

Stratigraphic Unit: **Brallier** Formation

Comments: Interbedded shales and siltstones, only one set measured, there are many joints present with diverse orientations, possibly four sets in all, so estimate of intensity is lower than actual

<u>Set</u>	<u>N</u>	<u>Spacing (cm)</u>	<u>Pseudovalue (cm<sup>-1</sup>)</u>
N67E±7	10	2	.478
		1	.625
		3	.318
		2	.478
		1	.625
		1	.625
		4	.143
		4	.143
		4	.143
		3	.318

STATION NUMBER: 15

Stratigraphic Unit: Mahantango Formation

Comments: Shales, no jointing apparent

STATION NUMBER: 16

Stratigraphic Unit: **Needmore** Formation

Comments: Shale

<u>Set</u>	<u>N</u>	<u>Spacing (cm)</u>	<u>Pseudovalue (cm<sup>-1</sup>)</u>
N86E±7	11	17	.224
		26	.147
		16	.233
		12	.265
		4'0	.009
		10	.28
		10	.28
		19	.208
		14	.249
		11	.272
		33	.081

<u>Set</u>	<u>N</u>	<u>Spacing (cm)</u>	<u>Pseudovalue (cm<sup>-1</sup>)</u>
N28E±2	11	7	.229
		10	.075
		7	.229
		8	.179
		10	.075
		3	.416
		2	.460
		4	.371
		6	.277
		8	.178
		20	-.541
N50W±2	9	70	.15
		70	.15
		6	.273
		8	.27
		20	.25
		170	-.186
		20	.25
		8	.27
		20	.25

STATION NUMBER: 17

Stratigraphic Unit: Brallier Formation

Comments: Interbedded shales and siltstones,  
siltstones 10 cm to 20 cm thick

<u>Set</u>	<u>N</u>	<u>Spacing (cm)</u>	<u>Pseudovalue (cm<sup>-1</sup>)</u>
N19W±8	10	100	-.097
		10	.200
		80	-.013
		29	.152
		32	.144
		4	.214
		24	.165
		4	.214
		22	.171
		30	.149

<u>Set</u>	<u>N</u>	<u>Spacing (cm)</u>	<u>Pseudovalue (cm<sup>-1</sup>)</u>
N34E±2	10	26	.043
		11	.201
		8	.23
		5	.257
		27	.031
		11	.201
		23	.077
		27	.031
		10	.211
		25	.054
N71E±3	9	10	.225
		14	.192
		49	-.178
		6	.256
		11	.217
		23	.113
		34	.003
		20	.141
		11	.217

STATION NUMBER: 18

Stratigraphic Unit: Brallier Formation

Comments: Interbedded shales and siltstones,  
siltstones 10 cm to 25 cm thick

<u>Set</u>	<u>N</u>	<u>Spacing (cm)</u>	<u>Pseudovalue (cm<sup>-1</sup>)</u>
N02W±5	21	17	.058
		14	.068
		10	.081
		28	.021
		6	.093
		18	.055
		9	.084
		18	.055
		25	.031
		19	.052
		22	.042
		6	.093
		34	-.001
		11	.078
		17	.058
		9	.084

<u>Set</u>	<u>N</u>	<u>Spacing (cm)</u>	<u>Pseudovalue (cm<sup>-1</sup>)</u>
		5	.096
		25	.031
		17	.058
		39	-.019
		17	.058

STATION NUMBER: 19

Stratigraphic Unit: **Brallier** Formation

Comments: Interbedded shales and siltstones,  
siltstones approximately 10 cm to 20 cm thick

<u>Set</u>	<u>N</u>	<u>Spacing (cm)</u>	<u>Pseudovalue (cm<sup>-1</sup>)</u>
N27E±7	6	28	.084
		22	.092
		34	.075
		62	.029
		100	-.059
		22	.092
N84E±2	11	2	.108
		5	.103
		2	.108
		4	.104
		11	.092
		13	.088
		9	.095
		9	.095
		12	.09
		60	-.02
		175	-.618

STATION NUMBER: 20

Stratigraphic Unit: Brallier Formation

Comments: Predominantly siltstones; 15 cm  
to 20 cm thick: fracture zone present;  
zone contains several closely spaced  
fractures and cuts through the outcrop,  
extent unknown; yellowish white residue  
present in this zone

Set	<u>N</u>	<u>Spacing (cm)</u>	<u>Pseudovalue (cm<sup>-1</sup>)</u>
N78W±7	15	84	.078
		52	.121
		40	.136
		151	-.027
		117	.03
		77	.088
		39	.137
		48	.126
		48	.126
		8	.173
		3	.178
		3	.178
		5	.176
		3	.178
		6	.175
N39E±2	12	29	.137
		35	.111
		36	.106
		20	.174
		24	.158
		25	.154
		32	.124
		8	.220
		34	.115
		8	.220
		34	.115
		47	.056
N36E±8	10	12	.167
		16	.084
		30	-.254
		20	-.004
		12	.167
		10	.207
		12	.167
		6	.282
		5	.301
		16	.084

STATION NUMBER: 21

Stratigraphic Unit: Marcellus Formation

Comments: Shale, no systematic jointing observed

STATION NUMBER: 22

Stratigraphic Unit: **Needmore** Formation

Comments: Shale, some jointing in southeastern  
part of exposure occupies small percentage  
of total exposure surface area, exposure  
otherwise unjointed

STATION NUMBER: 23

Stratigraphic Unit: **Brallier** Formation

Comments: Interbedded shales and siltstones,  
siltstones 9 cm to 15 cm thick

<u>Set</u>	<u>N</u>	<u>Spacing (cm)</u>	<u>Pseudovalue (cm<sup>-1</sup>)</u>
N01W±7	10	26	.062
		10	.116
		13	.106
		9	.119
		20	.083
		24	.069
		18	.01
		49	-.034
		17	.093
		32	.039
N76E±7	6	26	.095
		12	.129
		42	.05
		61	-.018
		44	.044
		12	.129

STATION NUMBER: 24

Stratigraphic Unit: Marcellus Formation .

Comments: Shale, several small faults present,  
the shale is also folded, **discon** folds  
(Wheeler, 1978) are present, slip line  
and slip plane consistent with either  
**flexural** flow on **the** northwest limb of  
**Elkhorn** Mountain anticline or backthrusting

<u>Set</u>	<u>N</u>	<u>Spacing (cm)</u>	<u>Pseudovalue (cm<sup>-1</sup>)</u>
N82W±6	6	10	.070
		4	.47
		5	.415
		5	.415
		3	.522
		7	.292
N48W±8	5	10	-.059
		4	.446
		4	.446
		5	.379
		6	.307

STATION NUMBER: 25

Stratigraphic Unit: Marcellus Formation

Comments: Shale, cleavage present in the Purcell  
limestone

<u>Set</u>	<u>N</u>	<u>Spacing (cm)</u>	<u>Pseudovalue (cm<sup>-1</sup>)</u>
N53W±4	6	42	-.004
		11	.174
		28	.089
		10	.179
		38	.026
		9	.183
N71W±7	4	7	.251
		32	.172
		48	.097
		48	.097



Set	<u>N</u>	<u>Spacing (cm)</u>	<u>Pseudovalue (cm<sup>-1</sup>)</u>
N19W±6	5	6	.292
		14	.036
		12	.11
		10	.176
		10	.176

STATION NUMBER: 26

Stratigraphic Unit: Mahantango Formation

Comments: Shale, bedding is folded

Set	<u>N</u>	<u>Spacing (cm)</u>	<u>Pseudovalue (cm<sup>-1</sup>)</u>
N69W±2	10	6	.354
		11	.283
		48	-.474
		37	-.193
		5	.367
		8	.326
		10	.298
		8	.326
		5	.367
		4	.381
N54W±4	10	8	.296
		7	.326
		18	-.038
		18	-.038
		22	-.195
		3	.438
		3	.438
		5	.383
		6	.355
		10	.235
N50E±7	9	15	.234
		23	.107
		11	.291
		14	.249
		12	.277
		6	.358
		22	.124
		6	.358
		29	.0

STATION NUMBER: 27

Stratigraphic Unit: Marcellus Formation

Comments: Shale, bedding planes form outcrop face,  
no apparent folding or faulting, bedding  
is steeply dipping

<u>Set</u>	<u>N</u>	<u>Spacing (cm)</u>	<u>Pseudovalue (cm<sup>-1</sup>)</u>
N70W±6	20	2	.447
		3	.412
		5	.339
		8	.227
		13	.031
		16	-.093
		16	-.093
		17	-.136
		14	-.01
		1	.482
		8	.227
		10	.150
		5	.339
		9	.189
		6	.303
		4	.376
		4	.376
		5	.339
		8	.227
		12	.071
N51W±3	21	6	.332
		3	.377
		2	.392
		5	.347
		2	.392
		4	.362
		5	.347
		3	.377
		3	.377
		3	.377
		4	.362
		10	.27
		24	.036
		11	.254
		24	.036
		20	.106
		29	-.054
		30	-.073
		25	-.018
		28	-.036
		21	.088

STATION NUMBER: 28

Stratigraphic Unit: Brallier Formation

Comments: Interbedded shales and siltstones,  
siltstones are approximately 14 cm thick

<u>Set</u>	<u>N</u>	<u>Spacing (cm)</u>	<u>Pseudovalue (cm<sup>-1</sup>)</u>
N49W±2	10	24	.139
		27	.129
		32	.111
		14	.171
		24	.139
		38	.089
		15	.168
		36	.097
		25	.136
		16	.165
N27E±2	10	14	.064
		16	.021
		12	.105
		4	.254
		11	.125
		15	.043
		5	.237
		11	.125
		10	.145
		6	.219

STATION NUMBER: 29

Stratigraphic Unit: Mahantango Formation

Comments: Shale, bedding planes form outcrop surface,  
bedding is steeply dipping, no apparent  
folding or faulting

<u>Set</u>	<u>N</u>	<u>Spacing (cm)</u>	<u>Pseudovalue (cm<sup>-1</sup>)</u>
N72W±7	10	7	.272
		24	.026
		12	.207
		8	.259
		10	.234
		1	.343
		50	-.554
		5	.297
		5	.297
		8	.259

<u>Set</u>	<u>N</u>	<u>Spacing (cm)</u>	<u>Pseudovalue (cm<sup>-1</sup>)</u>
N47W±3	12	9	.182
		6	.258
		6	.258
		7	.233
		4	.306
		18	-.079
		8	.208
		3	.329
		20	-.144
		10	.155
		6	.258
		6	.258

STATION NUMBER: 30

Stratigraphic Unit: Marcellus Formation

Comments: Shale

<u>Set</u>	<u>N</u>	<u>Spacing (cm)</u>	<u>Pseudovalue (cm<sup>-1</sup>)</u>
	5	4	.343
		3	.760
		2	1.12
		4	.343
		4	.343
		7	.47
		6	.60
		4	.819
		5	.711
		3	.92
		9	.92
		3	.203
		14	-.636
		2	.979
		5	.679
		2	.979
		3	.884
		9	.189
		2	.979
		3	.884

STATION NUMBER: 31

Stratigraphic Unit: Marcellus Formation

Comments: Shale; nearby, the Purcell limestone  
is tightly folded; axial plane cleavage  
present; faulted

Set	<u>N</u>	<u>Spacing (cm)</u>	<u>Pseudovalue (cm<sup>-1</sup>)</u>
	6	1	.76
		4	.67
		2	.73
		8	.53
		4	.67
		4	.67

STATION NUMBER: 32

Stratigraphic Unit: Brallier Formation

Comments: Interbedded siltstones and shales,  
siltstones approximately 40 cm thick

<u>Set</u>	<u>N</u>	<u>Spacing (cm)</u>	<u>Pseudovalue (cm<sup>-1</sup>)</u>
N38W±4	11	5	.204
		8	.196
		14	.179
		22	.157
		30	.133
		81	-.047
		67	.008
		90	-.086
		30	.132
		20	.162
		26	.145
N02E±8	10	31	.148
		27	.153
		85	.064
		41	.134
		32	.146
		83	.067
		62	.102
		49	.122
		60	.105
		70	.089

<u>Set</u>	<u>N</u>	<u>Spacing (cm)</u>	<u>Pseudovalued (cm<sup>-1</sup>)</u>
N33E±3	10	17	.174
		26	.153
		110	-.113
		33	.135
		49	.092
		13	.184
		23	.16
		23	.16
		50	.089
		64	.049
N82E±3	10	51	-.156
		21	.133
		40	-.04
		27	.082
		35	.009
		7	.241
		4	.262
		10	.219
		12	.204
		23	.116

STATION NUMBER: 33

Stratigraphic Unit: Brallier Formation

Comments: Siltstones interbedded with shales,  
siltstones approximately 17 cm thick

<u>Set</u>	<u>N</u>	<u>Spacing (cm)</u>	<u>Pseudovalued (cm<sup>-1</sup>)</u>
N88W±7	6	10	.331
		13	.188
		7	.461
		8	.419
		20	-.208
		15	.085
N31W±1	10	69	.181
		68	.183
		18	.279
		13	.287
		52	.216
		55	.21
		72	.174
		32	.254
		59	.202
		17	.280

Set	<u>N</u>	<u>Spacing (cm)</u>	<u>Pseudovalued (cm<sup>-1</sup>)</u>
N18E±2	11	30	.236
		46	.18
		45	.183
		44	.187
		26	.249
		20	.268
		33	.226
		18	.275
		32	.229
		32	.229
		32	.229
N51E±6	10	12	.163
		9	.276
		8	.313
		11	.202
		12	.163
		10	.24
		12	.163
		9	.276
		6	.383
		14	.083

STATION NUMBER: 34

Stratigraphic Unit: Brallier Formation

Comments: Shales and siltstones, siltstones are  
5 cm to 32 cm in thickness

Set	<u>N</u>	<u>Spacing (cm)</u>	<u>Pseudovalued (cm<sup>-1</sup>)</u>
N25W±2	10	25	.258
		27	.253
		27	.253
		140	-.113
		30	.246
		32	.242
		18	.273
		28	.251
		40	.222
		38	.227

Set	<u>N</u>	<u>Spacing (cm)</u>	<u>Pseudovalue (cm<sup>-1</sup>)</u>
N45E±8	9	10	-.492
		2	.706
		9	-.317
		2	.706
		2	.706
		3	.579
		2	.706
		7	.01
		13	-1.07
N67E±7	18	108	.194
		126	.183
		189	.140
		147	.169
		220	.117
		165	.157
		97	.201
		10	.248
		4	.251
		1	.253
		6	.250
		2	.252
		12	.247
		6	.250
		1	.253
		3	.252
		8	.249
		6	.250

STATION NUMBER: 35

Stratigraphic Unit: Brallier Formation

Comments: Interbedded shales and siltstones, siltstones  
approximately 15 cm thick, N63E set coated  
with mm sized quartz crystals

Set	<u>N</u>	<u>Spacing (cm)</u>	<u>Pseudovalue (cm<sup>-1</sup>)</u>
N38W±2	4	17	.051
		16	.080
		7	.28
		10	.226
N15W±4	3	45	.119
		35	.171
		25	.211



<u>Set</u>	<u>N</u>	<u>Spacing (cm)</u>	<u>Pseudovalue (cm<sup>-1</sup>)</u>
N23E±3	2	67	.171
		67	.171
N63E±17	3	13	.255
		12	.263
		38	-.106

STATION NUMBER: 36

Stratigraphic Unit: Brallier Formation

Comments: Interbedded shales and siltstones,  
siltstones approximately 15 cm thick

<u>Set</u>	<u>N</u>	<u>Spacing (cm)</u>	<u>Pseudovalue (cm<sup>-1</sup>)</u>
N13W±7	5	22	.054
		7	.108
		27	-.011
		10	.167
		5	.202
N50E±7	3	11	.192
		31	-.253
		6	.237

STATION NUMBER: 37

Stratigraphic Unit: Brallier Formation

Comments: Primarily shale, some siltstones

<u>Set</u>	<u>N</u>	<u>Spacing (cm)</u>	<u>Pseudovalue (cm<sup>-1</sup>)</u>
N35W±6	2	24	.091
		24	.091
N02E±7	7	15	.107
		10	.122
		18	.098
		10	.122
		40	.016
		11	.119
		39	.021

STATION NUMBER: 38

Stratigraphic Unit: Brallier Formation

Comments: Predominantly siltstones, 2 m to 3 m  
 sequence of siltstones with individual  
 beds ranging from 9 cm to 53 cm in  
 thickness

Set	<u>N</u>	<u>Spacing (cm)</u>	<u>Pseudovalue (cm<sup>-1</sup>)</u>
N80W	8	15	.193
		26	.179
		10	.199
		9	.2
		72	.109
		55	.138
		74	.105
		60	.13
N45W±0	2	17	.165
		17	.165
N04W±7	4	3	.37
		23	.002
		24	-.026
		15	.104
N33E±8	3	40	.175
		38	.183
		53	.117

STATION NUMBER: 39

Stratigraphic Unit: Needmore Formation

Comments: Shale; several joints present with diverse  
 orientation, two sets were measured, a third  
 set may be present: estimate of intensity  
 may be low

Set	<u>N</u>	<u>Spacing (cm)</u>	<u>Pseudovalue (cm<sup>-1</sup>)</u>
N33E±2	11	24	-.03
		12	.181
		4	.298
		10	.211
		14	.149
		14	.149

<u>Set</u>	<u>N</u>	<u>Spacing (cm)</u>	<u>Pseudovalue (cm<sup>-1</sup>)</u>
		13	.165
		13	.165
		6	.27
		9	.226
		6	.27
N52E±3	10	9	.206
		11	.158
		12	.133
		10	.182
		9	.206
		5	.295
		3	.336
		12	.133
		14	.082
		12	.133

STATION NUMBER: 40

Stratigraphic Unit: Mahantango Formation

Comments: Shales, bedding steeply dipping, bedding  
surface forms outcrop face, no folding or  
faulting apparent

<u>Set</u>	<u>N</u>	<u>Spacing (cm)</u>	<u>Pseudovalue (cm<sup>-1</sup>)</u>
N08E±4	9	49	-.435
		14	.178
		11	.216
		10	.228
		11	.216
		18	.125
		11	.216
		14	.178
		8	.252
N88E±4	8	43	.068
		10	.231
		44	.062
		58	-.028
		14	.214
		35	.112
		5	.252
		17	.201

<u>Set</u>	<u>N</u>	<u>Spacing (cm)</u>	<u>Pseudovalue (cm<sup>-1</sup>)</u>
N48W±2	12	7	.23
		5	.243
		9	.217
		6	.236
		4	.249
		56	-.18
		47	-.088
		41	-.031
		7	.23
		9	.217
		17	.162
		17	.162

STATION NUMBER: 41

Stratigraphic Unit: Mahantango Formation

Comments: Shale

<u>Set</u>	<u>N</u>	<u>Spacing (cm)</u>	<u>Pseudovalue (cm<sup>-1</sup>)</u>
N80W±6	6	2	.756
		9	.312
		19	-.624
		7	.452
		4	.642
		14	-.099
N45W±4	17	20	.147
		8	.323
		2	.403
		37	-.147
		26	.05
		17	.193
		26	.05
		7	.336
		5	.363
		16	.208
		9	.309
		2	.403
		12	.267
		6	.35
		2	.403
		1	.415
		2	.403

<u>Set</u>	<u>N</u>	<u>Spacing (cm)</u>	<u>Pseudovalue (cm<sup>-1</sup>)</u>
N12E±3	9	35	-.641
		5	.447
		7	,396
		5	.447
		11	.286
		17	.102
		6	.422
		8	,369
		10	.314

STATION NUMBER: 42

Stratigraphic Unit: Marcellus Formation

Comments: Shale

<u>Set</u>	<u>N</u>	<u>Spacing (cm)</u>	<u>Pseudovalue (cm<sup>-1</sup>)</u>
±N	4	23	.086
		57	.016
		21	,089
		78	-.050
	10	24	.066
		78	-.011
		27	.063
		22	.068
		27	.063
		25	.065
		23	.067
		19	.071
		90	-.019
		25	.065

C. INTENSITY, MEAN PSEUDOVALUE,  
AND CONFIDENCE LIMITS ON THE MEAN

Station	K	Intensity (cm <sup>-1</sup> )	Mean Pseudovalue (cm <sup>-1</sup> )	Confidence Limits (cm-l)
1	44	.3	.31	±.08
2	26	.11	.11	±.05
3	28	.22	.19	±.08
4	15	.18	.17	±.06
5	8	.12	.10	±.06
6	25	.22	.16	±.07
7	8	.12	.08	±.11
8	15	.05	.05	±.02
9	27	.66	.61	±.18
10	35	.25	.21	±.08
11	20	.19	.19	±.06
12	7	.05	.04	±.04
13	9	.14	.14	±.04
14	10	.40	.39	±.13
15	0	≅0	≅0	≅0
16	31	.21	.19	±.06
17	29	.14	.13	±.04
18	21	.06	.06	±.01
19	17	.06	.03	±.08
20	37	.13	.13	±.03
21	0	≅0	≅0	≅0
22	0	≅0	≅0	≅0
23	16	.08	.07	±.03
24	11	.35	.34	±.11
25	15	.17	.14	±.06
26	29	.24	.22	±.08
27	51	.24	.20	±.05
28	20	.14	.13	±.03
29	22	.19	.18	±.09
30	20	.68	.63	±.18
31	6	.26	.23	±.05
32	41	.12	.11	±.03
33	37	.23	.22	±.04
34	37	.22	.20	±.10
35	12	.17	.16	±.06
36	8	.13	.09	±.11
37	9	.09	.09	±.03
38	17	.17	.15	±.04
39	21	.19	.19	±.04
40	29	.15	.14	±.06
41	32	.28	.25	±.10
42	14	.05	.05	±.02

D. Average Group Intensities and p-Values

Average intensity of jointing from each group of stations are listed. p-values have been calculated using the non-parametric Mann-Whitney U-test for comparison of group intensity.

	Group*							
	<u>1, 2</u>	<u>3</u>	<u>4</u>	<u>5</u>	<u>6</u>	<u>7</u>	<u>8</u>	<u>9</u>
Average Intensity	.14	.15	.61	.13	.27	.07	.20	.11
N*	8	7	1	6	8	6	3	3

Table 17

\*Stations comprising each group are listed below.

Group 1: 20  
Group 2: 13, 14, 17, 18, 19, 23, 28  
Group 3: 32, 33, 34, 35, 36, 37, 38  
Group 4: 9  
Group 5: 4, 5, 6, 7, 8, 11  
Group 6: 24, 25, 26, 27, 29, 30, 31, 39  
Group 7: 10, 12, 15, 16, 21, 22  
Group 8: 1, 2, 3  
Group 9: 40, 41, 42

Reference to structural and lithologic relationships of each group can be made on Figure



## p-Values\* for Group Comparisons

Group	<u>1,2</u>	<u>3</u>	<u>4</u>	<u>5</u>	<u>6</u>	<u>7</u>	<u>8</u>	<u>9</u>
1,2		.17N	.11N	.33N	.002G	.14N	.19N	.32N
3	.17N		.13N	>.5N	.02G	.09L	.19N	.26N
4	.11N	.13N		.14N	>.5N	.17N	.25N	.25N
5	.33N	>.5N	.14N		.001G	.20N	.08G	.27N
6	.002L	.02L	>.5N	.001L	-	.01L	.27N	.14N
7	.14N	.09G	.17N	.20N	.01G		.10G	.16N
8	.19N	.19N	.25N	.08L	.27N	.10L	-	.20N
9	.32N	.26N	.25N	.27N	.14N	.16N	.20N	

Table 18

\*The p-values were calculated using the nonparametric Mann-Whitney U-test. The n-value is the probability that two populations of joint intensity have the same distribution. (1-p) is the probability that one population is stochastically larger or smaller than the other. The relationship of the column to the row is indicated by the letters G, L, or N. G implies that the intensity of the column group is greater than that of the row group to which it has been compared; L, less than; N, no difference. p-values of 0.1 or less are considered small enough to indicate the relationship of G or L. However, the relationship of G or L is not considered statistically different unless  $p \leq .05$ .

### APPENDIX III

#### Stratigraphy

A. Thicknesses of Stratigraphic Units

Average thicknesses of stratigraphic units were calculated from thicknesses reported for measured sections of the county reports.

THICKNESSES OF STRATIGRAPHIC UNITS  
FOR DODDRIDGE AND HARRISON COUNTIES,  
WEST VIRGINIA  
(Hennen and White, 1912)

system	Series	Average Thickness (feet)
Pennsylvania	Monongahela Series	420
	Conemaugh Series	565
	Allegheny Series	243
	<b>Pottsville</b> Series	350
Mississippian	<b>Mauch</b> Chunk Series	203
	Greenbrier LS	71
	Pocono Series	441
Devonian	Catskill Series	686

THICKNESSES OF **STRATIGRAPHIC** UNITS  
FOR GRANT AND MINERAL COUNTIES,  
WEST VIRGINIA  
(Reger and Tucker, 1924)

system	Series	Average Thickness (feet)
Pennsylvanian	Conemaugh Series	797
	Allegheny Series	175
	Pottsville Series	421
Mississippian	<b>Mauch</b> Chunk Series	827
	Greenbrier Series	273
	Pocono Series	596
Devonian <b>(Upper)</b>	Catskill Series	1925
	Chemung Series	4047
	Portage Series	1780
	<b>Genesee</b> Series	313
	(Middle)	
	Hamilton Series	400
	Marcellus Series	637
	(Lower)	
Silurian	Oriskany SS	205
	Helderberg LS	600
	Salina FM	
	Bossardville LS	302
	Rondout SH and LS	528
	Bloomsburg SS and SH	61
	Niagara LS	184
	Clinton Series	532
	Tuscarora SS	276
	Juniata Series	1015
	Oswego SS	254

THICKNESSES OF STRATIGRAPHIC UNITS  
FOR HARDY AND HAMPSHIRE COUNTIES,  
WEST VIRGINIA  
(Tilton, Prouty, Tucker, and Price, 1927)

system	Series	Average Thickness (feet)
Devonian	Catskill Series	4755
	Chemung Series	2200
	Portage Series	1200
	<b>Genesee</b> Series	400
	Hamilton Series	500
	Marcellus Series	550
	Oriskany Series	336
	Helderberg Series	375
Silurian	Salina Series	
	Bossardville LS	334
	Rondout SH and LS	455
	Bloomsburg SS and SH	36
	Niagara LS	265
	Keefer SS	25
	Clinton Series	487
	Tuscarora SS	328
	Juniata Series	550
	Oswego SS	400

THICKNESSES OF STRATIGRAPHIC UNITS  
FOR MARION, MONONGALIA, AND TAYLOR COUNTIES,  
WEST VIRGINIA  
(Hennen and Reger, 1913)

System	Series	Average Thickness (feet)
Pennsylvanian	Monongahela Series	348
	Conemaugh Series	582
	Allegheny Series	231
	Pottsville Series	297
Mississippian	Mauch Chunk Series	205
	Greenbrier LS	91
	Pocono Series	414
Devonian	Catskill Series	834

THICKNESSES OF STRATIGRAPHIC UNITS  
FOR MARSHALL, TYLER, AND WETZEL COUNTIES,  
WEST VIRGINIA  
(Hennen and White, 1909)

system	Series	Average Thickness (feet)
Pennsylvanian	Monongahela Series	320
	Conemaugh Series	541
	Allegheny Series	270
	Pottsville Series	270
Mississippian	<b>Mauch</b> Chunk Series	101
	Greenbrier <b>LS*</b>	57
	Pocono Series	527

\*Additional information on the top of the Greenbrier taken  
from Cardwell (1978).



THICKNESSES OF STRATIGRAPHIC UNITS  
FOR PENDLETON COUNTY, WEST VIRGINIA  
(Tilton, Prouty, and Price, 1927)

System	Series	Average Thickness (feet)
Mississippian	<b>Mauch</b> Chunk Series	1722
	Greenbrier Series	399
	Pocono Series	345
Devonian	(Upper)	
	Catskill Series	2800
	<b>Chemung</b> Series	4000
	Portage Series	2674
	<b>Genesee</b> Series	196
	(Middle)	
	Hamilton Series	566
	Marcellus Series	447
	(Lower)	
	Oriskany Series	339
	Helderberg Series	633
Silurian	Salina Series	
	Bossardville LS	30
	Rondout SH and LS	320
	Bloomsburg SS and SH	374
	Niagara Series	231
	Clinton <b>Series</b>	378
	Tuscarora SS	188
	Juniata Series	445
	Oswego SS	101
Ordovician	Martinsburg SH	2033
	Chambersburg LS	350

THICKNESSES OF STRATIGRAPHIC UNITS  
FOR RANDOLPH COUNTY, WEST VIRGINIA  
**(Reger, 1931)**

System	Series	Average Thickness (feet)
Pennsylvanian	Pottsville Series	687
Mississippian	<b>Mauch</b> Chunk Series	958
	Greenbrier Series	248
	Pocono Series	102
Devonian	Catskill Series	685
	Chemung Series	2946

THICKNESSES OF STRATIGRAPHIC UNITS  
FOR TUCKER COUNTY, WEST VIRGINIA  
(Reger, Price, and Tucker, 1923)

system	Series	Average Thickness (feet)
Pennsylvanian	Conemaugh Series'	a39
	Allegheny Series	132
	Pottsville Series	544
Mississippian	Mauch Chunk Series	672
	Greenbrier Series	274
	Pocono Series	152
Devonian	(Upper)	
	Catskill Series	761
	Chemung Series	2890
	Portage Series	1460
	Genesee Series	170
	(Middle)	
	Hamilton Series	1000
	Marcellus Series	695
	Corniferous Series	155
	(Lower)	
	Oriskany Series	270

THICKNESSES OF **STRATIGRAPHIC** UNITS  
FOR UPSHUR AND **BARBOUR** COUNTIES  
AND THE WESTERN PORTION OF RANDOLPH COUNTY,  
WEST VIRGINIA  
(**Reger** and Teets, 1918)

System	Series	Average Thickness (feet)
Pennsylvanian	Monongahela Series	391
	Conemaugh Series	598
	Allegheny Series	298
	Pottsville Series	302
Mississippian	<b>Mauch</b> Chunk Series	391
	Greenbrier LS	103
	Pocono Series	330
Devonian	Catskill Series	586

THICKNESSES OF STRATIGRAPHIC UNITS  
FOR ROCKINGHAM COUNTY, VIRGINIA  
(see Table 1 of Brent, 1960)

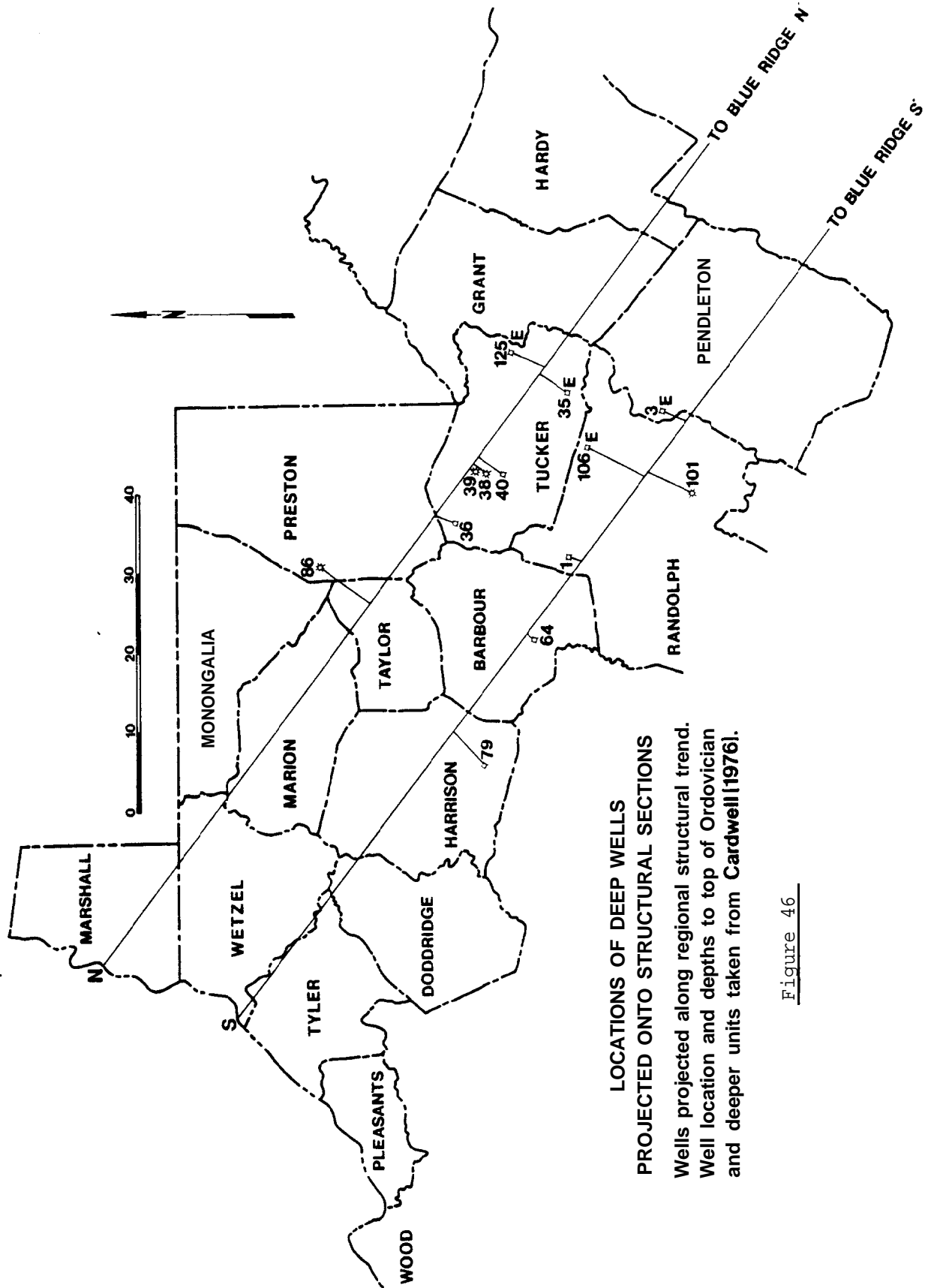
System	Series	Average Thickness (feet)
Mississippian	Pocono Fm	300+
Devonian (Upper)	Hampshire Fm	2000
	<b>Chemung Fm</b>	2000
	Brallier Sh	1200
(Middle)	Millboro and Onondaga Sh	400-500
(Lower)	Ridgely Ss	50-150
	Helderberg Ls	100-400
Silurian	Cayuga Group	220-600
	Clinton Fm	
	Massanutten Ss	500-700
	Clinch Ss	50-200
Ordovician (Upper)	Juniata Fm	250
	Oswego Ss	300-600
	Martinsburg Sm	1500-3000
(Middle)	Edinburg Fin	1500
	Lincolnshire Ls	50-150
	Newmarket Ls	50-200
(Lower)	Beekmantown Fm	2000
	Chepultepec Ls	500
Cambrian (Upper)	Conococheague Ls	2500
(Middle)	Elbrook Dolomite	2000
(Lower)	Rome ( <b>Waynesboro</b> ) Fm	1700
	Shady ( <b>Tomstown</b> ) Dolomite	1000
	Chilhowee Group	
	Erwin ( <b>Antietam</b> ) Quartzite	400
	Hampton (Harpers) Fm	900
	Weverton Fm	800-1600
	Loudoun Fm	0-200
Precambrian	Catoctin Greenstone	0-1000
	Swift Run Fm	0-100

THICKNESSES OF STRATIGRAPHIC UNITS  
FOR PAGE COUNTY, VIRGINIA  
(see Table 1 of Allen, 1967)

system	Series	Average Thickness (feet)
Devonian	Devonian (undivided)	30-200
Silurian	Cayuga Group	200-600
	Massanutten Ss	400-650
Ordovician	Martinsburg Fm	1000-3000
	Edinburg Fm	500-1500
	Lincolnshire Fm and New Market Ls	50-200
	Beekmantown Fm	2000-3000
	Chepultepec Fm	300-500
Cambrian	Conococheague Fm	2000-2500
	Elbrook Fm	2000-2500
	Rome Fm	2000
	Shady Fm	1000-1500
	Erwin (Antietam) Fm	800
	Hampton Fm	900
	Weaverton Fm	1000-1500
	Loudoun Fm	0-200
Precambrian	Catoctin Fm	0-2000
	Swift Run Fm	0-100
	Pedlar Fm	?

B. Deep Well Locations

Locations of deep wells that were projected onto the regional sections. Depths and locations are taken from Cardwell (1976).



LOCATIONS OF DEEP WELLS  
PROJECTED ONTO STRUCTURAL SECTIONS  
Wells projected along regional structural trend.  
Well location and depths to top of Ordovician  
and deeper units taken from Cardwell(1976).

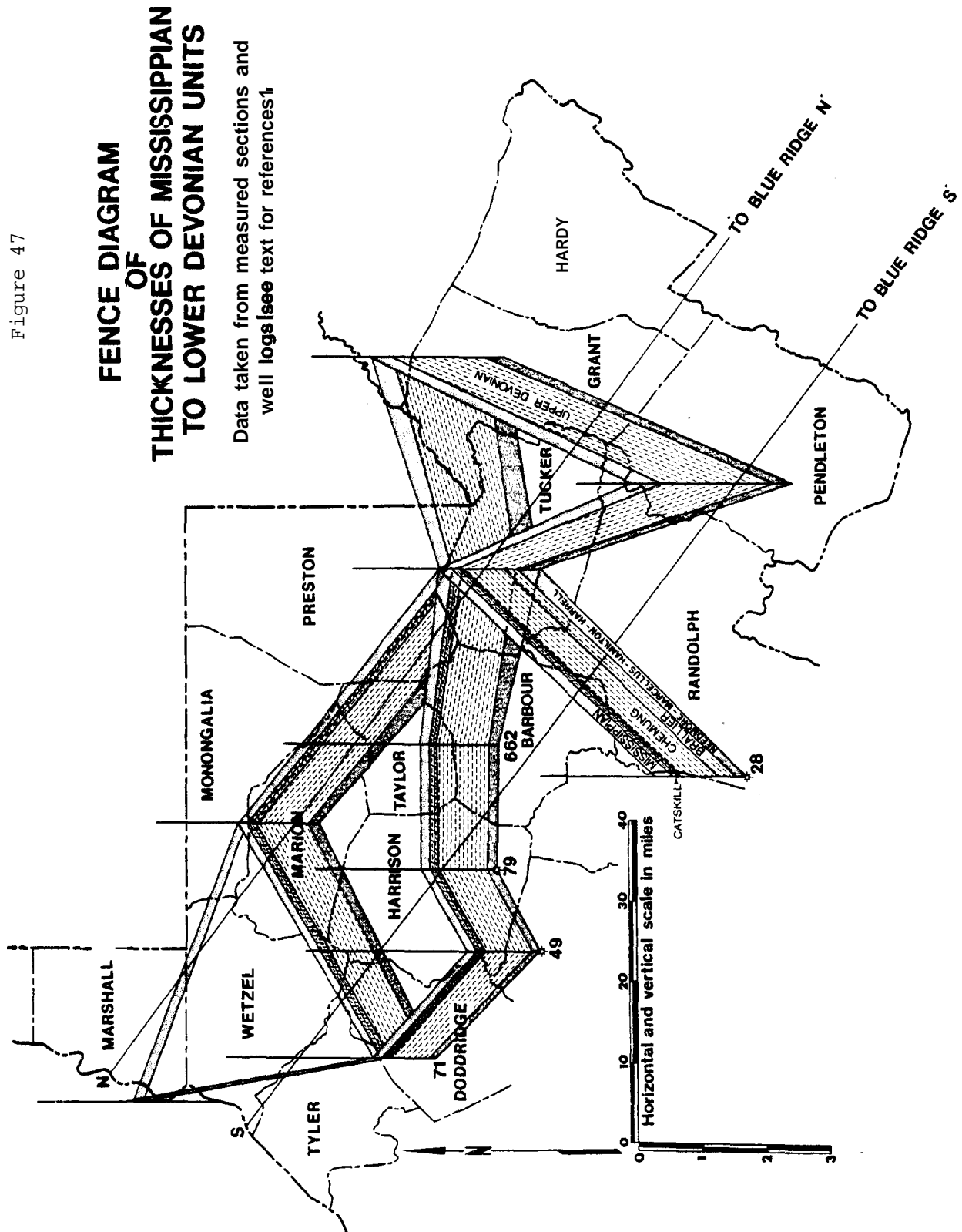
Figure 46

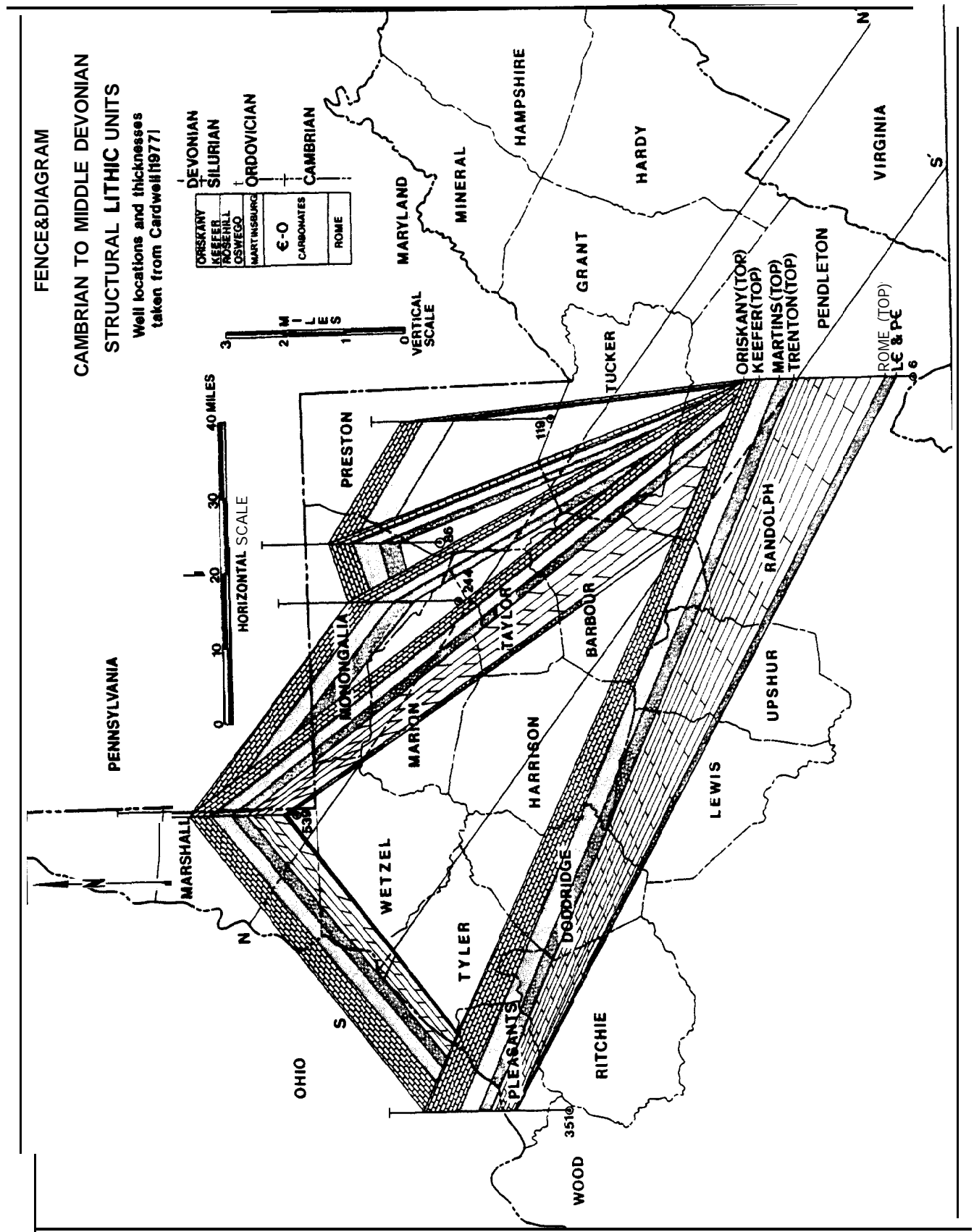


### C. Fence Diagrams

Fence diagrams are compiled from data presented in Cardwell (1976, 1976), Chen (1977) and Perry (1964). See section IVB, 1a for discussion.

Figure 47





#### APPENDIX IV

List of Pertinent Gravity Data for  
the Middle Mountain Gravity Profile

GRAVITY DATA - MIDDLE MOUNTAIN GRAVITY PROFILE

Station**	Elevation (feet)	Latitude (degrees)	Observed Gravity (mgals)	Latitude Corr. (mgals)	Elevation Corr. (mgals)	Terrain Corr. (mgals)	Terrain Corr.-- Bouguer Gravity
1	2110	38.845	-27.88	-.94	126.49	3.34	101.0
2	1767	38.838	-6.25	-.38	105.93	2.27	101.5
3	1505	38.834	9.42	-.02	90.23	2.27	101.9
4	1342	38.838	20.00	-.34	80.46	2.40	102.5
5	1262	38.837	24.22	-.23	76.66	2.27	102.9
6	1296	38.834	22.68	0.0	77.70	2.27	102.1
7	1289	38.832	22.68	0.19	77.28	2.40	102.6
8	1340	38.826	18.93	0.48	80.34	1.87	101.6
9	1408	38.827	15.29	0.64	84.41	2.27	102.6
10	1399	38.825	14.43	0.85	83.88	2.67	101.8
11	1419	38.823	12.30	0.97	85.08	2.80	101.2
12	1392	38.820	13.64	1.21	83.46	3.07	101.4
13	1400	38.817	13.35	1.49	83.93	2.14	100.9
14	1441	38.814	10.35	1.81	86.40	2.14	100.7
15	1446	38.811	9.77	2.00	86.70	2.27	100.7
16	1453	38.807	9.31	2.39	87.11	2.27	101.1
17	1472	38.805	7.81	2.57	88.25	2.27	99.2
18	1583	38.802	1.86	2.79	94.91	1.6	100.3
19	1581	38.795	1.70	3.45	94.79	1.73	101.3
20	1600	38.794	0.07	3.51	95.92	2.0	101.5
21	1626	38.794	-2.18	3.51	99.48	2.0	102.8
22	1671	38.795	-4.97	3.41	100.18	1.74	100.5
23	1752	38.796	-10.35	3.37	105.03	1.87	100.5
24	1979	38.797	-24.27	3.29	118.64	1.87	101.4
25	1985	38.798	-24.98	3.18	119.00	2.14	101.7
26	2072	38.798	-24.90	3.22	124.22	1.07	103.6
27	1977	38.772	-24.44	5.21	118.72	1.60	101.1
3ASE	1566	38.8341	0.0	0.0	93.89	4.27	98.2

"Observed gravity is relative to the gravity at the base station.

\*\*Station locations are located on Plate

**LEGEND:**

- 
- A vertical scale bar with a black background and white markings. The word "SCALE" is written vertically on the left side, and "MILLS" is written vertically on the right side. The scale has five major markings labeled 0, 1, 2, 3, 4, and 5 from bottom to top. Each marking is accompanied by a horizontal white line segment.





PLATE 4

